

Tomato bushy stunt virus
engineering:
design, development and tuning
of a tool for nanotechnology

PhD candidate:
Simone Grasso

Coordinator:
Prof.ssa Laura De Gara

Tutor:
Prof. Luca Santi



Università Campus Bio-Medico di Roma

Corso di dottorato di ricerca in

**"Scienze Biochimiche e Tecnologiche Applicate
agli Alimenti ed alla Nutrizione"**

XXV ciclo anno 2010

Tomato bushy stunt virus engineering:
design, development and tuning of
a tool for nanotechnology

Simone Grasso

Coordinatore:
Prof.ssa Laura De Gara

Tutore:
Prof. Luca Santi

- 26.03.2013 -

A handwritten signature in black ink, consisting of a large, stylized 'S' followed by a smaller 'G' and the name 'Simone Grasso' written in a cursive script.

Summary

Foreword.....	1
Introduction.....	3
Viral nano-biotechnology: an interdisciplinary field.....	4
Nanomedicine applications.....	6
Applications of VNPs in material synthesis.....	19
Tomato bushy stunt virus.....	28
The Genome - ORFs and replication.....	29
Proteins - function and synthesis.....	31
Plant molecular farming.....	35
Materials & Methods.....	41
General materials.....	41
<i>E. coli</i> strains.....	41
Plasmid.....	41
<i>N. benthamiana</i> plants.....	42
Relevant cloning techniques.....	43
<i>E. coli</i> cell culturing.....	43
Plasmid preparation.....	43
Agarose gel electrophoresis.....	44
Restriction digestion.....	44
DNA extraction from agarose gel.....	45
Ligation of DNA fragments.....	45
Preparation of electrocompetent cells and electroporation of <i>E. coli</i>	46
<i>In vitro</i> transcription of RNAs.....	47
<i>In vitro</i> annealing of oligonucleotides.....	47
Phosphorilation and de-phosphorilation.....	49
Polymerase chain reaction (PCR).....	49
Techniques for VNPs characterization.....	51
Plant infection.....	51
VNPs purification.....	51

VNPs quantification	52
SDS-PAGE	52
Western Blotting	53
Enzyme-Linked Immunosorbent Assay (ELISA)	54
Electron microscopy	55
RNA extraction and RT-PCR analysis.....	55
Analytical separation of VNPs on sucrose gradient.....	56
VNPs reversible swelling.....	56
RNase protection assay.....	57
VNPs biotinylation	57
Results	58
Genetic engineering	59
TBSV-Flag -cMyc, -HA, -V5 construction.....	60
TBSV-GFP construction.....	63
<i>In vitro</i> transcription constructs	64
<i>In planta</i> transcription constructs	66
Plant infection.....	69
VNPs characterization	73
Particle assembly	73
Heterologous peptide expression	75
Heterologous peptide display	77
TBSV chimeras genomic stability	78
VNPs modifications.....	81
Exploitation of the internal cavity of VNPs.....	81
Chemical derivatization of VNPs.....	83
Discussion	85
References	95



Acronyms

VNP: viral nanoparticle

CVP: chimeric virus particle

VLPs: virus-like nanoparticle

APC: antigen presenting cell

DC: dendritic cell

MHC: major hystocompatibility complex

HBV: Hepatitis B virus

HPV: Human papilloma virus

NV: Norwalk virus

TLR: toll-like receptors

CP: coat protein

HCRSV: Hibiscus chlorotic ring spot virus

mAb: monoclonal antibody

TR: translational repression

CPMV: Cowpea mosaic virus

QD: quantum dots

RCNMV: Red clover necrotic mosaic virus

OAS: origin-of-assembly

MRI: magnetic resonance imaging

Gd: gadolinium

CCMV: Cowpea chlorotic mottle virus

PET: positron emission tomography

TMV: Tobacco mosaic virus

TYMV: Turnip yellow mosaic virus

BMSC: bone marrow stromal cell

PEG: polyethylene glycol



SWCNTs: single-walled carbon nanotubes

LbL: layer-by-layer

TBSV: Tomato bushy stunt virus

sg: subgenomic

PMF: plant molecular farming

FDA: Food and Drug Administration

UHP: ultra-high-pure

EtBr: ethidium bromide

bd: bi-distilled

dpi: days post-infection

PVDF: polyvinylidene difluoride

HRP: horseradish peroxidase

NHS: N-hydroxysuccinimide

CDS: coding sequence

MCS: multi-cloning site

wt: wild-type

GFP: green fluorescent protein

NOS: nopaline synthase

HDV: Hepatitis delta virus

HRz: HDV ribozyme

A handwritten signature in black ink, consisting of a large, stylized 'S' followed by the name 'Simone' and a large, stylized 'G' followed by the name 'Grasso'.

Foreword

Developments during the past decade in biochemistry, physical chemistry, microscopy, and engineering have resulted in a dramatic upsurge of interest in the properties of nanoparticulate objects and their possible applications, making nanotechnology one of the most significant research areas emerged in the last years. Centered on the concept of creating applications based on components built at the very small (nano-) scale, nanotechnology is relatively young and it draws on well-established knowledge and expertise from all science and engineering disciplines, integrating aspects of physics, chemistry, biology, material sciences, and biological and chemical engineering. Taking inspiration from such a wide range of scientific disciplines, the nanotechnology is going toward a continuous and always increasing development. Currently, the prefix "nano" in common speech is used to denote products or applications very trendy, nevertheless there is yet a high degree of misinformation and also an apparent disparity of opinion as for the meaning of the term "nanotechnology". Nanotechnology is sometimes referred to as a general purpose technology because, in its advanced version, it will have significant impact on almost all industries and all areas of society. However, nanotechnology is largely a field of science and not a technology, alike some believe, since it involves fundamental research on the structure of matter and, in that sense, "nanoscience" is perhaps a more appropriate name. One of the definitions provided in the literature mentions nanotechnology as « the principle of atom manipulation atom by atom, through control of the structure of matter at the molecular level » (K. Eric Drexler, *Engines of Creation*). Nevertheless, this definition is too narrow because it restricts

nanotechnology as a discipline to building materials; therefore, there are many other routes being actively pursued by researchers spreading from drug delivery to imaging techniques. As such, in general nanotechnology refers to any application of science dealing with elements between 0,1 and 100 nanometers, where size is critical to performance. Nanotechnology can be divided into two discrete classes depending on whether the focus is on scientific research and development of particular nano-properties, which will make up the building blocks for applications (nanomaterials), or on the creation of functional systems (nanodevices). Numerous techniques are used to fabricate different nanomaterials. In particular nanoparticles can be produced using two main building strategies, either a "top down" or a "bottom up" approach. With the first approach, nanomaterials are generated by breaking up bulk materials, whereas with the second approach the nanomaterials are built from individual atoms or molecules that have the capacity to self-assemble. Over the past two decades, scientists and engineers have been mastering the intricacies of working with nanoscale materials. As a matter of the fact, researchers have now a clearer picture of how to create and manipulate nanoscale materials making nanotechnology-based commercial products available today.

Introduction

Currently, nanotechnology is described as a revolutionary discipline in terms of its possible impact on a wide range of applications because it offers potential solutions to many problems using emerging nano-techniques. Together with nanotechnology, biotechnology represents one of the most promising technologies of the 21th century. While the former deals with the creation, investigation and utilization of systems that are 1000 times smaller than the average diameter of an eukaryotic cell, the latter deals with metabolic processes and microorganisms. Convergence of these two sciences results in growth of a new discipline called "nanobiotechnology". This hybrid discipline can also mean making atomic-scale devices by imitating or incorporating biological systems at the molecular level. Depending on the strong interdisciplinary character of nanobiotechnology, this is expected to create innovations and play a vital role in various research fields.

Viral nano-biotechnology: an interdisciplinary field

In nanotechnology, submicroscopic particles ranging from 1 to 100 nm in diameter are usually referred to as nanoparticles. In recent years, there has been a great deal of development of nanoparticles different in size, chemical nature and structure. Nanoparticles can be developed from inorganic as well as organic compounds, or can be based on naturally occurring biomolecules. Biological nanoparticles mainly derive from the assembly of one or more protein subunits in defined macromolecular structures. Although naturally occurring biological nanoparticles such as ferritin and the heat shock protein cages, which are both individually able to self-assemble into nanometer sized spherical cages, have received particular attention (Yamashita, Iwahori et al. ; Flenniken, Liepold et al. 2005), viruses and virus derived nanoparticles (VNPs) are considered the most promising protein cages. Despite the first virus was discovered and recognized as an infectious agent only at the end of the 19th century, today more than 5000 viruses have been described and for a great part of these detailed knowledge about the structure and function is available. Viruses are designed by nature to form well defined super molecular structures during their infection cycle and therefore they have received much attention since the early days of nanotechnology. VNPs offer several advantages over non-biological nanoparticles as they are homogeneous in size (monodispersion), they bear an intrinsic robustness being at the same time naturally biodegradable, and have a repetitive and symmetric macromolecular organization. Another important aspect of the nanoparticles is that the smaller they get, the larger their relative surface area become, leading to greatly improved activity in respect to particle number concentration. A common requirement for advanced nanoscale applications is to fully take advantage of multivalency and payload containment and transport. Different strategies for the modification of VNPs' outer and inner surfaces as well as for entrapment of molecules in their inside have been addressed in order to thoroughly take advantage of and to tune the natural virus properties (Grasso and Santi 2010). Intact virus particles, able to

replicate and infect their natural host system, have been extensively used especially as nanoscaffolds for the display of biomolecules, such as short peptides (Donini, Lico et al. 2005), entire proteins (Cruz, Chapman et al. 1996), nucleic acids (Strable, Johnson et al. 2004), carbohydrates (Kaltgrad, O'Reilly et al. 2008). Genetic modifications of simple virions, consisting in many cases of one or just a few subunits, have led to the development of chimeric virus particles (CVPs) with new biological properties, involved in immunogenicity, cooperative affinity, specificity and tropism. Many viral structural proteins, also when individually expressed outside the context of their viral genome, retain the ability to self-assemble into organized macromolecular structures identical or similar to the cognate virion. These "empty shells", known as virus like particles (VLPs), lack of their genomic content and are therefore non-infectious. VLPs production can be achieved by unloading VLPs of their genome or by means of heterologous expression in several systems such as bacteria, yeast, mammalian and insect cells, whole plants and plant derived suspension cultures. In fact, the possibility to insert the structural protein coding sequence directly in a particular expression cassette and then move it into the desired biological production system has reduced dramatically the need of dealing with the native infectious agent. Bacteriophages (Bar, Yacoby et al. 2008; Newton-Northup, Figueroa et al. 2009), animal (Santi, Batchelor et al. 2008; Murata, Lightfoote et al. 2009) and plant viruses (Gonzalez, Plummer et al. 2009; Lico, Mancini et al. 2009) have been all investigated for their use as tools in a broad range of applied fields, extending from biomedicine to materials science (Lewis, Destito et al. 2006; Nam, Kim et al. 2006).

Nanomedicine applications

In general, nanomedicine refers to the medical application of nanotechnology focusing onto the development and fine-tuning of novel nanomaterials, which can be used for disease diagnosis, therapy and prevention. Historically, the first and currently the most advanced medical application of VNPs concerns vaccine development. The size of VNPs has been shown to be favorable for the uptake by antigen presenting cells (APCs) during the first stages of the immune response. As a result, their ordered, dense and repetitive structures are able to activate innate immunity through pattern recognition and to stimulate a potent humoral as well as T-cell mediated immunity (Thanavala, Mahoney et al. 2005; McCormick, Corbo et al. 2006). At the base of a proper immune response induction is the propensity of VNPs for being uptaken by dendritic cells (DCs), followed by their transport to lymph nodes, and the subsequent cross-presentation of the VNP derived peptides onto both the major histocompatibility complex (MHCs) molecules (Kurts, Robinson et al. ; Storni and Bachmann 2004). Three are the main strategies that have been employed in vaccine production: *i)* the first and most used vaccine technology takes advantage from viruses that are rendered non-infectious by chemical treatment whereas retaining their macromolecular cues; *ii)* genome-free VLPs produced in heterologous expression systems and consisting of capsid proteins able to initiate an immune response; and *iii)* chimeric VNPs used as molecular platforms for genetic fusion or chemical attachment of heterologous antigenic epitopes (Grasso and Santi 2010). Currently, vaccines that provide protection against infectious diseases have still primarily relied on attenuated or inactivated pathogens (Cox, Brokstad et al. 2004; Plotkin 2005), and the reason reside on both economic issue and the effectiveness of the formulations. Furthermore, although the production of VNP based vaccines is usually less expensive compared to live attenuated and killed viruses, manufacturing costs are in some cases too high, discouraging their utilization, especially when massive immunization programs are taken into account. Several VLPs produced in heterologous systems have been tested for

their ability to generate an immune response, which can be used for both prophylactic and therapeutic purposes. Due to the lack of the genomic content, these kinds of subunit recombinant vaccines are unable to replicate, but still exhibit the same structural immunological determinants of the virus they are derived from. For this reason, they are considered a safer alternative compared to traditional vaccines based on killed or attenuated viruses, which still bear the theoretical risk of viral replication. Several preclinical studies have underlined the ability of VLPs to generate a neutralizing protective response against various infectious agents (Correia-Pinto, Csaba et al. 2013). A number of VLP based vaccines are now at different stages of clinical development, however the only recombinant vaccines currently marketed are based on VLPs derived from the *Hepatitis B virus* (HBV) and the *Human papilloma virus* (HPV) (McAleer, Buynak et al. 1984; Harper, Franco et al. 2004; Villa, Costa et al. 2005). The production of correctly assembled VLPs in different plant systems has been also widely reported (Santi, Huang et al. 2006), and a number of plant-produced VLPs have already been shown to retain antigenicity and immunogenicity upon different administration routes. A clear example of the dramatic potential of the plant production platform has been set by *Norwalk virus* (NV) derived VLPs, which were produced in tobacco leaves, potato tubers and tomato fruits. In this case, immunogenicity of the plant-purified VLPs was tested in mice upon oral administration, and a clear specific humoral and mucosal antibody response was detected (Santi, Batchelor et al. 2008). In addition, VNPs as well as VLPs have been used as scaffolds for the display of non-native epitopes on their surface, creating a general strategy for the development of vaccines uncoupling the specific immune determinants from the original molecular display scaffold (Lico, Mancini et al. 2009). As such, the epitope display platform combines the distinctive advantages of the recombinant subunit and the whole virus vaccines under the same system. CVPs derived from plant and bacteria pathogens are particularly valuable in this field because they are not only biocompatible and biodegradable, but they are also considered non-infectious

and non-hazardous in humans and other mammals. On the other hand, there is increasing evidence that suggests the viral genome could play an additional role in stimulating the immune response. On these basis, phages as well as plant CVPs still enclose their genome, usually represented by a single stranded RNA unable to replicate in vertebrates, which may however interact with the intracellular toll-like receptors (TLRs) 7/8, activating downstream pathways important for DC maturation (Baum and Garcia-Sastre). Finally, VNPs provide a useful platform for development of novel vaccines because their highly repetitive structure, particulate nature and pathogen associated molecular patterns (PAMPs) increase their potential immunogenicity. The unique properties of VNPs such as their regular geometries, well characterized surface properties, stability over a wide range of physic-chemical conditions and also a relative easy and cheap production, candidate them as the next nanomedicine devices for therapeutic as well as diagnostic purposes. Therapeutic advantages regarding cargo containment of such molecular devices are interesting, particularly for what concerns cancer treatment. Although VNPs appear to be closed shells in almost their representations, virus capsids contain pores on their surfaces and are structurally highly dynamic themselves. Small molecules can diffuse freely between the bulk medium and the capsid through these pores or can be entrapped within the core of the VNPs by means of complex coat protein (CP) rearrangements. Furthermore, the ability to decorate nanoparticles with specific ligands means these payloads can be delivered to particular cells. Conventional small chemotherapeutic agents are commonly non-specifically administered and affect both pathological and normal cells with consequences concerning general toxicity of the drug. The combination of drug containment and active targeting using VNPs can offer a very promising approach to prolong drug systemic circulation lifetime, decrease dosage and enhance preferential drug uptake. Certain disease tissues express different receptors to the corresponding healthy tissues and such receptors can be targeted specifically using appropriate ligands to deliver therapeutic

agents. In a notable work, *Hibiscus chlorotic ring spot virus* (HCRSV) VNPs were used to target the ovarian cancer derived cells OVCAR-3 through folic acid/folate receptor binding. Folic acid is involved in cell division and DNA synthesis, playing a crucial role in cellular metabolism. Its uptake is mediated by its specific interaction with the cell surface folate receptor, which expression is upregulated during cellular proliferation and is thus overexpressed on tumor cells. Ren *et al.* (2007) demonstrated HCRSV derived VNPs, displaying chemically attached folic acid on their surface and delivering the chemotherapeutic agent doxorubicin within their core (**Fig. 1**), mediated a significantly higher uptake of doxorubicin, which resulted in higher cytotoxicity compared to doxorubicin loaded particles not exposing folic acid and also in respect to free drug (Ren, Wong *et al.* 2007). Another relevant example of VNPs employed to achieve tumor targeted and capsid mediated drug delivery has been achieved by the Bar *et al.* (2008) work. In this study, the filamentous phage M13 has been dual functionalized onto the surface through the chemical conjugation of the antibiotic hygromycin and by chimeric expression of an IgG binding capability moiety. Then, the M13 CVPs conjugated with hygromycin were decorated *in vitro* with a monoclonal antibody (mAb) to achieve a targeted delivery to ErbB2 overexpressing human breast adenocarcinoma SKBR3 cells. By using a cell killing assay, an impressive potency improvement relied to these VNPs was shown, resulting in more than 1000 folds over free hygromycin administration (Bar, Yacoby *et al.* 2008). The ability to target specifically a tissue or single cell types by ligand-receptor binding gives rise the possibility of delivering gene expression constructs directly to patients and to replace the activity of a non-functional or dysfunctional protein. On the other hand, antisense technology with the purpose to inhibit expression, upon mRNA hybridization with specifically designed nucleic acid, can be the solution when there is a necessity to down-regulate the production of specific proteins believed to be involved in the development of a disease. Both these strategies hold a great potential in the battle against genetic diseases and cancer. In the

history of gene delivery, adenoviral vectors represent one of the first and the most used platforms, due to their specific features such as low pathogenicity in humans, relative broad range of tissues able to transduce and the abilities to infect both dividing and non-dividing cells (Kay, Holterman et al. 1995; Lieber, Vrancken Peeters et al. 1995; Nguyen, Spitz et al. 1996; Mizuno, Yoshida et al. 1998). More recently, several gene therapy vector systems have been developed to specifically deliver constructs to particular cell types. Studies using a GFP reporter gene construct *in vivo* and *ex vivo* confirmed the high transfection efficiency and specificity of a system based on HBV derived L nanoparticles (Yamada, Iwasaki et al. 2003). These are singular VLPs obtained by heterologous expression in yeast of HBV 110 L protein monomers, which, once embedded in the endoplasmic reticulum membrane, are able to form organized and monodispersed vesicles of 80 nm in diameter. Taking advantage of the phospholipidic nature of these VLPs, which allowed a loading strategy based on simple electroporation of DNA plasmids, and exploiting the natural tropism of the HBV L protein for receptor binding on human hepatocytes, it has been possible to deliver the gene coding for the clotting factor IX (hFIX) into a mouse xenograft model of hepatic tumor. Plasmatic concentration of hFIX were regularly detected for at least 1 month after VLPs administration and the measured level were estimated to be sufficient to convert severe hemophilia to moderate hemophilia in humans (Yamada, Iwasaki et al. 2003). On the opposite, an example of packaging of nucleic acids to pursue specific protein expression inhibition is offered by the icosahedral MS2 bacteriophage VLPs (Wu, Sherwin et al. 2005). In this case, preferential loading of exogenous material has been achieved exploiting the peculiar translational repression (TR) operator RNA stem loop sequence contained in the MS2 genome. The TR RNA sequence is naturally involved in the genome encapsidation during virion assembly by binding CP dimers. This specific interaction has been used by Wu and colleagues (2005) to direct selective loading of antisense oligonucleotides designed on the p120 nucleolar gene and fused to the TR RNA sequence. The human p120 nucleolar protein

is a cell cycle related protein, which is uniquely localized to the nucleolus and appears to play a fundamental role in proliferation-associated nucleolar activity (Busch 1990). The nucleolus of eukaryotic cells is a subnuclear organelle mainly responsible for rRNA synthesis and ribosome biogenesis (Raska, Koberna et al. 2004). Nucleolar pleomorphism is usually exhibited by cancer cells, reflecting the increased need for ribosome biogenesis associated with their active proliferation. Taking advantage of antisense technology, short single-stranded DNA oligonucleotides were synthesized to specifically down-regulate p120 gene expression by interaction with cellular mRNAs and thus inducing their cleavage. The MS2 particles carrying the DNA/RNA hybrid oligonucleotides were also conjugated on the outer surface with transferrin molecules to exploit the specific binding with the transferrin receptor and to mediate virus internalization into the intracellular environment. In fact, the circulatory iron carrier transferrin is greatly demanded during proliferation and its surface cellular receptor is significantly overexpressed in cancer cells (Gomme, McCann et al. 2005). The resulting MS2 VNPs containing the short oligonucleotides cargo were used to treat a promyelocytic leukemia cell line over-expressing the p120 gene. The induction of a specific down-regulation of gene expression, thus resulting in apoptosis and tumor killing, was observed (Wu, Sherwin et al. 2005). In addition to gene function replacement and antisense therapy, nucleic acid delivery can also be used for chemotherapeutic aims. The nucleotide analogue 5-fluorouridine (5fU) has been often chosen for this purpose due to its well-known features (Armstrong and Diasio 1980). The incorporation of 5-fluoro-2'-deoxy-uridine (5fdU) as 5' and 3' extension of the 19 nt long TR RNA stem loop sequence combined the possibility to mediate its specific loading into empty MS2 particles with the exploitation of this nucleotide analogue toxic nature. Furthermore, VNPs were decorated by covalent attachment of monoclonal antibodies directed against a cell surface antigen, which is associated with human breast tumors (Fig. 1).

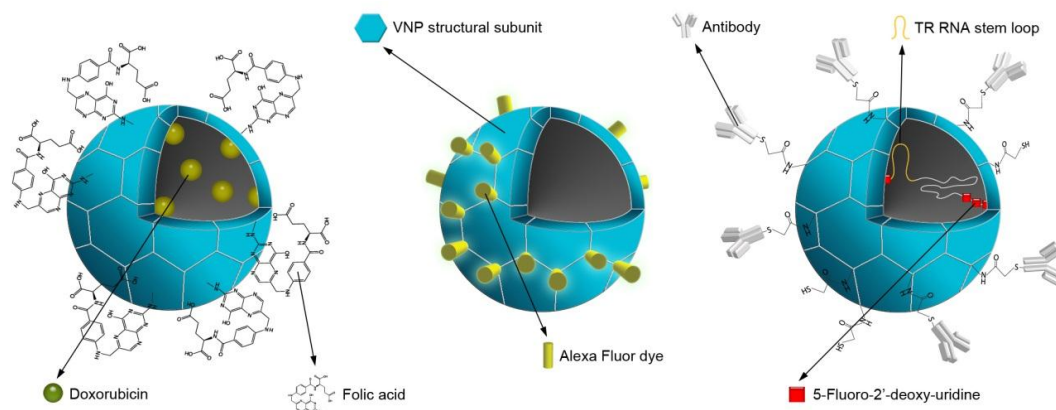


Figure 1 | Schematic representation of selected VNPs modification strategies. (left) Chemical conjugation and encapsidation for outer surface display and entrapment of small molecules (Ren, Wong et al. 2007); (center) Chemical conjugation for outer surface display of fluorophores (Lewis, Destito et al. 2006); (right) Chemical conjugation and selective encapsidation for outer surface display of antibodies and selective entrapment of nucleic acids (Brown, Mastico et al. 2002).

The cytotoxicity of such targeted VNPs was tested on breast carcinoma cells expressing the surface antigen at high levels. At lower concentrations, results showed a higher toxicity of the targeted VNPs compared to naked 5fdU containing oligonucleotides. This result supports the idea that the engineered particles enhanced the toxicity of the oligonucleotide by protecting it from degradation and by increasing the level of specificity and uptake (Brown, Mastico et al. 2002). Targeted nanoparticles are also particularly valuable for diagnostic purposes because they can increase the signal-to-noise ratio of imaging reagents by both avoiding background staining and concentrating the reporter molecule where it is required. Non-invasive imaging has an enormous potential for early detection, timely treatment and subsequent follow-up of diseases; moreover, this is also able to retrieve important information on anatomic-pathological structures, inflammation, angiogenic progression and diffusion. In a remarkable study, it has been recently demonstrated that *Cowpea mosaic virus* (CPMV) particles carrying fluorescent labels can be used for intravital vascular imaging in mouse and

chicken embryos (Lewis, Destito et al. 2006). Commercial fluorescent dyes have been successfully conjugated to these VNPs up to a density of 120 dyes per particle (**Fig. 1**), providing fluorescence intensity significantly higher than conventional vascular imaging. After injection, fluorescent CPMV derived VNPs distributed over all organs, reaching even the smallest capillaries, and thus overcoming the inadequate tissue penetration observed for common fluorescent agents. The visualization of the vasculature persisted for at least 72 hours with no visible deleterious effects (Lewis, Destito et al. 2006). This result was possible because labeled VNPs were specifically internalized by endothelial cells *in vivo* through a natural biospecific interaction mediated by the mammalian protein vimentin. Vimentin is a cytosolic protein predominantly expressed in the mesenchymal cells, even if it has been also found at high-level of expression on the surface of endothelial cells surrounding tumor tissues (van Beijnum, Dings et al. 2006). In fact, it has been shown that overexpression of vimentin in tumor endothelium correlates well with the uptake of CPMV in tumor endothelial cells of the chick chorioallantoic membrane tumor model (Lewis, Destito et al. 2006). The fluorescent CPMV were internalized through active endocytosis and were not detected outside the endothelial layer. This property is particularly beneficial to map areas involved in neovascularization, providing for instance high-resolution images of vessels entering and exiting tumor masses. Loading techniques can also be used to design hybrid VNPs with fluorescent cores for their use in advanced cellular imaging applications. Confinement of the imaging agent inside the VNPs has the advantage of leaving the external surface addressable with targeting moieties. Common strategies for live imaging within cells utilize bioconjugation techniques for the covalent attachment of imaging molecules onto the exterior surface of the particles. However, exterior surface modifications of the VNPs are typically not desired as they can alter and interfere with the natural functions of the capsid such as receptor recognition. Synthetic fluorescent quantum dots (QDs), paramagnetic materials and other metallic structures are useful for imaging

applications, and their introduction inside VNPs ensures biocompatibility, prevents aggregation, enhances stability and reduces toxicity. QDs are promising nanoscale visualization tools for biological applications, due to their long fluorescence lifetime with broadband absorption and narrow emission (Michalet, Pinaud et al. 2005). Formed as semiconductor clusters of II-VI, III-V, and IV-VI column elements, with diameters of several nanometers, QDs are emerging as a powerful class of visualization tools, even if caution should be exercised when considering *in vivo* toxicity. Recent studies on QDs in biological applications have revealed significant cytotoxicity effects (Cascio, di Martino et al. 2004), in fact oxidation of the exposed CdSe core can release Cd²⁺ ions, leading to liver toxicity. The confinement of QDs within VNPs molecular cage in order to enhance their safety has been attempted. Lommel and Franzen group using the *Red clover necrotic mosaic virus* (RCNMV) achieved functionalization of the corresponding VLPs core exploiting the viral origin-of-assembly site (OAS), a sequence that initiates CP monomer binding and promotes capsid self-assembly (Sit, Vaewhongs et al. 1998). Artificial OAS sequences have been introduced on QDs and when mixed with RCNMV CP monomers *in vitro*, this led to the self-assembly of RCNMV VLPs around the templated cores (Loo, Guenther et al. 2006). The magnetic resonance imaging (MRI) is another powerful, non-invasive *in vivo* imaging tool, which is based on the alignment of protons in a strong magnetic field. Contrast agents, such as gadolinium (Gd), are typically used to increase the brightness of the image, and hence the sensitivity of the technique. VNPs can carry several hundred of Gd³⁺ ions as they can be complexed with encapsidated RNA molecules or bound at intrinsic metal binding sites at CP interfaces (Allen, Bulte et al. 2005; Anderson, Isaacman et al. 2006; Hooker, Datta et al. 2007; Prasuhn, Yeh et al. 2007). In a recent work, paramagnetic nanoparticles have been successfully generated loading *Cowpea chlorotic mottle virus* (CCMV) VNPs with the lanthanides Gd³⁺ and Tb³⁺. CCMV protein cage offers 180 intrinsic metal-binding sites at the threefold axis. However, under physiological

conditions, Ca^{2+} ions are bound to these sites and contribute to stabilize the capsid by minimizing the electrostatic repulsion between two adjacent CP subunits (Jonhson and Spear 1997). Exploiting the physic-chemical properties of the amino acidic negatively charged groups involved in metal binding, it has been possible to replace the Ca^{2+} cations with Gd^{3+} and Tb^{3+} . Up to 180 lanthanidies can be bound, and the interaction was found to be stable under physiological conditions (Allen, Bulte et al. 2005). However, *in vivo* local high concentration of Ca^{2+} could compete with Gd^{3+} for VNPs binding, destabilizing the Gd^{3+} CCMV association with repercussions on toxicity due to the release of free Gd^{3+} . This problem could be potentially overcome using Magnevist, a strong chelate of gadolinium, most commonly used as a MRI contrast agent. Activated Magnevist was conjugated on MS2 VNPs using surface exposed lysines, resulting in the incorporation of 500 Gd-chelates per VNP (Anderson, Isaacman et al. 2006). The material properties of lanthanidies-VNP complexes have been evaluated and results showed that these formulations could be excellent candidates for further development as MRI contrast agents. Using a similar approach, the small fluorescent dye rhodamine has been infused and stably entrapped in RCNMV derived VNPs (Loo, Guenther et al. 2008). Like other plant viruses, RCNMV particles undergo structural transition and reversible surface pore opening in presence of specific pH and metal ions concentration. In the opened conformation and in presence of the RNA molecules, the small positively charged rhodamine molecules can freely diffuse into the interior cavity of the particles, where these bind to the negatively charged viral nucleic acid via electrostatic interactions. Interestingly, it was shown that pore re-opening does not release the trapped materials (Loo, Guenther et al. 2008). Most recently, VNPs have been explored as tools for positron emission tomography (PET) non-invasive imaging applications. MS2 derived VNPs have been labeled with [^{18}F]-fluorobenzaldehyde and evaluated after injection in rats. These experiments showed that while free [^{18}F]-fluoro-benzaldehyde is rapidly cleared from the circulation, [^{18}F]-MS2 VNPs can persist for at least 3 hours (Hooker, O'Neil et

al. 2008). The combination of a magnetic iron oxide core and an imaging reagent such as [^{18}F]-flfluorobenzaldehyde will be useful for specific delivery by external magnetic guidance. Another important and rapidly expanding field of nanomedicine, which could take advantage of the intrinsic properties of VNPs, is tissue engineering (**Fig. 2**).

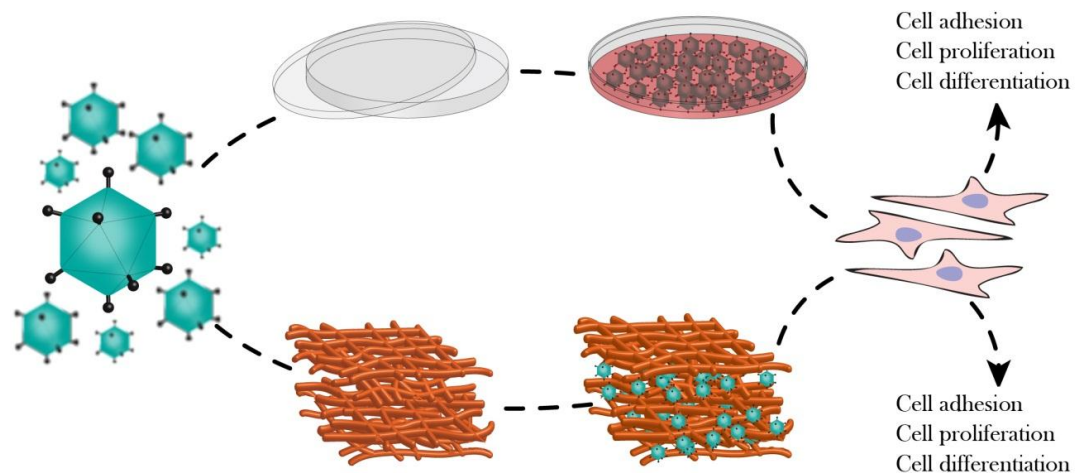


Figure 2 | Examples of tissue engineering. VNPs can be adsorbed onto supports for cell culture or embedded into 3D scaffolds displaying relevant mechano-structural properties. Cells can be cultured in the two conditions and then characterized for viability, proliferation and differentiation.

The design and synthesis of materials for tissue engineering was dominated by polymer chemists and materials scientists, however the advent of VNPs has brought the combined skills and expertise of molecular biologists, biochemists and cell biologists into the field. Initial research focused on the deposition of unmodified VNPs such as CPMV onto glass surfaces by non-specific adsorption, followed by an assessment of their ability to promote cellular growth compared to non-treated control slides (Lin, Su et al. 2008). Similar results were obtained when glass slides were coated with either the rod-shaped *Tobacco mosaic virus* (TMV) or the icosahedral *Turnip yellow mosaic virus* (TYMV) and were subsequently used as substrate for cell culture. In these cases, the functionalized supports not only improved cellular

proliferation but also encouraged bone marrow stromal cells (BMSCs) to undergo osteogenic differentiation at significantly enhanced rates compared to cells grown under standard conditions (Kaur, Valarmathi et al. 2008; Kaur, Valarmathi et al. 2010). VNPs interact with the environment primarily at the external surface and, modifying their capsid with relevant ligands, it could be possible to direct the protein cage toward specific interactions with both biological and non-biological surfaces (**Fig. 2**). An example is reported by the addressable TMV platform used by Kaur and colleagues (2010) to introduce chemical cues for differentiation, and to complement the natural biogenic properties of such VNPs. Exploiting chemical bioconjugation techniques, TMV particles were densely decorated with phosphate groups and, once embedded into biofilm, VNPs allowed Ca^{2+} ions attraction onto the tissue culture surface thus increasing calcium uptake by BMSCs. The induction of BMSCs differentiation into osteoblasts has been also demonstrated by the upregulation of several relevant markers (Kaur, Wang et al. 2010). The use of chemical ligands for tissue engineering can be complemented by genetically modified viral coat proteins to generate VNPs displaying specific peptides. In a recent work, the M13 bacteriophage was engineered to display the extensively studied RGD and IKVAV peptide sequences on its surface. M13 derived VNPs displaying cell binding motifs were deposited in parallel arrays on solid supports and enabled directionality growth of neural progenitor cells (Merzlyak, Indrakanti et al. 2009). The presentation of multiple growth factors will be necessary to accurately mimic the extracellular matrix and activate stem cell differentiation; VNPs can be modified in many ways, both chemically and genetically, indeed such nanoscale platforms may in the future offer a unique template to control tissue differentiation. When developing novel materials for nanomedicine, although VNPs offer clear advantages over synthetic nanomaterials primarily because they are biocompatible and biodegradable, it is essential to understand their *in vivo* properties, particularly any potential toxic effects. Due to their nature, VNPs derived from bacteriophages and plant viruses are

considered to be much safer for human administration, because humans are not their natural hosts. This supposition has been also supported by recent studies evaluating the biodistribution, pharmacokinetics and potential toxicity of CPMV, CCMV, Qb and M13 nanoparticles in mice. In all cases, VNPs were detected in a wide variety of tissues throughout the body of the animals, but there was no apparent toxicity despite broad biodistribution (Gatto, Ruedl et al. 2004; Srivastava, Kaido et al. 2004; Singh, Prasuhn et al. 2007). Besides these considerations on the safety of unmodified VNPs, when synthetic materials are combined with such biocompatible VNPs to develop hybrid systems, it is also fundamental to determine the pharmacological properties of the hybrid materials and evaluate potential toxic side effects, as these may differ from those of the individual components. Furthermore, immunogenicity is desirable for development of vaccines, but it reduces the efficacy of nanomaterials employed in those nanomedicine applications where the function is directly carried out by VNPs themselves. In these cases, the elicitation of an immune response against the VNPs is not desirable and for that reason efforts have been made to shield VNPs from the immune system. The most popular approach is the attachment of polyethylene glycol (PEG) chains, a non-toxic, non-charged and hydrophilic polymer, to the external surface of the nanoparticles. This method, also known as PEGylation, has been shown to be effective by reducing the biospecific interactions and immunogenicity of VNPs while increasing plasma circulation time and stability (Raja, Wang et al. 2003; Lewis, Destito et al. 2006; Steinmetz and Manchester 2009). As a matter of the fact, an appropriate balance between tissue penetration and systemic clearance is required because the optimal balance is expected to differ for therapeutic VNPs and those designed as imaging tools. Therefore, longer circulation times allow drugs and reagents to accumulate in target tissues, but the risk of toxicity and increased background noise in imaging applications is higher. Clearly, design of the ideal nanoparticle vector is an extremely challenging task, and it should be handled on a case-by-case basis to satisfy the

requirements of the specific application field. In medicine, VNPs have been applied in diagnostic assays, as vaccines, imaging modalities, and targeted therapeutic devices. In conclusion, this area of research shows great promises, and the next phase of investigation will necessitate of a more detailed understanding of the *in vivo* performance of VNPs and their hybrid assemblies.

Applications of VNPs in material synthesis

From a materials science point of view, VNPs are incredibly interesting as they can be produced easily and in high yields, they are robust and stable, and notably they are able to self-assemble in monodispersed nanometer-sized particles, maintaining precision in assembly of each molecular unit. VNPs contain potentially two surfaces that can be exploited for a stable functionalization: the exterior capsid surface and the interior core. For icosahedral particles, the interface between adjacent coat proteins is another possible target, however this is addressable only for leaky interactions and thus it was not used so far. The critical factor in the development a biodirected self-assembly approach for material science is the identification of the appropriate compatibilities and combinations of biological with inorganic materials. At the base of such challenge lays the full-understanding and the controlling of the building block properties and interactions. In recent years, researchers employing VNPs for material synthesis seek to adapt the natural properties of virus coat proteins to allow the encapsulation of artificial cargos. Therefore, virus structures are now considered as nanocontainers and they are used to encapsulate synthetic nanomaterials. Loading of exogenous materials can be achieved through different strategies pointing to reversible structural transition of the viral cage, usually referred to as gating mechanism, or to the *in vitro* disassembly/re-assembly of the entire particle. Once inside the interior cavity, the compound of interest can be covalently attached to addressable amino acids on the interior surface of the capsid, or retention can be achieved exploiting the interactions with the

encapsidated genome. In the latter case, only small positively charged molecules or molecules with natural affinity for nucleic acids can be stably entrapped, and these interactions are typically non-covalent. On the other hand, *in vitro* self-assembly mechanisms can be successfully exploited to selectively entrap larger exogenous materials, otherwise unable to reach the core of the nanoparticles throughout the viral gated pores. By this strategy, VNPs are disassembled into respective CP monomers, which are then mixed with the molecules of interest and re-assembled. Besides using the well-understood gating mechanism of viruses such as CCMV or RCNMV (Tama and Brooks 2002; Loo, Guenther et al. 2008), the *in vitro* self-assembly mechanisms can also be employed for selective encapsidation of artificial nucleic acid or negatively charged polymers. Naturally, the *in vivo* self-assembly of VNPs is initiated by subtle electrostatic interactions between genome and the CP subunits. The basic principle by which the nucleic acid assists and stabilizes particle formation has been exploited by mixing CP monomers with negatively charged compounds. In this process, also referred to as templating, capsid assembly is initiated via electrostatic interactions and results in VLPs encapsulating the artificial cargo (Sikkema, Comellas-Aragones et al. 2007; Hu, Zandi et al. 2008). Attempts to encapsulate neutral molecules such as fluorescein-labeled dextran failed, demonstrating that encapsidation is based on electrostatic interactions between the negatively charged polymers and the positively charged interior of the capsid proteins (Ren, Wong et al. 2006). Furthermore, several studies demonstrated that core particle sizes are directly correlated with the formation of VLPs differing in both dimensions and symmetries. In general, VLPs assembled from smaller cores are smaller than those assembled from larger cores. However, despite the flexibility and dynamic properties of viral coat proteins, it has been observed that VLPs do not assemble when the templating core provided is larger than the inner diameter of viral cage. Therefore, attempts to self-assemble RCNMV VLPs around a 20 nm gold core were not successful because, while the RCNMV capsid has an exterior diameter of 36 nm, the

interior cavity diameter is only 17 nm in length (Sherman, Guenther et al. 2006). In a more accurate study of Sun and colleagues (2007), the effect of VLP size and symmetry was systemically evaluated by using carboxylate-terminated PEG-coated gold cores of 6, 9, 12, 15 and 18 nm. When purified BMV CP monomers were independently incubated with templating cores of such dimensions, the most efficient encapsulation occurred with gold cores with a diameter of 12 nm, yielding VLPs similar to wild-type particles and with an high degree of homogeneity. As a result, BMV CP monomers mixed with smaller gold cores assembled into smaller VLPs, while VLPs assembled from larger gold cores resulted in larger structures (Sun, DuFort et al. 2007). Interestingly, tiny nanoparticle cores, which typically yield smaller VLPs, can be contained in multiple copies within the generated VLPs. For instance, self-assembly of VLPs around 4 nm-sized PEG-carboxylate-coated QDs yielded VLPs resembling *pseudo* $T=2$ symmetry and that, in the majority of cases, contained two or three QDs (Dixit, Goicochea et al. 2006). These data suggests that filling of the inner core is a fundamental prerequisite not only to confer stability during particle assembly but also to preserve the macromolecular organization. The exploitation of naturally occurring protein structures such as VNPs for synthesis of materials is referred to as biotemplating, a process that mimics the natural biomineralization by which, in living organism, proteins orchestrate the formation of complex inorganic structures with high level of control (Hildebrand 2008; Kroger and Poulsen 2008). Efforts have been made toward employing VNPs as scaffolds or templates for inorganic materials synthesis; therefore, nanocrystals can be specifically nucleated and grown on the surface of VNPs. Also the inner core of VNPs can be utilized as a constrained reaction vessel for controlled synthesis of monodisperse nanocrystals. In this circumstance, precursor materials diffuse into the interior cavity of assembled VNPs, where nucleation and mineralization of the material takes place leading to the synthesis of inorganic nanocrystals. In this context, virus size and shape play an important role as these physical properties determine the size and shape of

nanocrystals being grown. The first efforts to utilize VNPs for material synthesis were carried out about fifteen year ago, when CCMV VLPs were employed as size-constrained reaction vessels for mineralization of the polyoxometalate species paratungstate and decavanadate (Douglas and Young 1998). The pH-dependent gating mechanism of CCMV were exploited to load the aqueous molecular precursors into the particles being in swollen conformation, then by lowering the pH two different effects were coupled: the reversal structural transition of the CCMV cage from the swollen form to the compact form, and a pH-dependent oligomerization of the inorganic polyoxometalate species, which were readily crystallized as well-defined sized ammonium salts (Douglas and Young 1998). This mineralization reaction was electrostatically driven and occurred only at the interior surface of the capsid. The CCMV core is highly positively charged and thus provides an interface for the negatively charged paratungstate and decavanadate anions nucleation via electrostatic interactions. These principles can be extended to generate a range of materials within the CCMV cage, with the only requirement that the precursors are negatively charged. However, the potential of using VNPs as templates stays in the possibility to modify their charge properties by using genetic engineering. It was demonstrated that by altering the interior surface charge of CCMV particles from cationic to anionic, the resulting VNPs favored the encapsulation of cationic species (Brumfield, Willits et al. 2004). A CCMV mutant bearing negatively charged amino acids in place of all the basic residues on the N-terminus of the CP was produced. The resulting particles thanks to the electrostatic alterations favored strong interaction with ferrous (Fe^{2+}) and ferric (Fe^{3+}) ions, leading to sized-constrained formation of iron oxide (Fe_2O_3) nanoparticles within the viral cage. Rod-shaped TMV particles and filamentous M13 phages have been extensively used as templates for the synthesis of semiconducting tubes and wires for potential applications in the next-generation electronics. The versatility of TMV as a biotemplate for fabrication of a range of nanotubular inorganic materials via metal deposition has been largely demonstrated. The

exterior and interior capsid surface can be regarded as two chemically distinct environments, and thus each of them is exploitable for nucleation of materials. In particular, amino acid side chains on the interior surface are predominantly carboxylic acids conferring a general negative charge under physiological conditions. Conversely, the exterior surface exhibits positive charge at around pH 7.0 due to the significant number of Lys and Arg side chains (Namba and Stubbs 1986). These different surface properties of the exterior and interior surface have been exploited to allow spatial and controlled deposition of metals. Nobile metals such as platinum, gold, and silver have been deposited on TMV to form metallic TMV nanotubular composites (Dujardin, Peet et al. 2003; Bromley, Patil et al. 2008). These results have been achieved by electroless deposition, in which the VNPs were exposed to a metalization bath containing metal ions and a reductant. Platinum and gold coatings were found on the exterior surface while silver nanoparticles were incorporated within the central 4 nm wide channel (Dujardin, Peet et al. 2003). The differential nucleation observed was explained by the opposite charge between the interior and exterior capsid surfaces. In fact, when a TMV mutant with reduced interior anionic charge was produced and exposed to silver precursors and reductants, nucleation events occurred preferably on the exterior versus the interior virus surface. Although all these data confirm that surface charge and electrostatic interaction are the key factors in the mineral deposition mechanism, the Belcher's research team has developed a more sophisticated technology to specifically bind and nucleate inorganic materials without requiring the precise understanding of the molecular mechanism. Phage display screening technology settles on the same approach traditionally used by pharmaceutical industry to identify specific peptide motif having high degree of affinity for biological targets (Cabilly 1999; Cesareni, Castagnoli et al. 1999). A combinatorial M13 phage library expressing random peptide fusions is synthesized, the virus library is exposed to a substrate and positive binding interactions of the fused peptides are allowed to occur. To ensure specific

binding to the substrate, the virus interactions are challenged by washing with detergents, thus only the successful binding viruses are isolated by disrupting the binding conditions. Finally, viruses being positive to target recognition undergo sequencing, and the identity of the genetically encoded peptides responsible for binding to the inorganic target is determined. The peptides can be engineered into the M13 minor pIII protein and thus be displayed onto the capsid end structure or, alternatively, they can be fused with the major CP pVIII and hence be displayed along the virus body. When the appropriate metal precursors are added to induce the nucleation, in the former case a crystal is obtained selectively at the end structure of the phage (Lee, Mao et al. 2002), whereas crystal growth throughout the virus body and highly oriented nanowires synthesis are observed in the latter circumstance (Mao, Flynn et al. 2003). The phage display technology also allowed the synthesis of heterostructures by expressing dual peptides. When M13 CVPs, displaying peptides specific for ZnS and CdS as pVIII fusion, were incubated with both Zn(II) and Cd(II) in the presence of sulfide anions, the particles nucleated both nanocrystals on the same phage and with a stochastic distribution (Mao, Flynn et al. 2003). Multifunctional M13 particles can also be produced by introducing different peptides in several locations of the same phage. For instance, M13 construct expressing a gold-binding peptide along the virus body and an anti-streptavidin peptide at the phage end structure has been produced (Huang, Chiang et al. 2005). The gold-binding peptide facilitated metallization with streptavidin-coated gold nanoparticles, while the streptavidin peptide allowed self-organization into macromolecular structures via interaction with adjacent gold-decorated particles. In order to be employed in functional devices, these functionalized VNPs must be incorporated into other materials, immobilized onto solid supports, or ordered into films or arrays. The potential of VNPs building blocks for manufacturing battery electrodes has been shown (Nam, Kim et al. 2006; Nam, Wartena et al. 2008; Lee, Yi et al. 2009). Besides initial studies focused on the development of cobalt-oxide-based battery electrodes, research has

turned toward using iron-phosphate-based materials. Utilizing M13 platform, multifunctional VNPs able to serve as a template for anhydrous FePO_4 growth throughout the virus body were generated; the minor CP pIII was further engineered to have binding affinity for single-walled carbon nanotubes (SWCNTs) and thus to allow network formation. Carbon nanotubes with their high aspect ratio and highly conducting properties were expected to lead to efficient movement of lithium ions through the porous matrix. The biomolecular recognition and attachment to conducting SWCNT networks created efficient electrical nanoscale wiring, enabling high-power performance. These electrodes were assembled and tested, showing high and stable capacity. Finally, the functionality of such M13-based electrodes was demonstrated in a lithium-ion battery powering a green LED (Lee, Yi et al. 2009). More recently, various approaches that address VNPs as building blocks for the construction of arrays have been attempted. A range of VNPs have been utilized as construction material to fabricate 1D and 2D arrays as well as multi-layered arrays. From a multi-dimensional point of view, a rod-shaped VNP can be regarded as a line and thus has 1D. Similarly, an icosahedral VNP, which can be regarded as a simple point in a 3D space, could also be referred to as a 1D structure when the functional groups on its surface are considered. In material science robust, monodisperse, and highly ordered nanofibers find applications, especially in nanoelectronic devices, where could be used to interconnect different electronic components. The rod-shaped VNPs with their high aspect ratio are excellent building blocks for the fabrication of such structures. Rods can be self-assembled both end-to-end, thus forming nanowires, or side-to-side to generate bundles. In the case of TMV, head to tail self-assembly can be spontaneously induced when exposing particles to acidic conditions. The head-to-tail alignment is favored as in this conformation repulsion between the carboxylic acid residues at assembly interface is minimal. When such structures are mineralized, a continuous metal coat bridging two or several TMV particles is formed (Shenton, Douglas et al. 1999). Continuous wires can also be synthesized in

the interior channel of the aligned rods (Knez, Bittner et al. 2003). In addition to the natural end-to-end conformation, assembly of TMV in organized macromolecular structures can be assisted and stabilized by aniline, an aromatic amine. This molecule binds to TMV via electrostatic interactions and hydrogen bonding, leading to the formation of a thin layer onto the virus surface through its polymerization. This *in situ* polymerization stabilizes and fixes the spontaneously formed head-to-tail structures, allowing fabrication of fibers with length up to 10 μm . By varying the pH, hydrophobic interactions between the polyaniline can be induced, promoting parallel alignment of such head-to-tail TMV assemblies, hence forming bundles (Niu, Bruckman et al. 2007; Wang, Niu et al. 2008). Multi-layered architectures are indeed of growing interest for the development of miniaturized sensors, reactors, and biochips and their assemblies can be achieved via layer-by-layer (LbL) deposition technique. LbL method grounds on multi-layered structures are self-assembled one layer at a time, interconnecting the layers through biospecific or electrostatic interactions. For instance, multi-layered thin films of CCMV and CPMV have been constructed using the biotin-streptavidin system (Suci, Klem et al. 2006; Steinmetz, Bock et al. 2008). To achieve this, biotinylated VNPs are immobilized on a solid streptavidin-coated support. Subsequently streptavidin is added and a second biotinylated VNP layer can newly be deposited. This process strictly depends on the tetrameric arrangement of the streptavidin, offering four binding sites for biotin, as well as on the multivalency of VNPs. The deposition cycle can be repeated until the desired number of VNP layers is obtained. The mechanical properties of the CPMV arrays have been finely tuned by adjusting biotin spacer length and density before VNPs bioconjugation. Steinmetz and colleagues (2008) demonstrated that a more regular and densely packed array was assembled when CPMV particles displayed a high number of biotin labels attached via longer linkers. In contrast, the formation of a viscoelastic array with less dense particle packaging was implied when CPMV particles displayed a low number of biotins attached via shorter linkers (Steinmetz, Bock et al. 2008).

In conclusion, the coat proteins of VNPs can be regarded as remarkably flexible, tunable, and programmable building blocks. Cargo can be entrapped using different strategies, the coat proteins itself can be chemically modified via bioconjugation, and the particles can be self-assembled. A variety of techniques have been developed allowing the fabrication of VNPs structures including bundles and wires, films, and multilayered arrays leading toward 3D structures. To date, there is no comparable synthetic material that allows this degree of flexibility, underlining the potential of VNPs for a variety of application that rely on their precise self-assembly.

Tomato bushy stunt virus

Tomato bushy stunt virus (TBSV) is the type member of the genus *Tombusvirus*, which in turn is considered the prototype genus of the large *Tombusviridae* family. The genus comprises several species showing a narrow natural host range, which is restricted to dicotyledonous plants, and a limited geographic distribution. TBSV represents an exception, it is widespread indeed, and causes economically important disease in several crops (Thresh 1982). The virus was described for the first time in 1935 in tomato plants (Smith 1935) and, since that date, epidemics in field- as well as greenhouse-grown tomato crops have been reported around the world (Gerik, Duffus et al. 1990). Symptoms induced by TBSV in tomato plants include severe stunting and bushy growth, deformation and appearing of chlorotic spots on young leaves, conspicuous darkening and veinal necrosis of older leaves. Despite the general symptoms are observed among all the susceptible hosts during TBSV infection, each plant can react differently depending on genetic background. In addition to the TBSV strains deriving from tomato plants, many other strains of TBSV have been isolated worldwide from diverse crops, and all these have been demonstrated to be serologically related at varying degree. The taxonomy of the genus *Tombusvirus* has been based on serology and resulted in unsatisfactory classification of the numerous isolates; nevertheless, differences between the symptoms induced in tomato crops by the various TBSV strains are usually not observed (Luis-Arteaga, Rodriguez-Cerezo et al. 1996). TBSV, and more in general the tombusviruses, are among the most extensively studied messenger sensed RNA plant viruses. These studies have made possible a deep understanding of the molecular biology of tombusviruses' infection cycle.

The Genome - ORFs and replication

As a member of the genus *Tombusvirus*, the TBSV genome is constituted by a unique molecule of single stranded sensed RNA that is approximately 4.8 kb in length. Interestingly, although the genome is messenger-sensed, it lacks of both 5'-cap and 3'-poly(A) while bears two highly conserved sequence at both terminal ends of the RNA molecule (Russo, Burgyan et al. 1994). Five open reading frames (ORFs) are encoded between the two untranslated regions (UTRs) located at the 5' and 3' portion of the viral genome. The 5'-proximally encoded ORFs are p33 and p92, which share the initiation codon and thus overlap partially in the same reading frame: these represent the RNA-dependent-RNA-polymerase (RdRp) and are both essential for viral RNA replication (Scholthof et al. 1995; Oster, Wu et al. 1998). The p41 ORF is positioned just downstream of p92 and encodes for the viral CP, the monomeric subunit which self-assembles in number of 180 copies into the TBSV capsid (Russo, Burgyan et al. 1994). Finally, the last two ORFs, p22 and p19, are proximally located upstream the 3'UTR: these have overlapping sequences but in different reading frames, thus resulting into two distinct proteins involved in viral cell-to-cell movement and suppression of gene silencing respectively (Voinnet, Pinto et al. 1999; Qiu, Park et al. 2002; Qu and Morris 2002). RNA replication is a central step in the infectious cycle of TBSV and it has been demonstrated to be a multistep process (**Fig. 3**) (Buck 1996). It first requires the translation of the RdRp proteins (p33 and p92) from the genomic RNA and their localization into the cellular replication sites, which are probably identified as the membranous multivesicular bodies (Burgyan, Rubino et al. 1996). The full-length antisense-strands are first synthesized by the viral replicase proteins and subsequently these will serve as templates to generate large numbers of sensed strand RNAs; part of the progeny genomes just generated are re-introduced into additional rounds of replication, thus enhancing the exponential amplification of the sensed strand RNA synthesis (**Fig. 3**).

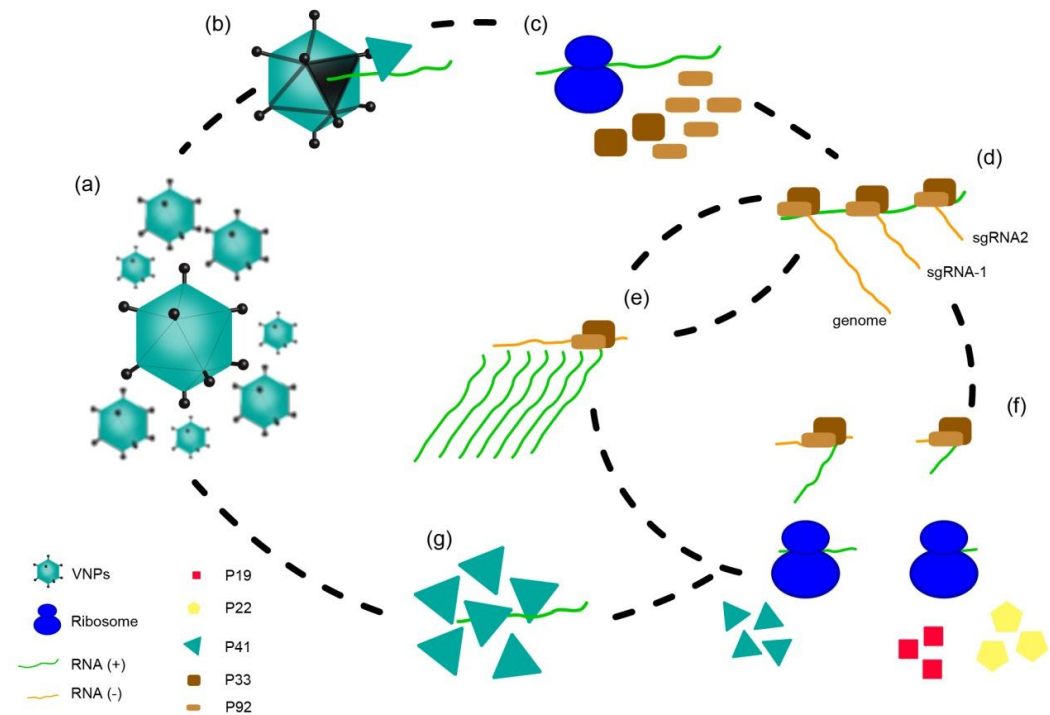


Figure 3 | Schematic representation of TBSV infection cycle. (a) Virions in native compact form. (b) Once the virus enters the plant cytoplasm, it undergoes several capsid structural modification leading to release of RNA genome. (c) The sensed genome is translated by cellular ribosomes into viral replicase proteins p33 and p92. (d) The active replicase protein complex (RdRp) starts viral transcription into anti-sensed full-length genomes and two sub-genomic RNAs. (e) The anti-sensed full-length RNA molecule is used as a template to transcribe the infectious genome, which in turn can be re-introduced in additional round of replication. (f) Meanwhile, the two sg-RNAs are transcribed into sensed messenger and translated by the cellular machinery into p41, p19 and p22. (g) When the right amount of CP and genome is produced, capsid starts to assemble around the RNA molecules and a new mature TBSV progeny is generated.

In general, it has been observed that overall RNA production is asymmetrical, leading to up to 100-fold excess of sensed strand RNA over the antisense-strand progeny. Besides its protein coding function, TBSV viral RNA is also directly involved in genome replication thanks to the action of *cis*-acting RNA elements. These RNA elements, including both replication's enhancers and silencers, which can stimulate sensed stranded RNA synthesis (Nagy, Pogany et al. 1999; Ray and White 1999; Pogany, Fabian et al. 2003) or can inhibit antisense-strand RNA production (Chang, Borja et al. 1995) respectively, are involved in the modulation of the efficiency of primer-independent initiation from the promoter elements. As a result of a great

number of studies about the role of these RNA sequences and secondary structures, it is becoming increasingly clear that mechanisms aimed to fine control the several steps of TBSV replication cycle relying on diverse and complex inter- and intra-genomic interactions.

Proteins - function and synthesis

Unlike most other RNA viruses, the synthesis of TBSV proteins has been found to involve an atypical translational mechanism related to the uncapped and non-polyadenylated nature of its genome. In eukaryotic cells, to achieve an efficient translation, the mRNA requires both 5'- and 3'-terminal structures; the 5'-cap is involved in binding the translation initiation factor, leading to the recruitment of ribosomal components (Kozak 1989), whereas the 3'-poly(A) is involved in head-to-tail interaction and circularization of the messenger (Gallie 1998). Studying *in vivo* the translational process by using various TBSV-derived mRNAs has revealed the presence of a 3'cap-independent translational enhancer (3'CITE) sequence, which can functionally mimic the translational recruitment activity of the 5'-cap through the formation of important RNA secondary structure (Wu and White 1999). Interestingly, once the translational machinery is recruited to the 3'CITE, this is delivered to the start codon at the 5' end of the viral message by means of specific RNA-RNA base pairing interaction between the translational enhancer and the 5' UTR. Moreover, the formation of kissing loops would act to circularize the viral messenger, analogously to the protein-mediated circularization of eukaryotic cellular mRNAs (Guo, Allen et al. 2001). The first proteins synthesized during the infection cycle of the TBSV are those that can be directly translated from the genome: p33 and p92. The two replication proteins are required simultaneously to trigger viral RNA synthesis, and they are accumulated within the cell at a relative ratio of 20:1 (p33:p92) (Panaviene, Baker et al. 2003). The different concentration between the two proteins can be explained throughout the mechanism at the base of their translation; in fact, p92 is translated from the genome by readthrough of a

leaky p33 termination codon, a process has been estimated to occur *in vivo* at rate of about 5% (Scholthof et al. 1995). Despite the lower cytoplasmic concentration, the p92 has been identified as the only active RdRp, while the role of p33 seems to be related to the assembly of the viral replicase/RNA template complex, and to the targeting of the viral RNA and of the RdRp itself to the sites of replication. Therefore, sequence analysis has revealed a single conserved RdRp motif within the readthrough region of p92, and an RNA-binding domain localized in the p33 C-terminal region (Russo, Burgyan et al. 1994; Rajendran and Nagy 2003). Because of the nature of the eukaryotic translational machinery, which generally accesses start codons by scanning from the 5' end of an mRNA, and, on the other hand, the polycistronic information indeed delivered by the TBSV genome, the expression of the 3'-proximal ORFs (p41, p22, and p19) requires the transcription of additional viral mRNAs, termed subgenomic (sg) mRNAs (Miller and Koev 2000). Also in this case, TBSV employs an unusual mechanism for synthesis of the sgRNAs involving both *cis*-acting RNA elements and viral proteins. Recent studies have revealed that triggering of sgRNA transcription involves a series of long-distance RNA-RNA base-pairing interactions (Zhang, Slowinski et al. 1999; Choi, Ostrovsky et al. 2001; Choi and White 2002), resulting in a secondary structure-mediated premature termination mechanism (White 2002). The model predicted suggests that antisense-strand synthesis is terminated prematurely to generate smaller antisense-sgRNAs, which then serve as templates for the transcription of sensed viral sgRNAs. As a result, two sgRNAs are transcribed during TBSV infection in a temporally coordinated manner. This sequential appearance of the sgRNAs acts as the primary mechanism to regulate the timing of production of 3'-encoded products. TBSV protein expression profile provides first the translation of the replication proteins, to achieve copy amplification of the genome and to transcribe sgRNAs, then the suppression of the host gene silencing system and invasion of adjacent cells, and finally the encapsidation of the genome progenies. Therefore, the smaller

sgRNA-2 delivering the information of both p22 and p19 is produced first. Whereas p22 ORF is directly translated over the sgRNA-2, p19 expression requires a leaky scanning event occurs. This process involves bypass of an upstream start codon by a scanning ribosome and its initiation at a second downstream start codon. During plant infection, TBSV needs for the membrane-associated p22 movement proteins to transfer the newly synthesized genomic RNA progeny into the adjacent not yet infected cells (Scholthof et al. 1995). Subsequently to the first rounds of genome replication, the p19 gene silencing suppressor protein becomes essential for TBSV to establish an efficient plant systemic invasion (Qiu, Park et al. 2002; Qu and Morris 2002). P19 explicates its function by binding to and sequestering the small interfering RNAs, which are produced by plant cells as a defensive response to viral infection; the gene silencing suppressor is fundamental for persistent infections and to accumulate large amount of TBSV progeny. Later in the infection, the larger sgRNA-1 is transcribed and directs translation of p41, the CP (Hillman, Hearne et al. 1989). TBSV encodes for a single CP subunit of about 41 kDa that assembles following a $T=3$ icosahedral symmetry into a spherical particle with a diameter of about 30 nm in length. X-ray single-crystal diffraction experiments performed by Harrison and Olson (1978) have elucidated the three-dimensional structure of TBSV and a model at 2.9 Å resolution is now available (Harrison, Olson et al. 1978; Olson, Bricogne et al. 1983). Tertiary structure of the TBSV-CP subunit consists of 3 domains: *i*) the N-terminus comprises the internally located random domain (R) which is thought to interact with viral RNA by means of positively charged amino acids; *ii*) a connecting arm links the R-domain to the internal surface of the capsid shell (S) domain, which in turn is connected through a four-residue hinge to the *iii*) carboxyl protruding (P) domain, projected outward from the assembled protein cage (Olson, Bricogne et al. 1983). Besides the well characterized three-dimensional structure of TBSV capsid, which provides shield to the enclosed genome during virus environmental spread, the real role of the CP during the infection cycle is not

yet understood. Studies have shown that CP is not required for either cell-to-cell spread or systemic invasion in hosts, but both types of movement are delayed in its absence (Scholthof, Morris et al. 1993), suggesting that assembled virions are probably important for the effective unloading of viruses from the vascular system into the leaf mesophyll.

Plant molecular farming

The recombinant production of biopharmaceuticals, industrial enzymes and functional secondary metabolites in plants is referred to as plant molecular farming (PMF). Since the first recombinant plant-derived pharmaceutical protein was produced (Sijmons, Dekker et al. 1990), there have been a great number of technological developments on many levels (Twyman, Stoger et al. 2003), and proof of concept has been established for the production of many therapeutic and prophylactic proteins, including antibodies, cytokines, growth factors, hormones, recombinant enzymes and human as well as veterinary vaccines (Twyman, Schillberg et al. 2005). Twenty three years on, attention has shifted from basic research towards commercial exploitation, as PMF is expected to challenge already established biopharmaceutical production technologies. The increasing market demand causes pressure for cost-effective alternatives for bulk manufacturing of pharmaceutical molecules, and in recent years PMF has demonstrated to represent a safe and profitable choice. Definitive confirmation of PMF potential was set in the second half of 2012, when the U.S. Food and Drug Administration (FDA) approved "Elelyso", the first plant-made pharmaceutical product obtaining marketing authorization (Sheridan 2012). ElelysoTM, the commercial name for taliglucerase- α , is a recombinant active form of the β -glucocerebrosidase, a lysosomal glycoprotein enzyme that catalyzes the hydrolysis of the glycolipid glucocerebroside to glucose and ceramide (Fabrega, Durand et al. 2002). ElelysoTM, today approved only in its injectable form, has been indicated for long-term enzyme replacement therapy for adults with a confirmed diagnosis of Type 1 Gaucher's disease. This is a rare genetic disorder in which individuals fail to produce the enzyme glucocerebrosidase, causing the most common form of lysosomal storage disease. The disorder is characterized by a dysfunctional metabolism of sphingolipids, which accumulate particularly in white blood cells, but also in all organs and tissues, eventually leading to liver and spleen damage (Levy, Or et al. 1991). Replacement therapy with ElelysoTM prevents lipids from accumulating and reduces all the associated

symptoms. Taliglucerase- α is produced by *Protalix BioTherapeutics*, an Israeli biopharmaceutical company that is focused on the development and commercialization of novel as well as biosimilar recombinant proteins through its licensed plant cell-based expression system. The plant cell platform is based on carrot and tobacco cell cultures technology, and it is able to synthesize recombinant proteins with a glycan and amino acid structure similar to naturally produced human counterparts. Protalix provides stable and optimized conditions for biotherapeutics production, maintaining low manufacturing costs thanks to the novel bioreactor system based on disposable plastic bags. As a result, ElelysoTM is priced at a 25% discount compared to Genzyme's Cerezyme, the market leader product for treatment of Gaucher's disease, thus undermining its leadership (Sheridan 2012). Traditionally, proteins have been produced using complex production systems such as bacteria, yeast, cultured mammalian and insect cells, and eggs. Plants are one of the world's most cost-effective protein producers and their exploitation for therapeutic commercial applications has several advantages. Plants lack human pathogens, oncogenic DNA sequences, prions, endotoxins, and indeed their use as bioreactors for biomedicine applications presents no biological hazard (Commandeur and Twyman 2004). However the main advantage is retained in the potential for very large-scale production. Greenhouse-based manufacturing facilities conditions can be quickly built for rapid and economic scale-up in order to meet market demands. Furthermore, growing plants in the field provides opportunities for virtually unlimited production. The easy system scalability makes possible to shift from laboratory to industrial production without an exponential increase of costs, typically related to fermentation technologies. From the industrial perspective, one of the driving forces behind PMF is the low initial investment required when compared with mammalian cell culture production (Bischoff 2004; Maliga and Graham 2004). Moreover, it has been estimated that proteins can be produced in plants at 2-10% of the cost of microbial fermentation systems and at 0.1% of the cost of mammalian cell

cultures or transgenic animals, as long as adequate yields can be achieved (Hood, Woodard et al. 2002). However, the production cost in the agricultural field constitutes only a fraction of the whole costs of a plant-derived pharmaceutical. When choosing a plant expression system all the downstream processes, ranging from good manufacturing practice requirements to quality control for approval, should be taken into account, as these represent a substantial proportion of the total cost of the final product. Furthermore, to provide efficiency, safety and stability of the final transgenic product a high level of protein purification is essential. When a PMF model is proposed as a substitute of a consolidated production system, expression stability and the biochemical activity of the final product are fundamental issues. A remarkable successful example comes from *Medicago Inc.*, a biopharmaceutical company developing novel vaccines and therapeutic proteins to address a broad range of infectious diseases. The company has demonstrated to be a worldwide leader in the development of recombinant vaccine antigens in plants through its proprietary VLPs and manufacturing technologies (Vezina, Daoust et al. 2011-05-01). Compared with traditional egg-based and cell production systems, plants are uniquely capable of efficient protein expression at very high yields. Medicago has reported positive results from its Phase II clinical trial with its avian flu H5 pandemic vaccine candidate. The vaccine was found to be safe, well tolerated and also to induce a solid immune response (Landry, Ward et al. 2010). In this light, Medicago and Philip Morris Products signed a commercial agreement in September 2012, granting the latter an exclusive license to develop, commercialize and manufacture Medicago's pandemic and seasonal influenza vaccines for the chinese market. Differently from current influenza vaccines, which are manufactured with an inactivated virus, Medicago's VLP-based antigen presentation vaccines consist only of protein shells made to look like viruses. As such the macromolecular structure allows them to be recognized readily by the immune system, however they lack the core genetic material and thus are unable to replicate (Vezina, Daoust et al. 2011-05-01).

Medicago has developed a proprietary high-throughput platform that accelerates enormously the discovery and development of new vaccines by rapidly expressing, purifying and testing candidate VLPs. Typically, from the identification of a new influenza strain it takes up to six months before the first dose of vaccine is produced in fertilized eggs, whereas Medicago's plant-based technologies potentially provide the best VLP-based vaccine within only a few weeks (D'Aoust, Couture et al. 2010). As a matter of fact, in January 2013 Medicago has been awarded a contract from the U.S. Department of Defense, obtaining to be listed as a company meeting all technical requirement standards for potential future manufacture and delivery of certain tobacco-produced proteins. Another important advantage of plants is the range and diversity of recombinant molecules that they can potentially produce. As higher eukaryotes, plants are preferred over prokaryotic hosts for the expression of recombinant proteins because most protein maturation events such as folding, disulfide-bond formation, and glycosylation are similar in mammals and plants (Frigerio, Vine et al. 2000; Ma, Drake et al. 2003). However, fundamental variations still remain in post-translational modifications making sometimes mammalian cell cultures a forced choice. PMF requires that DNA encoding the protein of choice is introduced into the plant and, thus far, multiple methods of human-directed foreign DNA transfer have been developed. The first strategy used to express stably genes in plants involves the delivery of the heterologous sequence of interest into the plant nuclear system. The major disadvantage associated with this technology is the unpredictability; unnecessary DNA insertions, deletions or re-arrangement of inserted genes within the chromosomes may occur, leading to variable and difficult to predict expression levels. In addition, expression performance of plant transformation techniques across different plant species is difficult to judge, because the same regulatory sequences may have a different intrinsic level of activity and specificity depending on the genetic background (Inaba, Zhong et al. 2007). Moreover, transgenic approaches require long development times and this aspect

represented an obstacle not only for their progress but also for technical improvements. For all these reasons, nowadays transient expression systems involving viral vectors or binary systems delivered by *Agrobacterium Tumefaciens*, are preferred to stable plant transformation. Transient delivery of heterologous gene is considered an effective way of obtaining adequate quantities of recombinant product in a very short time (Cramer, Boothe et al. 1999; Roggero, Ciuffo et al. 2001) and makes the expression of multiple genes in the same plant easier (Koprowski 2005). Comparing the overall yield that can be achieved by using *A. Tumefaciens* DNA transfer technique or virus based system, it has been demonstrated that the latter is more efficient as viruses can spread to all cells, thus enhancing product accumulation. Plant viral vectors are promising tools for the synthesis of pharmaceuticals (Pogue, Lindbo et al. 2002) because plant viruses are not infectious in humans or animals, they are able to synthesize large quantities of heterologous proteins inhibiting the host defensive mechanisms and, as the genes are not incorporated into the plant genome, they do not form a heritable trait. Besides the full viral genomes utilization, also a single or multiple parts of them can be exploited. In this case, deconstructed virus relies on *A. Tumefaciens* as a vector to deliver DNA of one or more viral RNA replicons to plant cells (Gleba, Klimyuk et al. 2007). As for stable plant transformation, the transient expression strategies require the right choice of the plant host species exploitable for the production cycle. Along with the susceptibility of the plant species to the viral infection, setup, scale-up and maintenance costs, length of production cycle, biomass yield, and costs of processing contribute together to the identification of the best platform (Schillberg, Twyman et al. 2005). A relevant example comes from tobacco plant, which has been adopted as a platform by several biotechnology companies and therefore is considered a well-established host for controlled transgene expression (Fischer, Stoger et al. 2004). In general *Nicotiana* species have long been considered model systems in plant biology and, more recently, they became particularly prominent as the field of plant molecular biology and plant transformation

has come of age. In particular *Nicotiana benthamiana*, which is a close relative of tobacco plant, offers the advantages of high expression levels, relatively short production times going from days to several weeks and ease of use in controlled growth conditions. Although *N. benthamiana* has become extremely important as a subject for the study of host-pathogen interactions, especially those involving plant viruses, nowadays it is considered a viable alternative for cost-effective protein production. The plant exhibits high susceptibility to many plant pathogens (Goodin, Zaitlin et al. 2008) and therefore *N. benthamiana* is used as a primary host for recombinant virus and agroinfiltration-based transient expression. Actually, tools and resources to support studies with *N. benthamiana* can be readily used across laboratories, in many cases without the need to consider plant effects other than those influenced by environmental and growth conditions. Furthermore, it is also a non-food and non-feed crop, hence transgenic material carries a reduced risk to contaminate feed and human food chains (Stoger, Ma et al. 2005). Although the use of non-food crops, to avoid accidental entry into the food chain, represents a solution for the safety issue, most regulatory processes do not readily accommodate PMF. In fact, current regulations have been developed only for food and feed crops. Guidelines for pharmaceutical crops are still a developing field and, made exception for strict confinement that is applied to limit any environmental exposure and possible transgene escaping (Menassa, Nguyen et al. 2001), in the EU the related technical issues and risks are considered on a case-by-case basis. In conclusion, even if in the last twenty years a lot of steps forward have been made, and the first plant derived pharmaceutical product has been released on market (Sheridan 2012), the development of a dedicated regulatory and the social acceptance are both fundamental for the real success of new biotechnology.

Materials & Methods

General materials

E. coli strains

The strain used to propagate a plasmid can have a substantial influence on quality of the purified DNA. The slower growing strain XL1-Blue strain allows blue-white color screening for recombinant plasmids and is an excellent host strain for routine cloning applications using plasmid vectors. The XL1-Blue cells are endonuclease (*endA*) deficient, which greatly improves the quality of plasmid DNA preparation, and are recombination (*recA*) deficient, improving insert stability. The *hsdR* mutation prevents the cleavage of cloned DNA by the *EcoK* endonuclease system. The *lac^FZAM15* gene on the F' episome allows blue-white screening for recombinant plasmids that provides α -complementation. When lacZ expression is induced by IPTG in the presence of the chromogenic substrate X-gal, colonies containing plasmids with inserts will be white, whereas colonies containing plasmids without inserts will be blue.

Plasmid

The pBluescript SK (+) is a vector designed to simplify commonly used cloning and sequencing procedures, *in vitro* generation of RNA transcripts and site-specific mutagenesis. The pBluescript SK (+) has an extensive polylinker, which is flanked by T7 and T3 RNA polymerase promoters, placed in inverted orientation. The β -galactosidase gene is present in the pBluescript SK (+) vector, but the coding sequence is interrupted by the large polylinker. A pBluescript SK (+) vector having no inserts in the polylinker

will produce blue colonies in the appropriate strains of bacteria (eg., XL1-Blue); conversely, vectors that have inserts will produce white colonies using the same strain, because the inserts disrupt the coding region of the *lacZ* gene fragment. The pBluescript SK (+) vector allows also a positive clone selection onto ampicillin supplemented growth media.

N. benthamiana plants

N. benthamiana is a close relative of tobacco and is considered by scientific community as a model organism for performing plant research. In this work, *N. benthamiana* plants were grown in a greenhouse at 25°C and 16-h-light/8-h-dark cycles. For each set of experiments, 6- to 8-week-old plants that were typically at the six leaf stage were used, and each experiment was repeated at least three times. A representative set of plants was selected for each experiment.

Relevant cloning techniques

E. coli cell culturing

E. coli host cells were usually grown over-night at 37°C in Luria-Bertani (LB) culturing media at pH=7.0. *E. coli* cells were grown in either LB broth or LB agar, which is obtained after the addition of agar to a final concentration of 2% (w/v). Immediately before using, sterile LB culturing media were supplemented with the appropriate antibiotic to achieve positive selection during cloning steps and preventing unwanted external contaminations. Typically, filter-sterile ampicillin (Amp) stock solutions were directly diluted in LB media up to a final concentration of 100 mg/L.

Plasmid preparation

Candidate clones were used to inoculate 5 to 100 mL cultures of LB broth containing the appropriate antibiotics and were incubated at 37°C over-night under constant shaking. *E. coli* cells were harvested after approximately 12-16 hours of growth, which typically corresponds to the transition from logarithmic into stationary growth phase. The media was subjected to centrifugation at 5.800 xg in a benchtop centrifuge for 10 minutes and, after removal of the supernatant, the bacterial pellet was gently resuspended for plasmid extraction. Depending on the initial culture volume, plasmid DNA was prepared by a MiniPrep or MidiPrep kit (Qiagen) in accordance with the manufacturer protocol. Briefly, supercoiled plasmid DNA was extracted by alkaline lysis of cells through the addition of NaOH/SDS and in presence of RNase, and after a while the reaction was stopped neutralizing the mixture. At this point, the bacterial lysate was cleared from genomic DNA, proteins and cell debris by centrifugation for 15 minutes at 12.000 xg; the resulting supernatant was saved for further purification steps. The plasmid raw material was left to bind to QIAGEN Anion-Exchange Resin under appropriate low-salt and pH conditions. Remaining RNA, proteins, and low-molecular-weight impurities are not retained on the silica resin and thus are

removed by wash. Finally, plasmid DNA is eluted in ultra-high-pure (UHP) water. To determine extraction yield, DNA concentration was determined by UV spectrophotometry at 260 nm. In addition to the $OD_{260/280nm}$ and $OD_{260/230nm}$ ratios, qualitative and quantitative analysis of the isolated DNA was performed by agarose gel electrophoresis. Plasmid DNA obtained has been used for a variety of routine applications including restriction enzyme digestion, *in vitro* transcription, PCR amplification, sequencing, ligation and transformation.

Agarose gel electrophoresis

The appropriate amount of agarose was dissolved in the proper volume of Tris·borate/EDTA (TBE) x1 or Tris·acetate/EDTA (TAE) x1 buffer by boiling and allowed to cool to around 50°C before the addition of ethidium bromide (EtBr) to a final concentration of 0,5 µg/mL. The gel mix was then poured into a gel casting apparatus containing the appropriate well-forming comb and allowed to set. After setting, the gel was placed in a gel tank and topped up with the appropriate buffer until just covering the gel. DNA or RNA samples were mixed with a gel loading buffer solution 1x, containing glycerol and Bromophenol Blue, and then were loaded into the gel. Electrophoresis was carried out at either 80 V or 120 V constant voltages, depending on gel dimension, for 1 hour. Finally, results of electrophoretic separation were visualized under a UV light and documented by photo capturing (ChemiDoc, BioRad).

Restriction digestion

Restriction digestions are enzymatic reactions catalyzed by endonucleases. These enzymes are able to cut the DNA with molecular precision in presence of specific recognition sites, usually represented by palindromic nucleotide sequences. The enzymatic digestions of plasmid DNA were performed in accordance with the manufacturer protocol accompanying each restriction enzyme. In general, the quantity of enzyme to be employed in a reaction was

decided considering that 1 enzymatic unit is able to cut 1 μg of double stranded DNA in 1 hour, when the mixture is incubated at the optimal temperature for enzyme activity. Double digestions are also possible as long as the two enzymes retain their endonucleolytic activity within the same pH, salt concentration and temperature. In the case the two enzymatic conditions are not compatible, the restriction digestions have to be sequentially performed after an adjustment of settings. All the restriction enzymes used in this work are produced by New England Biolab Inc. (NEB).

DNA extraction from agarose gel

Enzyme contamination of DNA samples can interfere with subsequent downstream applications along cloning procedures. To circumvent unwanted interferences relied on such contamination and to achieve physical separation of different-sized digested products, DNA samples were run on agarose gel and molecules were divided depending on their migration mobility. To recover target DNA fragments from the gel, the QIAquick gel extraction kit (Qiagen) was used. Briefly, agarose gel slices containing the DNA were solubilized in the appropriate buffer providing the best conditions for subsequent binding of DNA to the silica membrane. During the DNA adsorption step, unwanted primers and impurities, such as salts, enzymes, unincorporated nucleotides, agarose, dyes and EtBr did not bind to the silica membrane but flowed through the column. Salts were quantitatively washed away by the ethanol-containing buffer, and any residual ethanol trace was removed by an additional centrifugation step to avoid interferences with subsequent enzymatic reactions. Finally, the pure DNA is eluted with UHP-water.

Ligation of DNA fragments

Ligation is the process during which the formation of phosphodiester bonds between double stranded DNAs with 3'-hydroxyl (3'-OH) and 5' phosphate (5'-PO₄) termini occurs in the presence of ATP. During cloning procedures,

vector and insert DNAs are both appropriately restriction digested to generate complementary protruding single stranded ends; after the annealing of fragments via molecular recognition occurs, their joining into a unique structure is required to avoid they separate again. Some endonucleolytic enzymes generate *blunt* ends after DNA cleavage, and fragments such generated can be fused together without base pairing requirements in a not directionally manner. For the setting up of the ligation reaction the following calculation was applied:

$$(\text{ng}_{\text{insert}} / \text{kb}_{\text{insert}}) : (\text{ng}_{\text{vettore}} / \text{kb}_{\text{vettore}}) = \text{molar ratio}$$

The calculation allows normalizing the quantities (expressed as masses) of vector and insert DNAs for the number of molecules; therefore, the nucleotide dimension of vector and insert is used to substantially differ. The reaction mixture was incubated over-night at 16°C, followed by one additional hour at 37°C. After ligation, the mixture was desalted by means of a cross-linked agarose gel filtration based matrix (Sephacrose CL-6B, Sigma-Aldrich). The high-pure DNA product such generated was finally left to evaporate up to a volume of 5 µL before *E. coli* transformation.

Preparation of electrocompetent cells and electroporation of *E. coli*

An over-night culture from a single colony of *E. coli* XL1-blue host strain was diluted in fresh LB broth supplemented with tetracycline and was left growing up to OD_{600nm} = 0.6. At this point the bacteria were harvested by centrifugation at 3.500 xg for 20 minutes at 4°C. The supernatant was discarded and the cellular pellet underwent 4 washing steps in sterile bi-distilled (bd) H₂O at 4°C to remove residual salts. During each rinse, the volume of bdH₂O used to resuspend the pellet was progressively reduced up to 1/200 of the initial one. Finally, the concentrated electrocompetent cells were aliquoted, snap frozen in liquid nitrogen and stored at -80°C. For transformation, frozen aliquots were thawed on ice, then mixed with the

ligation product and incubated on ice for 30 minutes, and lastly transferred in a pre-cooled electroporation cuvette (gap 0,2 cm). Electroporation settings were 2,5 kV and 5 ms single-pulse. For reconstitution, the transformed bacteria were immediately transferred into pre-warmed LB medium without antibiotics and were left for 30 minutes at 37°C. In the end, the suspension was spread on LB agar plates with the appropriate antibiotics and grown overnight at 37°C.

In vitro transcription of RNAs

T7 transcription was the standard method of producing RNA *in vitro*. It is easy, quick, and produces relatively good quality RNAs up to many micrograms per reaction. T7 polymerase is one of a group of very active phage polymerases that use a short promoter sequence to initiate transcription at a specific base in the template. The transcription of single- or double-stranded DNA has good fidelity and goes on until the end of the template strand is reached. In fact, circular plasmid templates will generate extremely long and heterogeneous RNA transcripts. For this reason, plasmid DNA templates were linearized with the appropriate restriction enzyme downstream of the sequence to be transcribed, and the results of the digestion were checked on a gel to confirm that cleavage is complete. After linearization the transcription reaction was assembled following the MEGAscript kit (Ambion) manufacturer protocol. Finally, the reaction mixture was incubated at 37°C for 3-4 hours and the integrity of the transcribed RNA was verified by TBE agarose gel electrophoresis.

In vitro annealing of oligonucleotides

It is a routine procedure that allows complementary strands of nucleic acids to anneal and form double strands. The technique requires denaturing any complementary strand by rising temperature, thus removing also possible secondary structure, and then allowing the strands to hybridize. Two factors influence the efficiency of oligonucleotide hybridization: salt concentration

and the rate of temperature decrease. Annealing occurs most efficiently when the temperature is slowly decreased after denaturation, especially when the oligonucleotides have high GC content or form hairpin structures. All the oligos used in this work were synthesized at MWG-Biotech and were annealed following the same procedure. Two μg of each single stranded oligonucleotide were mixed with UHP-water up to a volume of 40 μL , meanwhile water in a large glass beaker were brought to boil on a hotplate. The tube containing the oligonucleotides was incubated in the boiling water for 5 minutes, and then the hotplate was turned off leaving to slowly cool to room temperature. Lastly, the volume of the annealing mixture was checked and the double strands such generated were ready to use for next cloning steps.

Flag-For	CGGTGGTGGAGGAGATTATAAGGATGATGATGATAAGT GATTAAT
Flag-Rev	TAATCACTTATCATCATCATCCTTATAATCTCCTCCACCA CCGGCC
cMyc-For	TGGTGGTGGAGGAGACAAAAGCTTATTTCTGAAGAGG ATCTTGGCCCGGTGATTATAAGGATGATGATGATAAGT GATTAAT
cMyc-Rev	TAATCACTTATCATCATCATCCTTATAATCACCGGGCCC AAGATCCTCTTCAGAAATAAGCTTTTGTTCCTCCACCA CCAAGCC
HA-For	TGGTTATCCTTATGATGTTCCAGATTATGCTGGCC
HA-Rev	CAGCATAATCTGGAACATCATAAGGATAACCAAGCC
V5-For	AGGAAAGCCTATTCCTAATCCATTGCTTGGATTGGATTCT ACTGGCC
V5-Rev	CAGTAGAATCCAATCCAAGCAATGGATTAGGAATAGGC TTTCCTGGCC
HRz-For	CCGGTTCGGCATGGCATCTCCACCTCCTCGCGTCCGACC TGGGCATCCGAAGGAGGACGCACGTCCACTCGGATGGCT AAGGGAGGGATC
HRz-Rev	CCGGATCCCTCCCTTAGCCATCCGAGTGGACGTGCGTCC TCCTTCGGATGCCAGGTCCGACCGCGAGGAGGTGGAGA TGCCATGCCGAC

Table 1 | List of the oligonucleotides used in the cloning experiments. In the left column the names of the oligos are reported. In the right column are reported the nucleotide sequences 5'-3' oriented: in italic and bold are highlighted the protruding ends generated after the *in vitro* annealing of the complementary oligonucleotides pairs; the recognition site of the restriction enzymes are evidenced as italic and underlined sequences.

Phosphorilation and de-phosphorilation

In the course of cloning strategies, sometimes there was the necessity to decrease the vector background to achieve an easier identification of the clone of interest. This was obtained using Antarctic phosphatase (NEB) catalyzing the removal of 5' phosphate groups from double stranded DNA as well as oligonucleotides. Since phosphatase-treated DNA lacked the 5'-phosphoryl termini required by ligases, mono-digested cloning vectors self-ligation was prevented. Conversely, when synthetic oligonucleotides had to be joined with de-phosphorilated vector, they needed for the addition of 5'-phosphates to produce the subsequent ligation. The transfer and exchange of P_i from the γ position of ATP to the 5'-hydroxyl terminus of polynucleotides was catalyzed by the T4 polynucleotide kinase (NEB) in accordance with the manufacturer protocol.

Polymerase chain reaction (PCR)

PCR is a rapid and efficient method to amplify specific nucleotide sequence by means of a DNA polymerase enzyme and 2 directionally inverted circumscribing primers. The reaction starts with the denaturation of the DNA template, followed by annealing of primers thorough nucleotide complementarity, and finally concluding with DNA synthesis. All these processes depend on substantially different temperature to occur and, governed by a thermocycler instrument, can be repeated a defined number of times to obtain exponential amplification of the DNA template region delimited by primers. Template should be high-quality purified DNA and its concentration should not be high as, in both cases, amplicon specificity decreases, particularly when a large number of cycles are employed. Generally, a primer is 20-30 nucleotides in length, the GC content should be in the range 40-60% with calculated melting temperatures (T_m) from 42°C to 65°C, and secondary structure (e.g., hairpins) within each primer as well as potential dimerization between the primers need to be avoided. In addition, a substantial physic-chemical equilibrium within the primer pairs is required.

All these aspects were carefully taken into account during *in silico* design process of all primers. A standard PCR reaction mix (EuroTaq, EuroClone), supplemented with magnesium and each nucleotide at concentration of 2,0 mM and 200 μ M respectively, was used for routine amplification procedures. During clone screening, to quickly check the inclusion of the ligation product in the *E. coli* cells, single colonies were directly used in a colony-PCR reaction as the template. When robust amplification performance and fidelity of product were required for cloning procedures, Phusion High-Fidelity DNA Polymerase (NEB) was preferred as it has an error rate 50-fold lower than that of *Taq* DNA polymerase.

ScreenCP	TGCACTGTCTCTAACCTACC
TBSV-2Back	AAGATCCAAGGACTCTGTGC
GFP-For	TAAAGGGCCCGGTGGTGGAGGTATGAGTAAAGGA GAAGAACTTTTCACTGG
GFP-Rev	CGCCCTTAATTAAGGCCTATTATTTGTATAGTTCAT CCATGCC
TBSV-35S-For	CGC <i><u>GGA</u></i> TCCGCAGGTCAACATGGTG
TBSV-35S-Rev	CCTCTCCAATGAAATGAACTTCC
TBSV-5' context-For	GGAAATTCCCCAGGATTTCTCG
TBSV-5' context-Rev	AAAATGTCC <i><u>ACCGG</u></i> TGCCGTC
PCR-NOS-For	TCCC <i><u>CCGGG</u></i> CGATCGTTCAAACATTTGG
PCR-NOS-Rev	GCTC <i><u>GCGAG</u></i> CTCGATCTAGTAACATAGATGAC
RT-PCR1For	TGACATTTTCGTGCAACTGG
TBSV-1For	TCTGACACATGCAGCTCC
ScreenNOS-Rev	ATCATCGCAAGACCGGCAAC

Table 2 | List of the primers used in the cloning, screening and sequencing experiments. In the left column the names of the primers are reported. In the right column are reported the nucleotide sequences 5'-3' oriented: the recognition site of the restriction enzymes are evidenced as italic and underlined sequences.

Techniques for VNPs characterization

Plant infection

Six to eight weeks old *N. benthamiana* plants, grown in controlled conditions (24°C, 16 hours light/8 hours dark), were mechanically inoculated with different TBSV constructs by abrading the adaxial side of 2 leaves per plant, using the TBSV infectious RNAs or the TBSV *in planta* expression vectors mixed with carborundum (silicon carbide) powder (VWR International). cDNA template of TBSV constructs owning the T7 promoter upstream the genome sequence were linearized by restriction digestion and used for *in vitro* transcription reaction following the manufacturer's instructions (MEGAscript®T7 High Yield Transcription kit, Ambion); approximately 2-3 µg of the *in vitro* transcribed RNA, diluted in UHP-H₂O up to a volume of 50 µL, were used to inoculate each leaf. Plasmidic DNA of TBSV constructs inserted within *in planta* expression cassette was used to directly inoculate 2 healthy leaves per plant (30 µg for each leaf). To verify the genomic stability and infectivity of virus particles, reinfections were performed using saps from infected leaves. Briefly, a raw leaf sap was prepared by homogenizing the symptomatic systemic tissue of an infected plant in Phosphate Buffered Saline (PBS; 151 mM NaCl, 8,4 mM Na₂HPO₄ · 12 H₂O, 1,86 mM NaH₂PO₄ · H₂O).

VNPs purification

Several methods were tested to purify viral particles from infected plants. Comparing yield and quality of the all procedures utilized, the best results were achieved applying the protocol of Burgyan and Russo (1998) with some modifications. Briefly, leaves showing typical signs of virus infection were collected 7-9 days post-infection (dpi) and ground to a fine powder in liquid nitrogen using a mortar and pestle. Next, samples were homogenized with 3 mL/g of 50 mM sodium acetate, pH 5.3, supplemented with 1% ascorbic

acid and a cocktail of protease inhibitors (P9599, Sigma). The extract was immediately filtered through miracloth filters (Calbiochem) and incubated on ice for 1 hour, leaving plant proteins and macro-particulate to precipitate; a raw extract was obtained by clarifying the solution by low-speed centrifugation (8.000 xg for 15 minutes at 4°C). At this point, the pH of the supernatant was adjusted to pH=5.0 with NaOH, as during the homogenization plant material lowered the pH of the extract. The solution was then ultra-centrifuged for 1 hour at 90.000 xg at 4°C. The obtained pellet was left gently resuspending by incubating over-night at 4°C in 50 mM sodium acetate, pH 5.3. Finally, purified viral particles were evaluated for yield and quality.

VNPs quantification

The amount of protein in plant raw extracts or plant purifications was quantified to establish the quality of the extraction protocol and to ensure equal loading in downstream analysis. Here, the Protein micro-Assay (Bio-Rad) was used, in which known bovine serum albumin (BSA, Sigma-Aldrich) concentrations, namely 1,2 to 10,0 µg/mL, were used as reference values. The method is based on the dye-binding Bradford assay, in which a differential color change of the dye occurs in response to various concentrations of protein (Bradford 1976). Prepared standard BSA concentration samples were read at absorbance 595 nm and a standard curve was drawn. Protein concentrations in unknown samples were extrapolated from the linear part of this curve.

SDS-PAGE

One of the routine analyses used in almost all laboratories for characterization of protein mixtures is the polyacrylamide gel electrophoresis in denaturing condition. This technique relies on the disruption of any macromolecular protein structure followed by a size-dependent migration throughout a molecular sieve. Protein samples are usually denatured by

boiling, after the addition of reducing agents, such as 2-mercaptoethanol (Sigma-Aldrich), and the anionic surfactant sodium dodecyl sulphate (SDS, Sigma-Aldrich); all these chemicals are contained within *Laemmli* buffer together with glycerol and the bromophenol blue dye (Laemmli 1970). The gel cast was assembled with proper spacers and tested with H_2O for leaks before pouring the gel solutions. A 13,5% (w/v) acrylamide *resolving gel* was chosen for protein separation and, as the crosslinking reaction was started by the addition of ammonium persulfate (10% w/v), the solution was immediately transferred into the cast and overlaid with isopropanol to stop air interfering with the crosslinking reaction. Once set, the isopropanol was removed and the *stacking gel* (acrylamide 4% (w/v)) was poured following the same procedure. Finally, the gel comb was inserted making sure no bubbles were in the wells, and the gel was allowed to set. The gel assembly was taken out of the casting apparatus, put into the gel tank, and then covered with *running buffer* (0,025 M Tris, 0,192 M Glycine, 0,1% SDS). Denatured protein samples were loaded into wells using a Hamilton syringe and ran against protein standards for molecular weight identification. Protein separation was carried out electrophoresing at 90-120 V constant voltage until loading dye migrated out of the gel. Proteins were either visualized by Coomassie blue staining (Coomassie R-250, Sigma-Aldrich) or Silver staining (AgNO_3 , Carlo Erba).

Western Blotting

This technique allows identifying a protein by exploiting the specific binding of antibodies to their target. Proteins were separated by SDS-PAGE and subsequently their transfer onto polyvinylidene difluoride (PVDF) membrane (Immobilon, Millipore) was performed. PVDF membrane was cut to the correct size for the gel and prepared for transfer by soaking in methanol. Gel was carefully removed from the glass slabs, placed onto PVDF membrane and finally sandwiched on both sides with extra-thick Wathman paper soaked in *transfer buffer* (0,025 M Tris, 0,192 M Glycine, methanol

20% (v/v)). Protein transfer was carried out using a semi-dry blotting apparatus (TE70X semi-dry transfer unit, Hoefler) set at 100 V constant voltages for 1 hour. Once the proteins were completely transferred, the membrane was blocked by incubating over-night at 4°C with a 5% powdered skim milk (w/v) solution in PBS. Next, the primary antibody, diluted in a 2% powdered skim milk (w/v) solution, was added and the incubation was left for 2-3 hours at 37°C and gently shaken. Before the addition of the secondary antibody, any trace of the primary antibody was removed by washing the membrane 3 times in PBS-Tween 0,2% (v/v) (Tween-20, Sigma-Aldrich) and consecutively 2 times in PBS. The membrane was incubated with the Horseradish peroxidase (HRP)-conjugated secondary antibody at 37°C for 1 hour, and then washed again following the procedure previously described. Finally, the chemiluminescent detection using the enzyme linked chemiluminescence (ECL) detection reagents (A and B) from Millipore was performed. The ECL reagent was incubated on the membrane for 5 minutes leading to catalysis of luminol in alkaline conditions. The luminol in the excited state decays in a chemiluminescent reaction, which was detected by ChemiDoc (Bio-Rad) or exposing Kodak films in dark-room. The primary antibodies and the respective dilutions used in this work were: mouse monoclonal M2 anti-Flag (1:4000; F3165, Sigma), rabbit polyclonal anti-cMyc, anti-HA, or anti-V5 (1:2000; PA1-22826, PA1-86676, PA1-32392 respectively, Thermo Scientific). For detection, anti-mouse IgG (NXA931, GE Healthcare) or sheep anti-rabbit IgG (PA1-84416, Thermo Scientific) HRP-conjugated secondary antibodies diluted 1:2500 were used.

Enzyme-Linked Immunosorbent Assay (ELISA)

This technique allows identifying a protein by exploiting the specific binding of antibodies to their target. Differently from WB, ELISA allows the detection of proteins in their native folding. Briefly, ELISA Maxisorp plate (eBioscience) was coated over-night at 4°C with 100µL of the protein sample per well; each sample was repeated at least in triplicate. After blocking with

5% skim milk (w/v) in PBS at 37°C for 2 hours, the plate was washed 3 times in PBS-Tween 0,2% (v/v) and consecutively 2 times in PBS. Next, the primary antibody, diluted in a 2% powdered skim milk (w/v) solution, was added and the incubation was carried out for 2 hours at 37°C. The plate was washed again and incubated for one additional hour at 37°C as 100µL of HRP-conjugated secondary antibody, diluted as the primary antibody, were added to each well. After washing thoroughly, colorimetric reaction was developed using 2,2'-azino-bis (3-ethylbenzthiazoline-6 sulphonic acid) substrate (ABTS, KPL) and read at 405 nm on an automated ELISA reader (Sunrise, Tecan). All the antibodies used in ELISA analysis are reported in Western Blotting paragraph (M&M).

Electron microscopy

Purified viral particles were collected on carbon/formvar film coated 400 mesh copper grids (Electron Microscopy Sciences) and stained with 2% (w/v) uranyl acetate aqueous solution. Grids were then analyzed by using a transmission electron microscope JEM 1200 EXII (Jeol) and images were acquired through a CCD Camera SIS Veleta (Olympus) at the Interdipartimental Center of Electronic Microscopy (Tuscia University).

RNA extraction and RT-PCR analysis

The viral stability and the presence of the heterologous sequences at the genomic level were verified by RT-PCR analysis. Seven to nine dpi, total RNA was extracted from symptomatic inoculated and systemic leaves by using an RNeasy plant mini kit (QIAGEN). Briefly, harvested tissues are first ground in liquid nitrogen, and then lysed and homogenized in the presence of a highly denaturing guanidine-thiocyanate containing buffer, which immediately inactivates RNAses to ensure purification of intact RNA. After lysis, samples were centrifuged to remove insoluble material and to reduce the viscosity of the lysates by disrupting gelatinous material often formed in plant. Subsequently, ethanol was added to provide appropriate binding

conditions, and the samples were then applied to an RNeasy Mini spin column, where the total RNA selectively bound to the membrane while contaminants were efficiently washed away. At the end of the procedure, high-quality RNAs were eluted in RNase-free water and RT-PCRs were performed by using a ProtoScript M-MuLV *Taq* RT-PCR kit (New England Biolabs) in accordance with the manufacturer's instructions. cDNA was synthesized by using random primers, and PCR was carried out with TBSV specific primers comprising the 3' *cp* region. The resulting fragments were evaluated by agarose gel electrophoresis, hence gel purified and finally sequenced at BMR Genomics.

Analytical separation of VNPs on sucrose gradient

A discontinuous sucrose density gradient was prepared by layering successive decreasing concentrations of sucrose solutions. Briefly, 2 mL each of 60, 50, 40, 30, 20 and 10 % (w/v) sucrose dissolved in PBS were poured into ultracentrifuge tubes and a volume of 200 μ L of a raw extract was loaded on top of the gradient. The analytical separation occurred by ultra-centrifugation at 90.000 xg for 2 hours at 4°C. Eleven fractions were collected from the top to the bottom of the tube and were finally analyzed by ELISA using specific antibodies for the detection.

VNPs reversible swelling

Conformational change in the TBSV icosahedral capsid was obtained varying ionic strength and pH. Approximately 4 μ g of purified TBSV were diluted in swelling buffer (0,1 M Tris, 50 mM EDTA, pH 8.5) or control buffer (0,1 M Tris, pH 5.5) with a volume ratio of 1:10, and were incubated at 4°C for 2 hours. To verify VNPs pore gating, EtBr was added during the incubation at a final concentration of 0,5 μ g/mL. Samples were resolved by electrophoresis in 1 % agarose gel using an electrophoresis buffer containing 38 mM glycine and 5 mM Tris at pH 8.5. The gel was prepared in the same buffer and, after samples run, it was stained in swelling buffer with the addition of EtBr at a

final concentration of 0,5 µg/mL. Detection of the viral particles was achieved by either visualization under UV light of the encapsidated RNA or Coomassie staining of the viral capsid protein.

RNase protection assay

Purified viral particles were treated in swelling buffer or control buffer as described above. After 2 hours 50 ng of ribonuclease A (NEB) were added to the reaction and the incubation was left at 4°C for additional 30 minutes. Encapsidated RNA was extracted by the addition of an equal volume of a 1:1 phenol-chloroform solution (v/v) and SDS at a final concentration of 1% (w/v). The mixture was agitated vigorously and then centrifuged to separate the two phases. The aqueous phase was recovered and the RNA was precipitated by the addition of 1/10 volume of 3 M sodium acetate and 3 volumes of ice cold ethanol. Finally, the RNA was sedimented by centrifugation and the pellet resuspended in RNase free water. An aliquot of viral RNA was analyzed by TBE agarose gel electrophoresis and visualized under UV light after EtBr staining.

VNPs biotinylation

In vitro biotinylation of the surface-exposed lysines of VNPs was performed following the EZ-Link® Micro NHS-PEO₄-Biotinylation Kit (Thermo) manufacturer's instructions. Approximately 200 µg of VNPs were mixed with N-hydroxysuccinimide (NHS) PEO₄-biotin reagent at 10-fold molar excess and incubated 2 hours in ice and then one additional hour at 4°C. The excess non-reacted and hydrolyzed biotin reagent remaining in the solution was removed by chromatography (Zeba™ Desalt Spin Column, 7000 MWCO; Thermo Scientific) and the purified samples were analyzed by Western blotting and ELISA using a streptavidin HRP-conjugated as probe (N100, Pierce).

Results

In this study is presented the development of an efficient and versatile system for VNPs production in *N. benthamiana*, based on the TBSV pepper isolate (Szittyá, Salamon et al. 2000). In particular, the construction of a vector, which allows the generation of genetic fusion at the C-terminal end of the TBSV CP, thus resulting in the display of peptides onto the viral protein capsid, is reported. Four commonly used protein tags have been exposed onto the surface progressively, one after the other, by fusion of their coding sequences (CDSs) in a modular fashion to the *cp* gene. The chimeric constructs showed to retain infectivity upon *in vitro* transcription of their RNA genomes and inoculation of plant leaves. The correct exposure of all fusion peptides, including the 56 additional amino acids of the longest chimera, was proved. Next, one of the generated chimeras was chosen to be addressed by bioconjugation of biotin and to be exploited for cargo loading through virus reversal permeability. Finally, with the prospect of a scaled up process, *in planta* expression cDNA based constructs were assembled to propose a cheaper alternative for plant infection.

Genetic engineering

Several studies have demonstrated that the C-terminal portion of the TBSV CP is exposed on the exterior surface of the assembled virion (Harrison, Olson et al. 1978; Olson, Bricogne et al. 1983). On this ground, a TBSV based vector for the generation of a peptide display system was designed (**Fig. 4**).

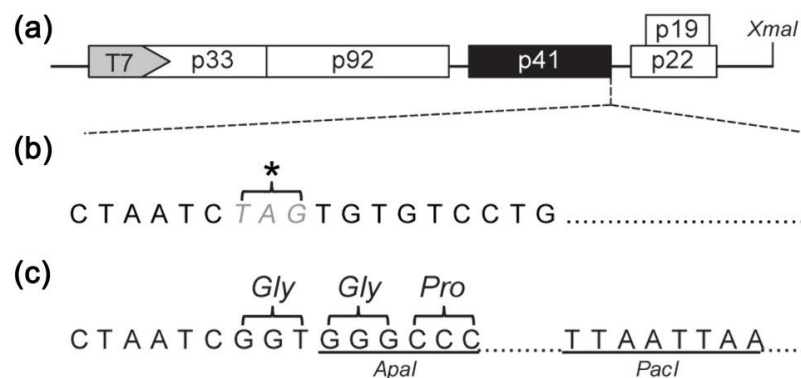


Figure 4 | Schematic representation of TBSV-vector cDNA construct. (a) Genome organization of TBSV-P (Szittyá, Salamon et al. 2000). The five open reading frames (ORFs) encoding the respective proteins with their molecular masses (in kDa) are represented as boxes: p33 and p92 (RNA-dependent RNA polymerase), p41 (coat protein), p22 (movement protein), p19 (silencing inhibitor). (b) Sequence detail of the original and (c) of the genetic engineered CP stop codon context. The first amino acids of all fusion peptides were reported. The underlined sequences represent the restriction enzyme sites used to clone the peptides of interest.

Briefly, a subclone containing the *cp* C-terminal CDS of the TBSV-P (Szittyá, Salamon et al. 2000) (**Fig. 4a**) was generated by digestion with *NotI*/*NcoI* and subsequent introduction of the generated fragment into the pBluescript SK (+) vector. Hence, a multi-cloning site (MCS) was inserted in place of the CP stop codon first by transforming the *amber* sequence into a unique restriction recognition site by site directed mutagenesis, and then by subcloning the compatible polylinker fragment, harboring the *ApaI* and *PacI* sites, through traditional vector digestion and ligation (**Fig. 4b,c**). Considering that these restriction recognition sites were not present in the TBSV-P sequence, they allowed the subsequent cloning of the CDSs of interest. At this stage, the modified 3'-terminal *cp* sequence was moved back into the TBSV genome

context upon *NotI/NcoI* digestion generating the TBSV-vector. This construct was designed to contain the heterologous peptides CDSs genetically fused to the 3' end of the viral *cp* gene.

TBSV-Flag, -cMyc, -HA, -V5 construction

Once the peptide display system allowing easy and rapid cloning of the CDS of interest was generated, the TBSV-vector was tested for the ability to accommodate 4 peptide modules sequentially inserted to obtain increasingly longer fusion proteins. The first chimeric construct to be produced was the TBSV-Flag (**Fig. 5a**), a CVP carrying a 15 amino acids long heterologous peptide onto the outer surface of the viral protein cage. In this circumstance, a flexible peptide linker constituted by the GGPGGGG sequence was introduced between the last CP amino acid and the Flag tag (DYKDDDDK, Chiang and Roeder 1993) in order to decrease the negative influence of the heterologous portion during CP native folding. TBSV-vector was prepared upon digestion with *ApaI* and *PacI*, the 2 unique restriction recognition sites introduced within the MCS, and subsequently the compatible Flag sequence, which was produced by *in vitro* annealing of synthesized sense and antisense oligonucleotides (Flag-For, Flag-Rev; see M&M for sequence), was introduced by ligation. After transformation of electro-competent cells the colonies grown under selection were screened by PCR using the primers (ScreenCP, TBSV-2Back; see M&M for sequence). Colonies giving an amplification product of the correct size (~470 bp) were selected for plasmid extraction. Final confirmation of successfully introduced CDS was obtained through *NotI/PacI* digestion of the cDNA construct and visualization of the released fragment (~1130 bp) on agarose gel. Before proceeding with subsequent cloning steps, the clone was verified by sequencing at BMR Genomics with TBSV-2Back primer (see M&M for sequence). The second chimera to be produced after TBSV-Flag generation was the TBSV-cMyc (**Fig. 5b**), bearing the EQKLISEEDL cMyc peptide (Kawarasaki, Yamada et al. 2003), derived from the c-myc proto-oncogene product, in addition to the Flag sequence.

Also in this case, two synthetic oligonucleotides containing the cMyc-Flag CDSs (cMyc-For, cMyc-Rev; see M&M for sequence) were *in vitro* annealed to generate a double strand fragment presenting digested-like *ApaI* and *PacI* trimmings. Simultaneously, TBSV-Flag construct was digested in the same manner and a vector owning compatible ends was thus obtained. Ligation between insert and backbone fragments was carried out, and after a colony-PCR with the primers ScreenCP and TBSV-2Back (see M&M for sequence) positive clones were identified. Additional confirmations were then obtained by both *NcoI/PacI* restriction digestion of the extracted cDNA and sequencing. The new chimeric CP bore the cMyc tag placed just after the last amino acid of the linker and divided from the adjacent Flag peptide by an additional GPG spacer. At this point, after the introduction of the second peptide module, the chimeric protein resulted in an extension of 28 amino acids compared to the wild-type CP. Going further in the progressive addition of peptide CDSs, the last two sequential fusions were generated. Here, the TBSV-cMyc construct was opened at the unique *ApaI* restriction recognition site, located in between the cMyc and the Flag CDSs, and subsequently was de-phosphorylated in order to prevent vector self-ligation events. On the other hand, a complementary pair of synthetic oligonucleotides (HA-For, HA-Rev; see M&M for sequence) encoding for the HA tag peptide derived from the influenza Hemagglutinin (YPYDVPDYA, Laize, Ripoche et al. 1997) was *in vitro* annealed, generating a fragment owning *ApaI* compatible protruding ends. Due to the un-phosphorylated nature of both the DNA synthesized oligos and the prepared vector, the double strand fragment was incubated with a kinase in presence of ATP to achieve 5' terminal phosphorylation necessary for proper ligation into the prepared vector. Electro-competent cells were then transformed with the ligation product and, after over-night incubation at 37°C, the colonies grown were screened for the inclusion of the cDNA construct of interest. In this circumstance, the preparation of the TBSV-cMyc backbone by simple *ApaI* linearization allowed the insertion of the fragment in two possible orientations, usually

referred to as unidirectional subcloning, and also in multiple copies through concatemers formation. To isolate the proper TBSV-HA clone of interest (**Fig. 5c**), a PCR with primers for correct orientation screening was performed, whereas the visualization on agarose gel of the size of the amplification product (~580 bp) enabled the discrimination for fragments copy number. Finally, the same strategy was used to clone the V5 module (V5-For, V5-Rev; see M&M for sequence), corresponding to the GKPIP NPLLGLDST epitope derived from the P/V proteins of the paramyxovirus simian virus 5 (SV5, Kolodziej, Pourfarzad et al. 2009), thus creating the TBSV-V5 (**Fig. 5d**).

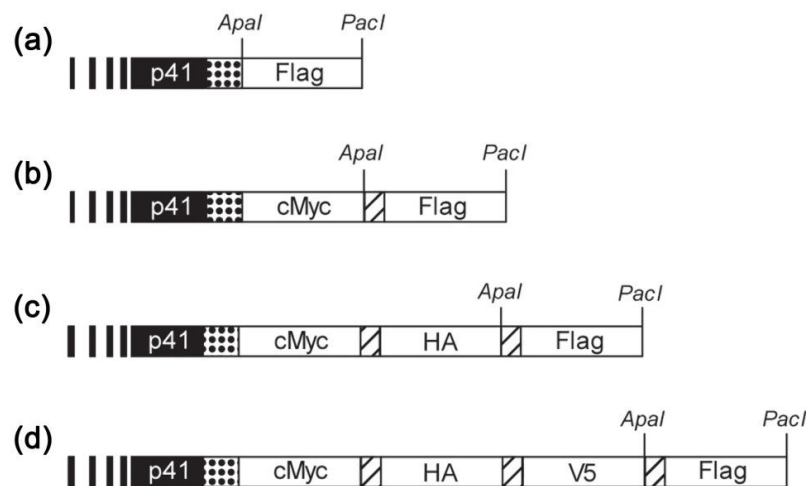


Figure 5 | Schematic representation of TBSV cDNA chimeras' constructs. As simplification, is illustrated only the 3'-CP engineered region of the (a) TBSV-Flag, (b) TBSV-cMyc, (c) TBSV-HA, (d) TBSV-V5 constructs. The dotted boxes represent a seven length glycine rich spacer and the striped boxes a Gly-Pro-Gly amino acidic linker.

When the introduction of the last 2 tag peptide modules were successfully confirmed by sequencing, the TBSV-HA and TBSV-V5 chimeric CPs resulted in respectively 40 and 56 amino acids extensions compared to the TBSV wild-type (-wt) CP. In all cases, the 5' end of each chimeric peptide CDS was designed *in silico* to generate, upon genetic fusion, a GGPGGGG linker peptide between the CP and the first tag module, providing flexibility to the exogenous fragment and avoiding undesirable interferences with virus

assembly. Moreover, to separate each tag module from the others, GPG spacer CDSs were introduced by design into the encoding sequence oligonucleotides. This sequence was employed primarily for the well documented ability of GPG to interrupt protein secondary structures, providing flexibility to the residing region and, consequently, promoting each peptide to assume its original conformation independently of other modules (Wriggers, Chakravarty et al. 2005). All the peptide CDSs as well as the amino acidic linker and spacers were cloned in the same reading frame with the CP. A novel stop codon was flanked at the 3' end of the last Flag module during the *in silico* design process. In fact the TBSV-vector was devoid of the original *cp amber* codon. In addition, all tags CDSs were *in silico* optimized for *N. benthamiana* codon bias to gain the highest expression level during *in planta* production.

TBSV-GFP construction

After the generation of the previously described 4 TBSV chimeric constructs, the attempt of displaying the entire green fluorescent protein (GFP) was carried out. TBSV-Flag was digested with *ApaI* and *PacI* to prepare the vector to sustain the introduction of the GFP CDS in place of the Flag CDS downstream the GGPGGGG linker peptide coding sequence. Differently from the 4 TBSV chimeras, whose tags CDSs were *in silico* designed and then synthesized at MWG in form of oligonucleotides, the GFP coding fragment to be inserted within the cDNA vector was produced by PCR using the pPVX204 expression vector (Baulcombe, Chapman et al. 1995) as a template. Since the pPVX204 lacks specific recognition restriction sites flanking the GFP CDS, two primers (GFP-For, GFP-Rev; see M&M for sequence) carrying clamps at the 5' ends, corresponding to the restriction site *ApaI* (GGGCCC) and *PacI* (TTAATTAA), were synthesized; some additional nucleotides were included upstream of the restriction site in both primer extensions to ensure maximum enzyme cutting activity. In this circumstance, the stop codon was already present at the end of the GFP coding sequence and thus it was not

introduced again by design. The amplification product (~640 bp) obtained by PCR was visualized on agarose gel for size confirmation and, subsequently to purification and quantification steps, it was digested to generate the proper sticky ends. Compatible backbone and insert were included in the ligation reaction and, after electro-competent cells were transformed, positive colonies containing the insert of the correct size were sent for sequencing. Alignment of the electropherogram output with GFP reference sequence resulted in 100% rate of identity, confirming the absence of error occurrences during *proof-reading* polymerase activity. As a result of the cloning procedure, the generated TBSV-GFP chimera carried 245 additional amino acids as CP C-terminal fusion.

In vitro transcription constructs

All the generated TBSV chimeras as well as the TBSV-P construct itself (Szittyá, Salamon et al. 2000) harbor the cDNA of the virus embedded in the context of a commercial plasmid for molecular biology. Plasmid DNA can be easily amplified inside *E. coli* cells, purified with high yields through miniPrep procedures, and finally used for all common genetic engineering procedures. Managing double-stranded DNA is by now relatively easy and allows even complex reactions otherwise impossible to be carried out with RNA. TBSV genome is constituted by a unique single-stranded RNA molecule with positive polarity, lacking both 5'-cap and 3'-poly(A). For this reason TBSV cDNA constructs need to be transcribed into corresponding RNA molecules in order to trigger plant infection. Once the viral genome reaches plant cell cytoplasm, it can be translated by cellular machinery into viral RdRp proteins, which initiate the TBSV infection cycle. Theoretically, even a single molecule of infective RNA is able to generate an abundant virus progeny. TBSV-wt and all the derived chimeras' genomes have been designed to be under control of the T7 phage promoter sequence (**Fig. 6a**).

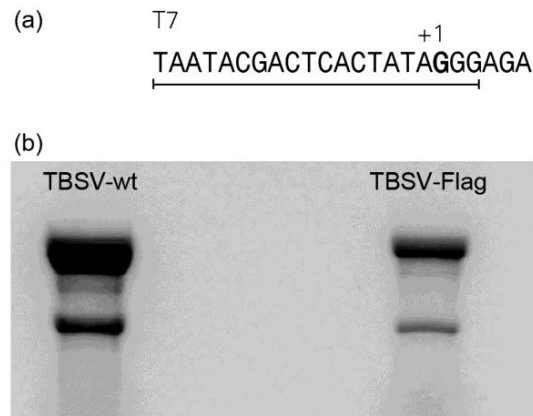


Figure 6 | Molecular aspects of T7 *in vitro* transcription technique. (a) T7 phage polymerase promoter. The minimal sequence needed for efficient transcription is underlined. The +1 base (in bold) is the first base incorporated into RNA during transcription. (b) TBE agarose gel electrophoresis of *in vitro* transcribed RNAs. Four microliters of the performed reaction are run on gel under denaturing condition. The upper bands of both TBSV-wt and TBSV-Flag lanes represent the transcribed RNAs, while the lower band is the linearized cDNA template used in the reaction.

Therefore, in this study T7 transcription was the standard method of producing RNA *in vitro*. T7 polymerase is a very active phage polymerase that uses a short promoter sequence to initiate transcription at a specific base in the template (**Fig. 6a**) and then goes on until the end of the template strand is reached. The enzyme is unable to recognize proper transcription termination sequences and thus using circular plasmid as a template will generate extremely long and heterogeneous RNA transcripts. As a matter of the fact, plasmid DNA templates need to be linearized with the appropriate restriction enzyme downstream of the sequence to be transcribed. At genome 3' end, all the TBSV cDNA constructs were designed to bear a unique *XmaI* restriction recognition site, which was used to generate linear templates indeed. Results of the digestions were always checked on a gel to confirm that cleavage was complete. After linearization, the transcription reaction was performed following the MEGAscript kit (Ambion) manufacturer protocol. Finally, the integrity of the transcribed RNA was verified by TBE agarose gel electrophoresis (**Fig. 6b**).

In planta transcription constructs

To produce an alternative approach for the plant infection, which is normally obtained through the inoculation of infectious *in vitro* transcribed RNA, an *in vivo* transcription model strategy based on the Cauliflower mosaic virus (CaMV) 35S promoter (Odell, Nagy et al. 1985) was designed (Fig. 7).

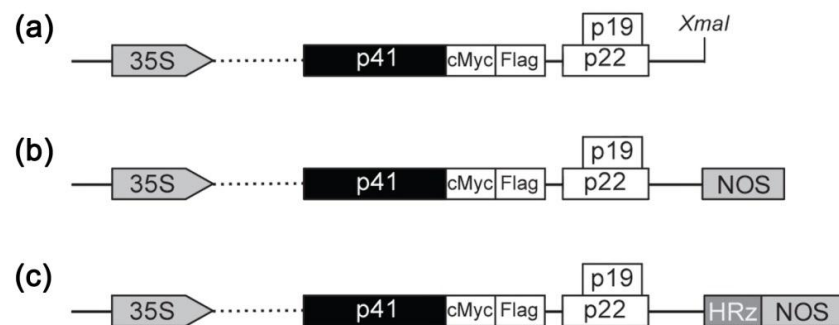


Figure 7 | Schematic representation of *in vivo* TBSV-cMyc expression vectors, based on Cauliflower mosaic virus 35S promoter and *A. tumefaciens* NOS terminator. (a) 35S-TBSV-cMyc, (b) 35S-TBSV-cMyc.NOS, (c) 35S-TBSV-cMyc.riboNOS. The dotted line represents schematically the whole genomic sequence between the first 5' TBSV nucleotide and the p41 ORF. The HDV anti-genomic ribozyme site was reported as a "HRz" named box.

Using the TBSV-cMyc construct as a template, the CaMV 35S promoter sequence was introduced in place of the original T7 promoter, residing in the original TBSV-P construct and in all TBSV derived chimeras, thus generating the 35S-TBSV-cMyc (Fig. 7a). The first step toward the generation of such *in planta* expression vector was the identification of unique restriction recognition sites surrounding the 5' region of the TBSV-cMyc construct: *Bam*HI and *Age*I sites, which were located upstream of the first T7 nucleotide and within the p33 ORF respectively, were selected. The CaMV 35S sequence was amplified by PCR using the pPVX204 expression vector as a template and a pair of specific primers (TBSV-35S-For, TBSV-35S-Rev; see M&M for sequence); both primers were designed to anneal exactly onto the first and last nucleotide of the 35S sequence, and to carry, in the case of the forward primer, an additional 5' *Bam*HI extension. In parallel, the 5' TBSV

genome context was amplified by PCR using a forward primer (TBSV-5'context-For; see M&M for sequence), covering the authentic 5' end of TBSV genome (Hearne, Knorr et al. 1990), and a reverse primer (TBSV-5' context-Rev; see M&M for sequence) with an additional 5' *AgeI* recognition sequence extension. Next, both PCR products were properly *BamHI* and *AgeI* digested, purified and included in a pre-ligation reaction in order to join the two fragments using the blunt ends generated by the *proof-reading* polymerase. Finally, the pre-ligation mixture, containing a compatible TBSV 5' genomic context under the control of a 35S promoter, was added with the TBSV-cMyc construct, previously digested *BamHI/AgeI*, to generate the 35S-TBSV-cMyc construct (**Fig. 7a**). At this stage of the cloning strategy, although the whole TBSV-cMyc sequence could be directly *in vivo* transcribed by the plant cell expression machinery, the vector still needed an enzymatic *in vitro* linearization as it lacked a termination signal at the 3' end of the genome. For this reason, 2 additional constructs, both harboring the cDNA of the TBSV-cMyc under the control of the CaMV 35S promoter, were assembled modifying the 3' end context downstream the virus sequence: the 35S-TBSV-cMyc.NOS (**Fig. 7b**) additionally contained the termination sequence of the nopaline synthase (NOS; Depicker, Stachel et al. 1982) gene of *A. tumefaciens*, and the 35S-TBSV-cMyc.riboNOS (**Fig. 7c**) had the Hepatitis delta virus (HDV) antigenomic ribozyme (HRz; Chowrira, Pavco et al. 1994) sequence introduced between the 3' end of the genome and the NOS sequence. Ribozymes are RNAs with enzymatic activity that are able to cleave themselves or other RNA molecules in a sequence-specific manner. Depending on the location of the processing site, ribozymes are classified as *trans*-acting, if the target is outside their sequence, or conversely *cis*-acting, when the RNA molecule can undergo self-cleavage. In any case, their activity is strictly correlated to their function (Doherty and Doudna 2001). HDV is a small single-stranded RNA satellite of HBV, and although it is a human pathogen, it shares a number of features with a subset of the small plant satellite RNA viruses. In fact, thanks to the extensive self-

complementarity of genome sequence, HDV is characterized by the presence of self-cleaving activity in both the genomic and antigenomic viral RNAs. The self-cleaving sequences are critical to viral replication as HDV needs to process *in vivo* the products of rolling-circle replication to unit-length RNA molecules (Been and Wickham 1997). This particular ribozyme element, already employed by Scholthof (1999), when properly inserted is capable, through auto catalytic activity, to generate 3' RNA terminal sequences identical to those of the TBSV genome, eliminating regions derived from nuclear transcription and normally not present on the infectious viral RNAs, such as the poly-adenylation signals. To generate these constructs, the unique *XmaI* restriction site, which was already employed for accurate cleavage at the last TBSV nucleotide during *in vitro* production of infective RNAs, and the *PacI* recognition sequence, located downstream the 3' terminal region of the 35S-TBSV-cMyc construct, were chosen for cloning assessment. Also in this case, the pPVX204 expression vector was used as a template, and the NOS sequence was amplified by PCR with a pair of specific forward and reverse primers (PCR-NOS-For, PCR-NOS-Rev; see M&M for sequence) owning a 5' *XmaI* or *SacI* extension respectively. The fragment containing the HRz sequence, and bearing *XmaI* protruding compatible sequences on both ends, was generated by *in vitro* annealing of two complementary sense and antisense oligonucleotides. Subsequently, the 35S-TBSV-cMyc construct and the NOS fragment were *XmaI/SacI* digested and included in a three fragments ligation with the *XmaI* compatible HRz fragment. To verify proper construct assembly, single colonies, grown overnight at 37°C on LB-agar medium, were used in a colony-PCR reaction as a template. Candidate constructs were screened for the presence of NOS, thus generating the 35S-TBSV-cMyc.NOS vector (**Fig. 7b**), or for both fragments in the correct orientation, thus obtaining the 35S-TBSV-cMyc.riboNOS construct (**Fig. 7c**). Finally, all clones were verified by sequencing at BMR Genomics with specific primers (TBSV-1For, TBSV-2Back and ScreenNOS-Rev; see M&M for sequence).

Plant infection

Aim of the work was the generation of an efficient and versatile system for VNPs production based on TBSV. As previously described, TBSV-P was widely genetically engineered to sustain the expression of heterologous peptides, going from small amino acidic tags to the entire GFP, and to display such portions outward the viral protein cage. Nature has tuned the TBSV genome by selecting only the genomic sequence able to ensure the best fitness during plant infection, thus leading to the loss of those coding as well as non-coding sequences unnecessary for virus replication cycle. As a matter of the fact, it was verified that each generated construct still retained the ability to establish viral infection on *N. benthamiana* plants after genetic modification. TBSV-P, that *in vivo* produces TBSV-wt particles and -Flag, -cMyc, -HA and -V5 vectors were all linearized exactly at 3' genomic end by digestion with *XmaI* restriction enzyme. The cDNA was then purified and used as a template for the *in vitro* transcription of infectious RNAs as previously described; therefore, TBSV genome does not require 5'-cap neither 3'-poly(A) to trigger plant infection. TBSV RNAs were used to inoculate 6-8 weeks old *N. benthamiana* plants by gently rubbing the surfaces of 2 leaves per plant with silicon carbide, and distributing on each leaf approximately 2-3 μg of RNAs. The symptomatology was constantly monitored and documented by photo capturing (**Fig. 8**). The appearance of the characteristic chlorotic local lesions onto inoculated leaves was observed at around 2-3 dpi. At 5-7 dpi symptoms appeared systemically showing mottling, severe distortion and stunting of the leaves (**Fig. 8b,c**). Necrosis of the apical shoots and finally the death of the plant occurred between 11 and 14 dpi (**Fig. 8d,e**). Despite the evident differences between TBSV-wt and its derived chimeras in terms of CP dimension and genomic length, plants inoculated with infectious RNAs of all construct showed comparable symptoms progression and severity.

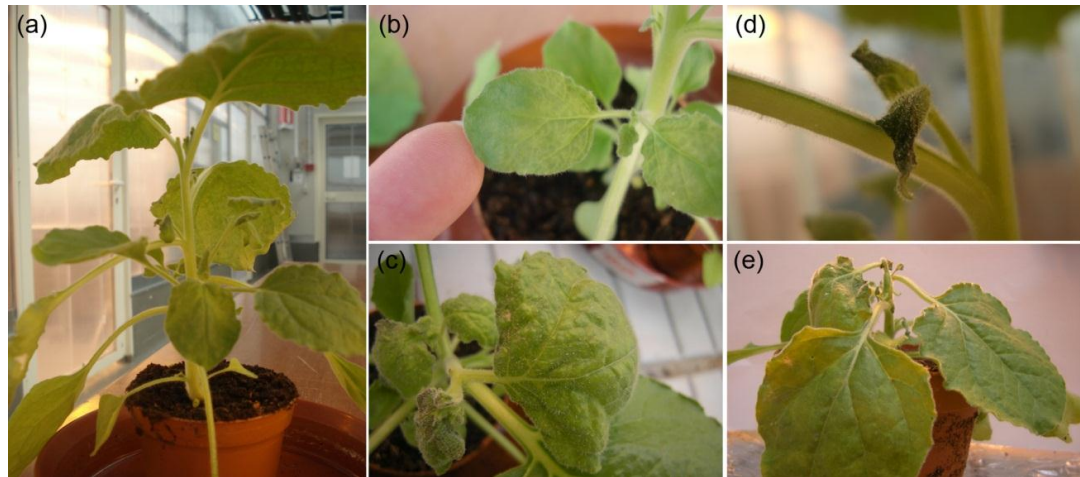


Figure 8 | Typical symptoms elicited by TBSV infection of *N. benthamiana* plants. (a) *N. benthamiana* not-infected plant; (b) particular of vein chlorosis on a systemic leaf; (c) severe distortion and stunting of the leaves; (d) necrosis of the apical shoots; (e) bushy appearance before death of the plant occurred.

To assess if the virus was still able to replicate even after the addition of a longer sequence, GFP CDS was added to the viral sequence. Differently from what experimented with the 4 TBSV chimeras expressing the tag peptides, when *N. benthamiana* plants were inoculated with the *in vitro* transcribed RNA of TBSV-GFP, no symptoms were detected on either inoculated or systemic leaves, even at 20 dpi. In addition, leaves were harvested and carefully observed under UV light in order to locate GFP, which was indeed undetectable as demonstrated by the absence of fluorescence emission. After several attempts to establish infection, we concluded that TBSV-GFP construct was unable to replicate *in vivo* and thus it was non-infectious. Although molecular aspects of such result were not further analyzed, the loss of infectivity could reside on either genomic or protein levels. Therefore, the expression of a large heterologous fusion peptide could impair CP function and, being reflected by a sensible extension of viral genome sequence, alter also the replication process. In the light of a large scale production, a great number of plants was directly inoculated with sap material deriving from first and second generation of infected tissues (**Fig. 9**).

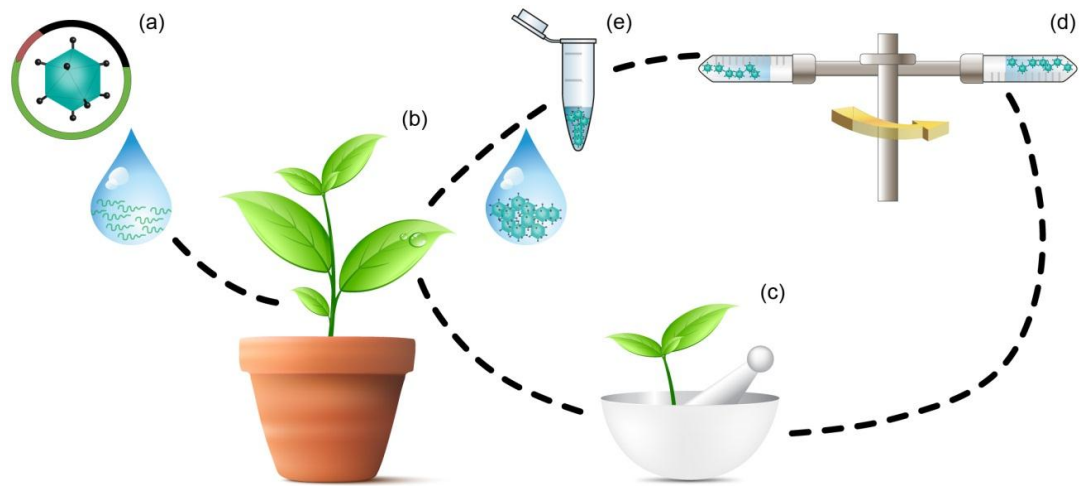


Figure 9 | Schematic representation of a typical VNPs production cycle. (a) TBSV-based cDNA vector is used as a template for the *in vitro* transcription of infectious RNAs. (b) *N. benthamiana* plants are inoculated with the infectious RNA or virus particles. (c) Infected leaves are collected 7-9 days post-infection and ground to a fine powder using a mortar and pestle. (d) Virus particles are purified through sedimentation by ultra-centrifugation. (e) Purified VNPs are used or stocked at -20°C.

When plants were infected with assembled VNPs instead of transcribed RNAs, symptoms progression did not change even if severity sometimes increased, especially on inoculated leaves. We hypothesized that this phenomenon could be related to the higher concentration of infectious agents associated with systemic infected tissues. Therefore, when plants were infected by using sap derived from inoculated leaves, which generally contained a lower quantity of virus, milder symptoms were observed. In any case, inoculated leaves as well as those showing systemic infection were harvested at 7-9 dpi, and VNPs were purified following the protocol of Burgyan and Russo (1998) with some modifications. The recovery among different CVPs was very similar and allowed to produce approximately 300 µg of VNPs per gram of fresh leaf tissue. The quality of each purification was always verified by a silver stained SDS-PAGE before employing the VNPs in downstream studies. As previously described, an alternative *in vivo* transcription model based on plant expression strategy was designed, and 3 different constructs were assembled: 35S-TBSV-cMyc, -cMyc.NOS and -cMyc.riboNOS. To test the infectivity of the 3 different expression vectors,

5 plants of *N. benthamiana* were inoculated using 2 leaves per plant with each of the different purified cDNA expression constructs at 3 different concentrations: 10, 20 or 30 μg . The symptomatology was accurately monitored and documented by photo capturing. Using 10 μg of plasmid none of the vectors was able to establish the infection. With 20 μg , at 10 dpi only upper leaves of plants inoculated with 35S-TBSV-cMyc.riboNOS vector showed evident systemic viral symptoms. With 30 μg the 35S-TBSV-cMyc.ribo-NOS vector produced systemic symptoms at already 6-8 dpi, whereas the 35S-TBSV-cMyc.NOS showed some mild signs of infection only at 19 dpi. All the attempts performed with linearized 35S-TBSV-cMyc vector, used at the 3 different concentrations, failed to induce both local symptoms development and systemic virus spread. As final biological prove of infection, a cycle of re-inoculations was performed using the sap obtained homogenizing the symptomatic systemic tissue of all infected plants. All primary infections were confirmed and, as expected, symptoms progression and severity returned identical to those obtained by inoculating infectious RNAs or assembled VNPs.

VNPs characterization

Observation of symptoms appearing during plant infection upon inoculation of the TBSV chimeric construct is a clear proof for proper replication and infection progression. However molecular evidence for correct assembly of chimeric VNPs needs to be demonstrated. All the experiments reported in the following paragraphs were carried out to demonstrate that assembly of all TBSV chimeras occurred during the infection cycle, and that VNPs properly expressed and displayed the heterologous portion outside the viral cage. Finally, a study on the genetic stability of the generated chimeras was performed.

Particle assembly

To verify proper particles assembly, in preliminary experiments TBSV-Flag was considered as representative for all chimeras. Crude extracts of symptomatic TBSV-wt or -Flag infected leaves were subjected to sucrose sedimentation analysis (**Fig. 10**).

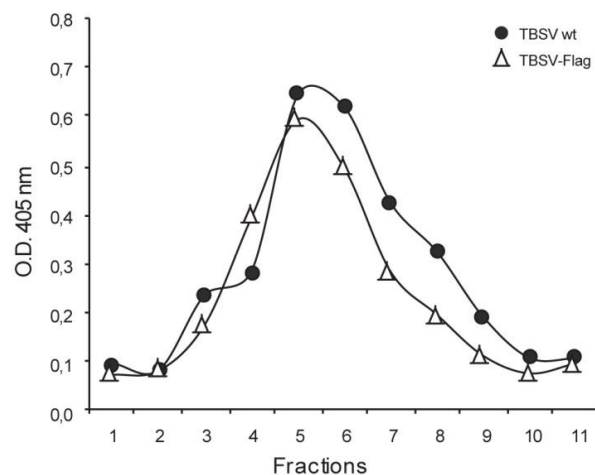


Figure 10 | Evaluation of TBSV wild-type and TBSV-Flag assembly. Crude extracts from TBSV wild-type and TBSV-Flag *N. benthamiana* infected plants were analyzed on a 10-60% sucrose gradient; 11 fractions were collected from top to bottom. The presence of TBSV particles in the collected fractions was determined by ELISA using anti-TBSV wild-type CP (●) and anti-Flag peptide (Δ) antibodies.

Viral suspensions were poured on top of a 10-60 % (w/v) sucrose gradient and depending on distinctive density of the molecules the analytical separation by ultra-centrifugation was allowed to occur. According to our experience, plant organelles and other macro-aggregates should sediment forming a pellet on the bottom of the tube, whereas smaller molecules such as plant proteins or the viral CP monomer should not be able to enter the sucrose gradient thus remaining on top; on the other hand, properly assembled VNPs, which owned an intermediate density, should penetrate the gradient forming a distinct band at the interface of a sucrose concentration able to prevent their migration. At the end of the analytical separation, 11 fractions were collected from the sucrose gradient and further analyzed by ELISA with specific antibodies against the viral CP or the Flag tag. The sedimentation profiles of TBSV-wt and -Flag crude extracts were similar, showing the center of the Gaussian distribution around 30% sucrose solution (**Fig. 10**). Besides physical proofs of nanoparticles formation, to obtain direct evidence of TBSV assembly purified TBSV-wt and all chimeras were subjected to transmission electron microscopy analysis (**Fig. 11**).

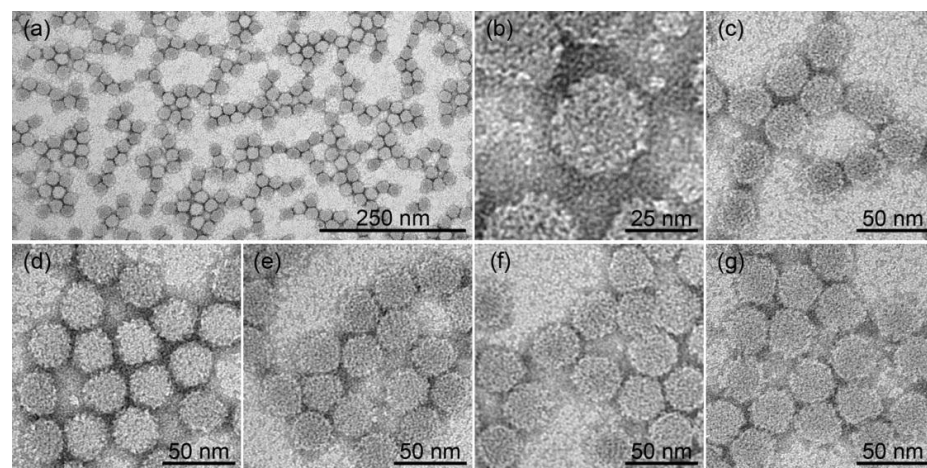


Figure 11 | Visualization by negative staining and high resolution electron microscopy of purified wild-type and chimeric TBSV particles. (a, b, c) Wild-type TBSV displayed at different magnifications; (d) TBSV-Flag; (e) TBSV-cMyc; (f) TBSV-HA; (g) TBSV-V5.

Samples were collected on electron microscopy grids and, after a staining with 2 % (w/v) uranyl acetate aqueous solution, images were acquired. Photos captured at several magnifications highlighted the absence of differences among each chimera and the TBSV-wt, with VNPs monodispersed in size and with a diameter of about 30 nm (**Fig. 11**).

Heterologous peptide expression

Obtained direct evidence of particles assembly, purified TBSV-wt and all TBSV chimeras were further characterized at proteomic level. Different protocols to avoid protein aggregate formation were tested after it was observed that sample migration on acrylamide gel tended to be prevented when VNPs were denatured by heating at 100°C in a classic Laemmli buffer (**Fig. 12**, lane 1), presumably due to cross-linking reactions between CP monomers. For this reason a different strategy involving the physico-chemical properties of TBSV was pursued. It has been demonstrated that TBSV capsid undergoes a pH- and metal ion-dependent structural transition (Heaton 1992), a mechanism probably exploited by the virus to unload the genomic content once entered the cell cytoplasm. Hence, a modified Laemmli buffer containing a Ca^{2+} chelator was generated by adding EDTA. In presence of EDTA and alkaline pH conditions TBSV particles tend to assume a relaxed form attributable to the repulsive charges generated at the interface of their capsomeric subunits for the chelation of divalent ions. Exploiting such thermodynamically unstable condition, it was possible to disassemble the VNPs without aggregate formation by decreasing both temperature and time of heat incubation. A far more efficient capsid denaturation was thus established resulting in a higher fraction of CP monomer that could be separated on acrylamide gel (**Fig. 12**).

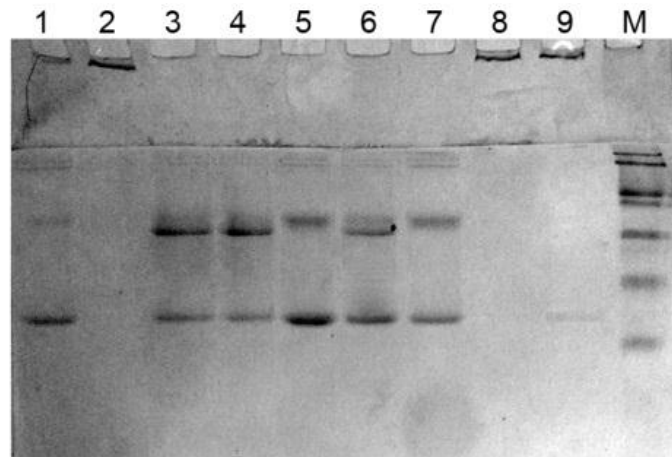


Figure 12 | SDS-PAGE of denatured TBSV particles. The same amount (1 μ g) of TBSV particles were analyzed by acrylamide gel electrophoresis upon different incubation conditions in Leammli buffer: (1) 100°C, 5'; (2) room temperature, 5'; (3) room temperature, 5' with EDTA; (4) 40°C, 1' with EDTA; (5) 60°C, 1' with EDTA; (6) 40°C, 5' with EDTA; (7) 60°C, 5' with EDTA; (8) 40°C, 5'; (9) 60°C, 5'. The EDTA was present at a final concentration of 5 mM. M= Marker.

In particular, it was observed a direct correlation between the increase of heating temperature and the amount of protein aggregates unable to enter the separating gel. Moreover, exploiting weak denaturing conditions a sensible increase of CP dimer signal (**Fig. 12**, upper bands) was observed. In fact, during particle assembly TBSV CP monomers interact one with the other to form dimer structures, representing the “assembly units” of the $T=3$ icosahedral symmetry (Harrison 2001). Finally, the best parameters found were to heat at 60°C for 1 minute in the presence of EDTA at a final concentration of 5 mM (**Fig. 12**, lane 5). Once the denaturation protocol was optimized, purified TBSV-wt and all TBSV chimeras were subjected to denaturation and the derived capsidic monomers were resolved by 13,5% silver stained SDS-PAGE (**Fig. 13**, upper panel). For all chimeric CPs, differences observed in the mobility throughout the acrylamide gel confirmed their expected sizes; all chimeras' derived monomers showed a clear and progressive shift in respect to wild-type CP migration and among each other, depending on their relative molecular weight. Since all chimeras displayed the Flag tag as part of the CP fusion peptide, the same samples were further

analyzed by western blotting using the anti-Flag specific antibody (**Fig. 13**, lower panel).

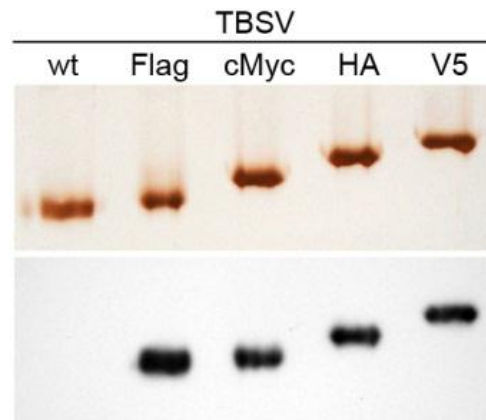


Figure 13 | SDS-PAGE analysis of denatured particles. TBSV wild-type and all the TBSV-chimeras CPs were analyzed by silver staining (upper panel) and Western blot (lower panel) using anti-Flag antibodies.

Made exception for the TBSV-wt, which in this case was considered as a negative control, results showed the presence of the Flag tag in all the fusion assemblies, confirming that mobility shift among the chimeric and wild-type CPs was clearly related to the respective sizes.

Heterologous peptide display

Once the expression of all chimeric CPs was demonstrated, to assess also those fusion peptides were correctly exposed onto the surface of properly assembled viral nanoparticles, an ELISA analysis with antibodies specific to each individual tag was performed (**Fig. 14**); in contrast with western blotting analysis, ELISA did not require protein denaturation, therefore the expected display of each exogenous peptide module was investigated directly on VNPs being in native form. A total protein raw extract was prepared from the infected tissue of plants inoculated with all the different constructs. Viral suspensions were quantified using the Bradford Reagent (Bio-rad), and an equal amount of normalized extracts were evaluated with ELISA; a crude extract of a not-infected *N. benthamiana* plant was used as a negative

control. Specific binding of the anti-tag antibodies directed against the chimeras was observed (**Fig. 14**).

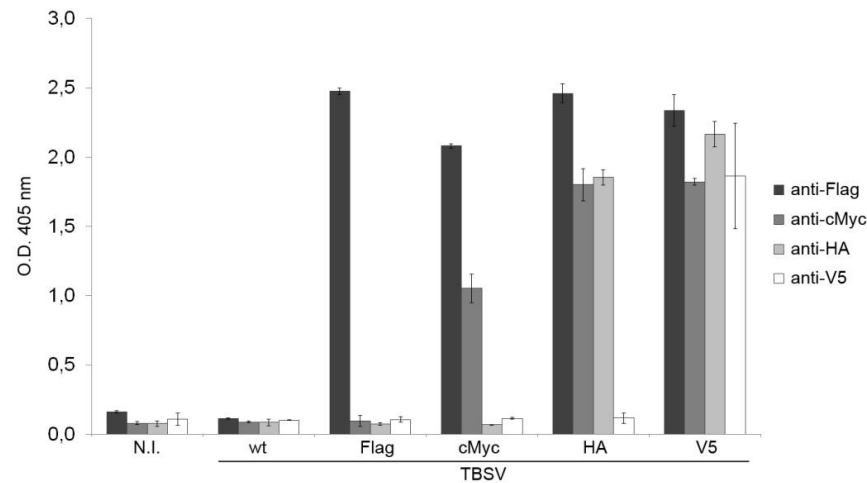


Figure 14 | ELISA analysis of properly assembled TBSV particles. TBSV wild-type and all TBSV chimeric VNPs were probed separately with specific anti-Tag antibodies. A total soluble protein extract from not-infected (N.I.) *N. benthamiana* plant was used as a negative control.

Anti-Flag, -cMyc, -HA and -V5 antibodies were able to recognize the corresponding tag peptide, expressed as C-terminal fusion of the CP, demonstrating the correct presence of the peptides at protein level, their exposure on virion surface and their individual accessibility for antibodies binding.

TBSV chimeras genomic stability

A relative instability for genetically modified viral based construct has been broadly reported in literature. In fact, whether the added or modified sequence impairs viral fitness, the viral genome tries to rearrange with single or multiple mutations in order to restore the natural genomic configuration able to guarantee an overall superior fitness. Sometimes even complete recombination events, resulting in total extrusion of the heterologous portion have been reported (Lico, Capuano et al. 2006; Avesani, Marconi et al. 2007). From a production point of view, construct stability over subsequent viral

generations is an important parameter as it allows the use of infected material to scale up the production process without affecting costs exponentially. As a matter of the fact, integrity of the sequence at nucleic acid level was evaluated. Leaves of primary infected plants showing systemic symptoms were harvested and the genetic stability of the chimeric *cp* genes was verified by RT-PCR and sequencing (**Fig. 15**).

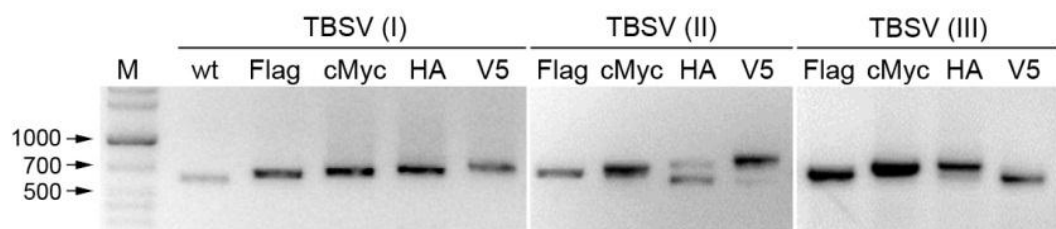


Figure 15 | Evaluation of the presence of the heterologous sequences at the genomic level. Agarose gel electrophoresis of RT-PCR covering the *cp* gene 3' region of the TBSV-wt and of all TBSV chimeras. Viral genomes were analyzed in the first (left panel), second (center panel), and third generation (right panel) of infection.

The mobility shift of PCR fragments on agarose gel represented the different length of the constructs at genomic level, and the sequencing of the bands confirmed the presence of the correct heterologous sequences (**Fig. 15**, left panel). Next, cycles of reinfections were performed by inoculating *N. benthamiana* plants with sap prepared from symptomatic systemic tissues of first or second generation infected plants. Symptomatic inoculated as well as systemic leaves were harvested at 7-9 dpi and total extracted RNAs were subjected to RT-PCR to amplify the genomic 3' *cp* region. The resulting fragments were resolved by agarose gel electrophoresis, and sequenced. Complete recombination of chimeric replicons at the second generation of infections was never detected (**Fig. 15**, center panel). Beyond second generation we have sporadically experienced some construct instability, especially when the largest fusions were concerned (**Fig. 15**, right panel). In any case, it has to be stressed that length of heterologous insertion at genomic

as well as protein level is not the only parameter to be considered; in fact each individual sequence used for the generation of a new chimera must be evaluated empirically on a case to case basis.



VNPs modifications

Exploitation of the internal cavity of VNPs

Many icosahedral plant viruses, in presence of specific physicochemical conditions, are subjected to the reversible opening of pores on their capsid surface. This process is usually referred to as swelling. In the case of the TBSV, it is reported that inner core can be reached by applying slightly alkaline conditions (pH 8.5) and divalent ion chelators (Heaton 1992). We have demonstrated that optimal particle denaturation is obtained by the addition of EDTA and in presence of a basic environment, settings by which TBSV virions tend to assume a relaxed form. To further test cations depletion and pH adjustment as prerequisites for the accessibility to the viral RNA contained in the VNPs' cavity, TBSV-wt or -Flag particles were challenged for susceptibility to RNase activity (**Fig. 16a**). Particles were independently incubated at 4°C for 2 hours in control (0,1 M Tris, pH 5.5) and swelling buffer (0,1 M Tris, 50 mM EDTA, pH 8.5) to induce a preferential capsid transition toward the compact or swollen conformation respectively. Finally, the RNase was added and left to act for additional 30 minutes. Viral genomic RNA was extracted from VNPs used in each treatment and then analyzed by agarose gel electrophoresis. The RNA enclosed in the TBSV nanoparticles incubated at pH 8.5 and supplemented with EDTA 50 mM was completely degraded (**Fig. 16a**, lanes 5, 6), whereas the genome within virions at pH 5.5 resulted fully protected (**Fig. 16a**, lanes 3, 4), as the untreated particles' controls (**Fig. 16a**, lanes 1, 2). Besides the evidence of capsid dynamics control by tuning surrounding molecular environment, access and release of small cargo molecules to and from the interior of the virion was attempted. As proof of concept, loading of the small EtBr molecule into swollen TBSV nanoparticles was tested (**Fig. 16**).

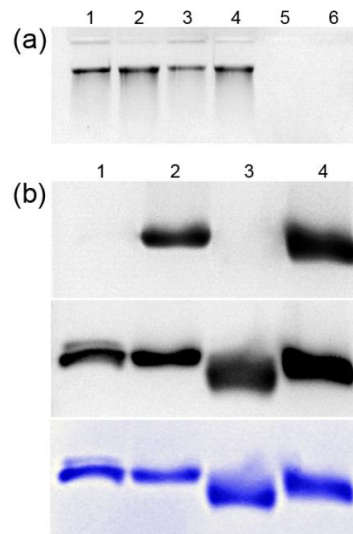


Figure 16 | Evaluation of TBSV internal cavity accessibility. (a) Ribonuclease A protection assay. Ethidium bromide stained agarose gel of TBSV extracted RNAs. Untreated TBSV particles were used as control of genome extraction (lane 1, TBSV-wt, and lane 2, TBSV-Flag). Purified particles were treated with ribonuclease A in compact (lane 3, TBSV-wt, and lane 4, TBSV-Flag) or swollen state (lane 5, TBSV-wt, and lane 6, TBSV-Flag) before RNA extraction. (b) Ethidium bromide loading by controlled TBSV capsid expansion. (Upper panel) Agarose gel of TBSV-wt (lane 1 and 2) and TBSV-Flag particles (lane 3 and 4) incubated with EtBr in swollen (lane 2 and 4) or compact state (lane 1 and 3). Further, the same gel was incubated in swelling buffer supplemented with EtBr (middle panel) and then stained with Coomassie Blue (lower panel).

Approximately 4 μg of purified TBSV-wt or -Flag particles were incubated in swelling buffer (**Fig. 16b**, lanes 2, 4) or control buffer (**Fig. 16b**, lanes 1, 3), both containing EtBr at a final concentration of 0,5 $\mu\text{g}/\text{mL}$, leading the dye molecule to move toward the VNPs core by passive diffusion. After the incubation, the purified viral suspension were resolved by agarose gel electrophoresis and visualized under UV light. According to the nature of the EtBr molecule, the signal was visible only when this compound penetrated into cavity of swollen particles intercalating the viral RNA (**Fig. 16b**, upper panel, lanes 2, 4). Therefore, fluorescence was not detectable in lanes containing the virions being in compact state (**Fig. 16b**, upper panel, lanes 1, 3). When the whole gel, after the run, was incubated in swelling buffer and fresh EtBr was added, the particles previously in compact state underwent swelling and became visible once exposed to UV light (**Fig. 16b**, middle panel, lanes 1, 3). Finally, the integrity of TBSV nanoparticles after the treatments was proved by staining the same gel with Coomassie Brilliant Blue, highlighting the co-migration of genomic RNA with capsid proteins (**Fig. 16b**, lower panel). We concluded that switching between the two conformational states of the capsid we were able to make the interior cavity of TBSV VNPs accessible to RNAase as well as to small guest cargo molecules.

Chemical derivatization of VNPs

After the display of peptides through genetic modification was exploited, the possibility to decorate VNPs' outer surface by *in vitro* chemical conjugation was explored (**Fig. 17**).

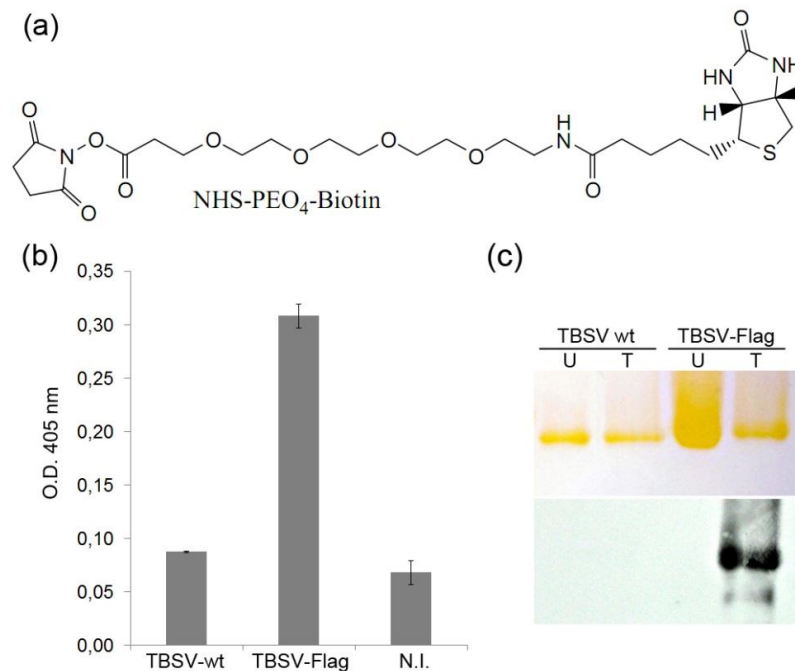


Figure 17 | Chemical derivatization of TBSV nanoparticles. Purified TBSV-wt and TBSV-Flag particles were used in reaction with a 10-fold molar excess of NHS-PEO₄Biotin for 24 h. Byproducts and not-reacted biotin reagent were removed by chromatography. (a) Chemical structure of biotin NHS ester reagent. (b) ELISA analysis of biotin bioconjugated VNPs using a streptavidin-horseradish peroxidase conjugate as probe. A total soluble protein extract from not-infected *N. benthamiana* plant was used as a negative control (C-). (c) SDS-PAGE analysis of denatured bioconjugated (T) and untreated (U) VNPs. TBSV-wt and TBSV-Flag CPs were further analyzed by silver staining (upper panel) and Western blot (lower panel) using a HRP-conjugate as probe.

In general, *in vitro* chemical modification relies on the covalent attachment of an activated conjugate to functional groups of amino acids residues of a protein. This technique has the advantage to use directly assembled VNPs, hence preventing all the problems related to CP folding and capsid formation, and gives the possibility to conjugate different molecules than peptides. The amine functional group of lysine is a common target for conjugation through

NHS ester based chemistry (Wang, Kaltgrad et al. 2002; Smith, Lindbo et al. 2006). NHS ester reagents react efficiently with primary amino groups (-NH₂) by nucleophilic attack, forming an amide bond and hence releasing the NHS moiety. Thirteen lysine residues are contained in the TBSV-wt CP, however due to folding rearrangement no primary amines are exposed and thus addressable on the outer viral shell (Hsu, Singh et al. 2006). Nevertheless, the Flag (DYKDDDDK) tag, which is the most distal peptide on each chimera, carries 2 genetically introduced lysine residues, one of those being at the very last carboxi-terminus. To probe for addressable reactive amine groups, *in vitro* biotinylation experiments were performed on TBSV-wt or -Flag particles following the EZ-Link® MicroNHS-polyethylene-oxide (PEO₄)-Biotinylation Kit (Thermo Scientific) manufacturer's instructions. The kit provided all the reagents required for labeling macromolecules containing addressable primary amino groups. In particular, due to general hydrophobicity of biotin moiety, a long hydrocarbon spacer arm (PEO, also called polyethylene glycol; **Fig. 17a**) was designed to impart water solubility and avoid that biotinylated molecules aggregate when stored in solution. Approximately 200 µg of VNPs were mixed with NHS-PEO₄ biotin reagent at tenfold molar excess and incubated for 2 hours in ice and then over-night at 4°C. The non-reacted biotin reagent and the byproducts of the reaction were then removed by chromatography during the desalting step on a spin column. A sample from each purified reaction was analyzed by ELISA and western blot using a HRP-conjugated streptavidin as a probe (**Fig. 17b**). The results demonstrated that TBSV-Flag particles were suitable for conjugation to biotin (**Fig. 17c**, lower panel, lanes 3, 4) whereas, as predicted, it was not possible to functionalize unmodified wild-type virions (**Fig. 17c**, lower panel, lanes 1, 2). Finally, the presence of TBSV CPs was detected through a silver stained SDS-PAGE (**Fig. 17c**, upper panel), which confirmed the molecular weight of the proteins in comparison with a marker. We concluded that bioconjugation of biotin on TBSV-Flag makes possible to redecorate VNPs surface.

Discussion

In recent years, there has been an upsurge of interest concerning nanotechnology and especially in nanoparticulate aggregations. Nanotechnology is not itself a single emerging scientific discipline but rather a meeting point of traditional sciences like chemistry, physics, biology and materials science. All these sciences bring together the required collective knowledge and expertise required for the development of novel technologies. Many believe that nanotechnology is ready to guide the next industrial revolution, taking part into a broad range of application fields from biomedicine to electronics. In an incredible short period of time, the emergence of nanoparticle tools has matched and even exceeded the capabilities of traditional imaging, delivery, and sensing devices (Gomme, McCann et al. 2005; Lewis, Destito et al. 2006; Bar, Yacoby et al. 2008; Hooker, O'Neil et al. 2008). In this context, viruses have received a great attention in nanotechnology as potential source of biological nanoparticles. VNPs are virus-based nanoparticle formulations that can be used as a building block for novel materials with a variety of properties. VNPs can be based on bacteriophages, plant or animal viruses, and they can be infectious as well as non-infectious (Grasso and Santi 2010). In particular, plant viruses have been extensively exploited in the development of novel nanotechnological tools for drug delivery, bioimaging, biomaterials and nanostructured electronic devices (Young, Willits et al. 2008). Plant viruses are spherical or rod shaped particles that usually contain a small, single stranded, sensed RNA genome, which can trigger the replication cycle once inside the plant cell cytoplasm. The limited genomes size, together with the precise knowledge of their sequence, make possible to retro-transcribe them into infectious cDNA clones that can be easily inserted within common

plasmid for molecular biology. The ease of handling of such cDNA constructs allows a rapid production of modified clones that can be further experimentally tested for their peculiar activity. In nanotechnology, chimeric VNPs can be developed to fine-tune and alter the surface properties of the wild-type protein cage. Nowadays, mutagenesis of viral capsids by operating at genomic level is a well-established technique, which allows alteration of the surface properties, such as the outer or inner charge of the cage (Dujardin, Peet et al. 2003; Brumfield, Willits et al. 2004), and also the display of peptides on the particle (Lee, Mao et al. 2002; Huang, Chiang et al. 2005; Lico, Mancini et al. 2009). In these terms, additional amino acid side chains can be introduced onto the capsid to allow chemical modification and the installation of additional functionalities (Peabody 2003). Moreover, plant viruses are completely safe for both human and animals as their replication cycle is confined within plants cells. This is an advantage not only in terms of safety issue but also as far as production is concerned. Therefore, plants have been extensively reported as excellent bioreactor systems. They are safe, cost-effective and support VNPs production in both laboratory setting and large scale production facilities (Santi, Huang et al. 2006). Finally, exploiting the particulate nature and the intrinsic resistance of VNPs to a variety of physicochemical conditions, purification from plant material is simple, efficient, high yielding and quick (Scholthof et al. 1996; Chen and Lai 2012). In this light, the TBSV pepper isolate infectious clone (Szittyá, Salamon et al. 2000) was used to develop a multivalent platform exploitable for nanobiotechnology applications (Grasso, Lico et al. 2012). Four commercial tag peptides were successfully cloned in a modular fashion to obtain chimeric CPs sequentially increasing in length. The correct expression of the fusion proteins as well as the exposition outward the viral protein cage was widely demonstrated, producing also compelling evidence of particle assembly by direct visualization through electron microscopy. In any case, homogeneity regarding both dimensions and shape was proved among different chimeras. Therefore, despite the presence of additional heterologous fusion peptides,

TBSV CP monomers seem to retain the ability to fold correctly in their secondary structure and then, interacting one with the other, assemble in icosahedral particles of 30 nm in diameter. Due to the complex nature of the intra- and intermolecular interactions necessary to form the viral capsid, we suggest that the presence of a GGPGGG linker peptide, spacing the CP from the heterologous portion, could play a fundamental role in chimeras' assembly. Hence, while glycine residues confer flexibility, the proline interrupts any protein secondary structure and, consequently, promotes adjacent portions to assume their own conformation independently from flanking regions. TBSV chimeric VNPs, being in their native arrangement, were independently probed with specific antibodies able to recognize and bind each tag peptide. Results obtained through ELISA analysis revealed that the progressive fusion of different peptides did not affect the structure required for their molecular recognition. In fact, even in the multiple modules assemblies (TBSV-cMyc, -HA and -V5) each tag was efficiently recognized when individually probed with the respective antibody. Also in this circumstance, the designed GPG spacers, interjected between adjacent peptide sequences, provided independent structural folding and allowed each tag to be recognized as a distinct domain. As far, the longest assembly we were successfully able to produce was the TBSV-V5, which displays 56 additional amino acids as C-terminal fusion of the CP. Albeit results obtained are already quite beyond the reported 16 amino acids long foreign peptide derived from the V3 loop of HIV-1 (Joelson, Akerblom et al. 1997), it has to be stressed that TBSV might sustain even longer fusions. Anyway, our attempt to clone the entire GFP coding sequence in frame with the TBSV *cp* gene resulted in a non-infectious construct. Several plants were inoculated with the *in vitro* transcribed RNA of TBSV-GFP vector but they all failed to produce the typical symptoms associated with viral infection. To confirm plant phenotype evidence of virus deficiency, inoculated and systemic leaves were further analyzed under UV light to locate GFP. However, protein fluorescence emission was undetectable even in those leaves showing

general mild signs of stress. Whether the expression of the entire GFP as a CP fusion failed, this result does not reduce the potential of such VNPs as display scaffold. In fact, getting things into perspective, the generation of GFP chimeric protein would result in an extension of more than 80% of the original size and it is probable that the amino acid linker is not long enough to provide the proper conformational independence to the two portions. It is also possible that other causes participated to abolish TBSV infective efficacy, in fact several studies suggest that CP of this genus of single-stranded sensed RNA viruses is dispensable for infection of certain *Nicotiana* species, even if the presence of the capsid enhances efficient systemic spread (Scholthof, Morris et al. 1993). In this light, it assumes particular importance to shift the attention from a translational to a transcriptional point of view. A progressive deep understanding of the molecular biology of tombusviruses has revealed how infection cycle relies on many diverse and complex inter- and intra-genomic interactions (Russo, Burgyan et al. 1994). Consequently, the introduction at genomic level of the GFP coding sequence could impair virus replication ability and thus justify the complete absence of symptomatology on inoculated plant. All constructs were evaluated for stability at nucleic acid level upon three subsequent generations of re-infection and an overall permanence of the heterologous sequences was observed. Although there is not a general rule and each chimera should be empirically evaluated, we experienced some construct instability beyond the second generation only with the largest fusions. This result is in clear contrast with previous studies on TBSV, where a tendency to loss heterologous sequences was observed. Scholthof and colleagues (1993) found that the foreign inserts are removed frequently from the TBSV vectors primarily when viruses move to the upper non-inoculated leaves. The apparent natural instability of the tombusvirus RNA (White and Morris 1994) probably facilitates the appearance of TBSV molecules devoid of the insert as the virus spreads throughout the plant. The competitive advantage of these deletion mutants results in infection of upper non-inoculated leaves without

significant levels of the heterologous peptide. In other studies, TBSV was also exploited as a vector for expression of foreign genes. This modified vector was devoid of p19, thus preventing severe systemic necrosis (Scholthof et al. 1995) that would otherwise interfere with optimum expression, and harbored foreign genes downstream of the first codons of an inactivated CP. Unfortunately, also in this circumstance a rapid recombination, along with the selective advantage of the mutants, precluded the use of TBSV as a replacement vector for stable transient expression of foreign genes in whole plants (Scholthof et al. 1996). In parallel with the translational fusion of small foreign peptides to viral CP, so that the resulting moieties project outwards on the VNPs, a general strategy to functionalize capsid surface with additional cues is represented by *in vitro* chemical modification. In this work, the employment of native or genetically introduced amino acid functional groups, such as the primary amine of lysine, to address TBSV VNPs with chemical molecules was reported. A commercially available biotin NHS ester reactive was successfully used to conjugate biotin molecules to properly assembled VNPs. As TBSV-wt lacked of addressable lysine residues, only the TBSV-Flag, owning 2 additional solvent exposed primary amines, resulted in the formation of biotin labeled VNPs. The final outcome achieved with such chimera is a clear example of a *gain-of-function* obtainable through genetic engineering of the virus genome. TBSV-Flag chimeric VNPs have indeed 180 copies of addressable sites that once biotinylated would allow the conjugation of streptavidin, avidin, or neutravidin fusion proteins by simple molecular recognition. Moreover, a protocol for loading a cargo inside the VNPs cavity has been developed. Indeed, changes in pH and bivalent cations concentration are able to promote reversible structural modifications, which result in the opening or closing of virus gated pores (Heaton 1992). Switching between the two conformational states, we were able to load EtBr inside the VNPs. Whether EtBr was used mainly for analytical reasons, as it could be revealed by the fluorescence emission derived from the intercalation with encapsulated nucleic acids, its size and chemical nature are in the range of

many drugs. Hence, the loading of TBSV core with EtBr provides a proof of concept that could be extended to other chemical molecules having pharmacological activity. We have also proven experimentally the accessibility of the genome enclosed inside the VNPs by its susceptibility to RNase degradation. Potentially, upon removal of the genetic materials, the inner cavity of such generated VLPs would become ideal for the encapsidation of larger functional cargo or exogenous nucleic acids, opening another opportunity for gene therapy and DNA vaccine delivery. In this work, we have found very convenient to use *in vitro* transcribed RNA directly for production purposes, and we believe that it is indeed feasible to use just first generation material for small scale production. Under this view and with the prospect of a scaled up process, to avoid the enzymatic treatment necessary for the *in vitro* transcription and also the RNA synthesis itself, we designed and assembled an *in planta* expression cDNA based system, which could be delivered to plants simply in the form of a circular DNA plasmid. To set the genome transcription under active control of plant cell machinery, the CaMV 35S promoter sequence was cloned upstream the 5' end of viral cDNA, replacing the original T7 promoter. Subsequently, three different constructs were generated by modifying the 3' context of TBSV genome in order to achieve transcription termination. In a case, the *XmaI* linearization site has been left, thus keeping unchanged the need for linearization reaction before plant inoculation (**Fig. 7a**). The remaining two constructs, which have been designed to be directly delivered into plant as circular DNA plasmid, harbored the HDV ribozyme sequence followed by the *A. tumefaciens* NOS terminator (**Fig. 7c**) or uniquely the NOS transcription termination signal (**Fig. 7b**). Plants were challenged testing different quantities of all cDNA constructs, however only the 35S-TBSV-cMyc.riboNOS resulted able to reproducibly establish infections comparable, with regards to symptomatology and progression, to the one generated by *in vitro* transcribed RNAs. This result can be explained by the molecular biology being beneath TBSV replication cycle, which requires specific terminal sequences on both 5'

and 3' genomic ends (Russo, Burgyan et al. 1994). Therefore, as a result of the eukaryotic transcription, the *in planta* generated RNA genomes bear a long 3' additional poly(A) sequence that would prevent them to be infectious. Only the employment of the HRz sequence, which promotes an autocatalytic process at RNA level, resulting in the cleavage of the acquired poly(A) tail and the restore of the correct viral 3' end, is able to provide an efficient infection (Chowrira, Pavco et al. 1994). Furthermore, to have a clear picture of the two infection techniques, it should be also considered the sensible difference existing between the quantity of DNA and RNA material used. Upon mechanical leaf rubbing inoculation, whether only a few micrograms of infectious *in vitro* transcribed RNA are already sufficient to establish consistent plant systemic infection, we observed that at least 30 µg of 35S-TBSV-cMyc.riboNOS vector are required to obtain the same result. This evident discrepancy is directly correlated with the different nature of the two molecules and consequently their fate. Sensed RNA genome molecules once entered the cytoplasm of plant cells are directly translated in viral replication proteins, which in turn are able to initiate autonomously the infection cycle. On the opposite, cDNA genomes require reaching the nucleus of the cells to be transcribed by eukaryotic polymerase and, when RNAs are produced, an autocatalytic cleavage must occur before mature infective TBSV molecules are generated. In general, self-processing ribozymes are highly active *in vivo* in their native context, however it has been reported that the presence of extra flanking sequences reduces the frequency of cutting events substantially (Chowrira, Pavco et al. 1994). This is likely due to non-productive, alternative folding of the ribozyme with adjacent sequences. In conclusion, in this study we presented the development and tuning of a cutting edge nano-technologic tool based on TBSV (Grasso, Lico et al. 2012). The system has shown to have several benefits. First of all, the plant production that is quick, easy and really up-scalable. Plants are one of the world's most cost-effective protein producers. An ideal host should support high-levels of foreign protein expression, while providing large biomass, with

easy and rapid growth profiles in both the greenhouse and field. In our study, *N. benthamiana* was used as a primary host for recombinant virus transient expression concluding in the production of TBSV derived VNPs. Although *N. benthamiana* has a relatively small biomass and does not grow well in the field compared to other *Nicotiana* species, greenhouse based manufacturing facilities conditions can be quickly built for rapid and economic scale up. The leaves of these plants are well suited to rapidly incorporate, in a non-permanent fashion, the genetic information required to produce high yields of VNPs. *N. benthamiana* plants are easy to grow and handle, being required only 8 weeks from seeds to the proper developmental stage for infection. Production time can be estimated in just 9-12 days from tissue inoculation to purified VNPs. The purification procedure is reliable, efficient and clean. The system consistently allows producing approximately 300 mg of purified VNPs per kg of fresh infected leaves and data collected from several independent experiments suggest that VNPs yield after purification was very similar among different chimeras. We provided evidence that TBSV offers an ideal scaffold for the development of functional nanoparticles. Depending on the specific application, VNPs can be potentially conjugated with a variety of molecules including fluorophores, metals, peptides, proteins, antibodies, nucleic acids, small molecules, and radioactive isotopes. There are a large number of chemistries available for labeling, most of which utilize the accessible reactive moieties on the surface of the VNPs. The simplest method for labeling the CP of TBSV is by taking advantage of the primary amine of lysine residues. Other possible side chains exploitable for conjugation include carboxyl groups, phenols and thiols. Carboxyl groups can be converted into reactive NHS esters, which in turn can then react with amine-containing small molecules (Li, Chen et al. 2010). Cysteine residues can be modified using maleimide functionalized groups and tyrosine can be modified using diazonium salts (Schlick, Ding et al. 2005; Sapsford, Soto et al. 2006). Recently, "click" reactions have become more widely used for labeling VNPs with large molecules and proteins due to their modular nature, specificity,

high yield and range of solvents and pH stability (Bruckman, Kaur et al. 2008). Click chemistry utilizes reaction precursors which do not react with common functional groups present in biological molecules and this allows the reactions to proceed with high-yield and a high thermodynamic driving force (Bruckman, Kaur et al. 2008). In some cases, when VNPs have a variety of reactive moieties, these simple strategies can be combined to create multiple modified VNPs. The genetic engineering approach has shown to be a successful mechanism for the modification of TBSV based VNPs and can be combined with direct chemical derivatization to create multifunctional nanoparticles for imaging, targeting, and other biotechnology applications. Targeted delivery of VNPs relies on the discovery of cell-specific marker and their incorporation onto the VNP moieties. Recent advances in the development of tumor-specific markers and their ligands have made new groups available for VNP conjugation and helped to create large advances in this field. Based on the functional group attached, VNPs can target tumor cells that specifically overexpress certain ligands as well as receptors. Targeted delivery also has the ability to increase the signal-to-noise ratio of imaging reagents by reducing non-specific background staining. In some cases, the external labeling of VNPs with fluorescent molecules can be detrimental as conjugation with multiple functional groups or large molecules could affect the properties and the uptake efficiency of the VNPs. To overcome this problem, efficient encapsidation strategies can be developed. VNPs core can be exploited to shield small molecules or functional groups from proteolytic degradation while controlling loading and unloading of cargos, including dye as well as chemotherapeutic drugs. Versatility and multi-functionality of the TBSV based VNPs represent two of the most important features desirable for a nanotechnology device. Particles could be modified inside and outside the viral protein cage, combining also different modification strategies. All these features together give the tool a high technological plasticity leading to a large plethora of possible applications. Actually, the TBSV system is already employed in several applications for

tissue engineering, vaccines, drug delivery. However any new functionality needs to be carefully evaluated in regard of the VNPs properties and fate.

References

- Allen, M., J. W. Bulte, et al. (2005). "Paramagnetic viral nanoparticles as potential high-relaxivity magnetic resonance contrast agents." Magn Reson Med **54**(4): 807-812.
- Anderson, E. A., S. Isaacman, et al. (2006). "Viral nanoparticles donning a paramagnetic coat: conjugation of MRI contrast agents to the MS2 capsid." Nano Lett **6**(6): 1160-1164.
- Armstrong, R. D. and R. B. Diasio (1980). "Metabolism and Biological Activity of 5'-Deoxy-5-Fluorouridine, a Novel Fluoropyrimidine." Cancer Research **40**(9): 3333-3338.
- Avesani, L., G. Marconi, et al. (2007). "Stability of Potato virus X expression vectors is related to insert size: implications for replication models and risk assessment." Transgenic Res **16**(5): 587-597.
- Bar, H., I. Yacoby, et al. (2008). "Killing cancer cells by targeted drug-carrying phage nanomedicines." BMC Biotechnol **8**: 37.
- Baulcombe, D. C., S. Chapman, et al. (1995). "Jellyfish green fluorescent protein as a reporter for virus infections." Plant J **7**(6): 1045-1053.
- Baum, A. and A. Garcia-Sastre "Induction of type I interferon by RNA viruses: cellular receptors and their substrates." Amino Acids **38**(5): 1283-1299.
- Been, M. D. and G. S. Wickham (1997). "Self-Cleaving Ribozymes of Hepatitis Delta Virus RNA." European Journal of Biochemistry **247**(3): 741-753.
- Bischoff, F. (2004). A Top-down View of Molecular Farming from the Pharmaceutical Industry: Requirements and Expectations. Molecular Farming, Wiley-VCH Verlag GmbH & Co. KGaA: 267-290.
- Bradford, M. M. (1976). "A rapid and sensitive method for the quantitation of microgram quantities of protein utilizing the principle of protein-dye binding." Anal Biochem **72**: 248-254.
- Bromley, K. M., A. J. Patil, et al. (2008). "Preparation of high quality nanowires by tobacco mosaic virus templating of gold nanoparticles." Journal of Materials Chemistry **18**(40): 4796-4801.
- Brown, W. L., R. A. Mastico, et al. (2002). "RNA bacteriophage capsid-mediated drug delivery and epitope presentation." Intervirology **45**(4-6): 371-380.
- Bruckman, M. A., G. Kaur, et al. (2008). "Surface modification of tobacco mosaic virus with "click" chemistry." ChemBiochem **9**(4): 519-523.
- Brumfield, S., D. Willits, et al. (2004). "Heterologous expression of the modified coat protein of Cowpea chlorotic mottle bromovirus results in the assembly of protein cages with altered architectures and function." J Gen Virol **85**(Pt 4): 1049-1053.
- Buck, K. W. (1996). "Comparison of the replication of positive-stranded RNA viruses of plants and animals." Adv Virus Res **47**: 159-251.
- Burgyan, J., L. Rubino, et al. (1996). "The 5'-terminal region of a tombusvirus genome determines the origin of multivesicular bodies." J Gen Virol **77** (Pt 8): 1967-1974.

- Burgyan, J. and M. Russo (1998). "Tombusvirus isolation and RNA extraction." Methods Mol Biol **81**: 225-230.
- Busch, H. (1990). "The Final Common Pathway of Cancer: Presidential Address." Cancer Research **50**(16): 4830-4838.
- Cabilly, S. (1999). "The basic structure of filamentous phage and its use in the display of combinatorial peptide libraries." Mol Biotechnol **12**(2): 143-148.
- Cascio, A., L. di Martino, et al. (2004). "A 6 day course of liposomal amphotericin B in the treatment of infantile visceral leishmaniasis: the Italian experience." J Antimicrob Chemother **54**(1): 217-220.
- Cesareni, G., L. Castagnoli, et al. (1999). "Phage displayed peptide libraries." Comb Chem High Throughput Screen **2**(1): 1-17.
- Chang, Y. C., M. Borja, et al. (1995). "Host effects and sequences essential for accumulation of defective interfering RNAs of cucumber necrosis and tomato bushy stunt tombusviruses." Virology **210**(1): 41-53.
- Chen, Q. and H. Lai (2012). "Plant-derived virus-like particles as vaccines." Hum Vaccin Immunother **9**(1).
- Chiang, C. M. and R. G. Roeder (1993). "Expression and purification of general transcription factors by FLAG epitope-tagging and peptide elution." Pept Res **6**(2): 62-64.
- Choi, I. R., M. Ostrovsky, et al. (2001). "Regulatory activity of distal and core RNA elements in Tombusvirus subgenomic mRNA2 transcription." J Biol Chem **276**(45): 41761-41768.
- Choi, I. R. and K. A. White (2002). "An RNA activator of subgenomic mRNA1 transcription in tomato bushy stunt virus." J Biol Chem **277**(5): 3760-3766.
- Chowrira, B. M., P. A. Pavco, et al. (1994). "In vitro and in vivo comparison of hammerhead, hairpin, and hepatitis delta virus self-processing ribozyme cassettes." J Biol Chem **269**(41): 25856-25864.
- Commandeur, U. and R. M. Twyman (2004). Biosafety Aspects of Molecular Farming in Plants. Molecular Farming, Wiley-VCH Verlag GmbH & Co. KGaA: 251-266.
- Correia-Pinto, J. F., N. Csaba, et al. (2013). "Vaccine delivery carriers: Insights and future perspectives." International Journal of Pharmaceutics **440**(1): 27-38.
- Cox, R. J., K. A. Brokstad, et al. (2004). "Influenza virus: immunity and vaccination strategies. Comparison of the immune response to inactivated and live, attenuated influenza vaccines." Scand J Immunol **59**(1): 1-15.
- Cramer, C. L., J. G. Boothe, et al. (1999). "Transgenic plants for therapeutic proteins: linking upstream and downstream strategies." Curr Top Microbiol Immunol **240**: 95-118.
- Cruz, S. S., S. Chapman, et al. (1996). "Assembly and movement of a plant virus carrying a green fluorescent protein overcoat." Proc Natl Acad Sci U S A **93**(13): 6286-6290.
- D'Aoust, M. A., M. M. Couture, et al. (2010). "The production of hemagglutinin-based virus-like particles in plants: a rapid, efficient and safe response to pandemic influenza." Plant Biotechnol J **8**(5): 607-619.
- Depicker, A., S. Stachel, et al. (1982). "Nopaline synthase: transcript mapping and DNA sequence." J Mol Appl Genet **1**(6): 561-573.
- Dixit, S. K., N. L. Goicochea, et al. (2006). "Quantum dot encapsulation in viral capsids." Nano Lett **6**(9): 1993-1999.
- Doherty, E. A. and J. A. Doudna (2001). "Ribozyme structures and mechanisms." Annu Rev Biophys Biomol Struct **30**: 457-475.

- Donini, M., C. Lico, et al. (2005). "Production of an engineered killer peptide in *Nicotiana benthamiana* by using a potato virus X expression system." Appl Environ Microbiol **71**(10): 6360-6367.
- Douglas, T. and M. Young (1998). "Host-guest encapsulation of materials by assembled virus protein cages." Nature **393**(6681): 152-155.
- Dujardin, E., C. Peet, et al. (2003). "Organization of Metallic Nanoparticles Using Tobacco Mosaic Virus Templates." Nano Letters **3**(3): 413-417.
- Fabrega, S., P. Durand, et al. (2002). "[The active site of human glucocerebrosidase: structural predictions and experimental validations]." J Soc Biol **196**(2): 151-160.
- Fischer, R., E. Stoger, et al. (2004). "Plant-based production of biopharmaceuticals." Curr Opin Plant Biol **7**(2): 152-158.
- Flenniken, M. L., L. O. Liepold, et al. (2005). "Selective attachment and release of a chemotherapeutic agent from the interior of a protein cage architecture." Chem Commun (Camb)(4): 447-449.
- Frigerio, L., N. D. Vine, et al. (2000). "Assembly, secretion, and vacuolar delivery of a hybrid immunoglobulin in plants." Plant Physiol **123**(4): 1483-1494.
- Gallie, D. R. (1998). "A tale of two termini: a functional interaction between the termini of an mRNA is a prerequisite for efficient translation initiation." Gene **216**(1): 1-11.
- Gatto, D., C. Ruedl, et al. (2004). "Rapid response of marginal zone B cells to viral particles." J Immunol **173**(7): 4308-4316.
- Gerik, J. S., J. E. Duffus, et al. (1990). "Etiology of tomato plant decline in the California desert." Phytopathology **80**(12): 1352-1356.
- Gleba, Y., V. Klimyuk, et al. (2007). "Viral vectors for the expression of proteins in plants." Curr Opin Biotechnol **18**(2): 134-141.
- Gomme, P. T., K. B. McCann, et al. (2005). "Transferrin: structure, function and potential therapeutic actions." Drug Discov Today **10**(4): 267-273.
- Gonzalez, M. J., E. M. Plummer, et al. (2009). "Interaction of Cowpea mosaic virus (CPMV) nanoparticles with antigen presenting cells in vitro and in vivo." PLoS One **4**(11): e7981.
- Goodin, M. M., D. Zaitlin, et al. (2008). "*Nicotiana benthamiana*: its history and future as a model for plant-pathogen interactions." Mol Plant Microbe Interact **21**(8): 1015-1026.
- Grasso, S., C. Lico, et al. (2012). "A plant derived multifunctional tool for nanobiotechnology based on Tomato bushy stunt virus." Transgenic Res.
- Grasso, S. and L. Santi (2010). "Viral nanoparticles as macromolecular devices for new therapeutic and pharmaceutical approaches." Int J Physiol Pathophysiol Pharmacol **2**(2): 161-178.
- Guo, L., E. M. Allen, et al. (2001). "Base-pairing between untranslated regions facilitates translation of uncapped, nonpolyadenylated viral RNA." Mol Cell **7**(5): 1103-1109.
- Harper, D. M., E. L. Franco, et al. (2004). "Efficacy of a bivalent L1 virus-like particle vaccine in prevention of infection with human papillomavirus types 16 and 18 in young women: a randomised controlled trial." Lancet **364**(9447): 1757-1765.
- Harrison, S. C. (2001). "The familiar and the unexpected in structures of icosahedral viruses." Curr Opin Struct Biol **11**(2): 195-199.
- Harrison, S. C., A. J. Olson, et al. (1978). "Tomato bushy stunt virus at 2.9 Å resolution." Nature **276**(5686): 368-373.

- Hearne, P. Q., D. A. Knorr, et al. (1990). "The complete genome structure and synthesis of infectious RNA from clones of tomato bushy stunt virus." Virology **177**(1): 141-151.
- Heaton, L. A. (1992). "Use of agarose gel electrophoresis to monitor conformational changes of some small, spherical plant viruses." Phytopathology **82**(7): 803-807.
- Hildebrand, M. (2008). "Diatoms, biomineralization processes, and genomics." Chem Rev **108**(11): 4855-4874.
- Hillman, B. I., P. Hearne, et al. (1989). "Organization of tomato bushy stunt virus genome: characterization of the coat protein gene and the 3' terminus." Virology **169**(1): 42-50.
- Hood, E. E., S. L. Woodard, et al. (2002). "Monoclonal antibody manufacturing in transgenic plants--myths and realities." Curr Opin Biotechnol **13**(6): 630-635.
- Hooker, J. M., A. Datta, et al. (2007). "Magnetic resonance contrast agents from viral capsid shells: a comparison of exterior and interior cargo strategies." Nano Lett **7**(8): 2207-2210.
- Hooker, J. M., J. P. O'Neil, et al. (2008). "Genome-free viral capsids as carriers for positron emission tomography radiolabels." Mol Imaging Biol **10**(4): 182-191.
- Hsu, C., P. Singh, et al. (2006). "Characterization of polymorphism displayed by the coat protein mutants of tomato bushy stunt virus." Virology **349**(1): 222-229.
- Hu, Y., R. Zandi, et al. (2008). "Packaging of a polymer by a viral capsid: the interplay between polymer length and capsid size." Biophys J **94**(4): 1428-1436.
- Huang, Y., C. Y. Chiang, et al. (2005). "Programmable assembly of nanoarchitectures using genetically engineered viruses." Nano Lett **5**(7): 1429-1434.
- Inaba, Y., W. Q. Zhong, et al. (2007). "Specificity of expression of the GUS reporter gene (*uidA*) driven by the tobacco ASA2 promoter in soybean plants and tissue cultures." J Plant Physiol **164**(7): 824-834.
- Joelson, T., L. Akerblom, et al. (1997). "Presentation of a foreign peptide on the surface of tomato bushy stunt virus." J Gen Virol **78** (Pt 6): 1213-1217.
- Kaltgrad, E., M. K. O'Reilly, et al. (2008). "On-virus construction of polyvalent glycan ligands for cell-surface receptors." J Am Chem Soc **130**(14): 4578-4579.
- Kaur, G., M. T. Valarmathi, et al. (2010). "Regulation of osteogenic differentiation of rat bone marrow stromal cells on 2D nanorod substrates." Biomaterials **31**(7): 1732-1741.
- Kaur, G., M. T. Valarmathi, et al. (2008). "The promotion of osteoblastic differentiation of rat bone marrow stromal cells by a polyvalent plant mosaic virus." Biomaterials **29**(30): 4074-4081.
- Kaur, G., C. Wang, et al. (2010). "The synergistic effects of multivalent ligand display and nanotopography on osteogenic differentiation of rat bone marrow stem cells." Biomaterials **31**(22): 5813-5824.
- Kawarasaki, Y., Y. Yamada, et al. (2003). "Stabilization of affinity-tagged recombinant protein during/after its production in a cell-free system using wheat-germ extract." J Biosci Bioeng **95**(3): 209-214.
- Kay, M. A., A. X. Holterman, et al. (1995). "Long-term hepatic adenovirus-mediated gene expression in mice following CTLA4Ig administration." Nat Genet **11**(2): 191-197.
- Knez, M., A. M. Bittner, et al. (2003). "Biotemplate Synthesis of 3-nm Nickel and Cobalt Nanowires." Nano Letters **3**(8): 1079-1082.
- Kolodziej, K. E., F. Pourfarzad, et al. (2009). "Optimal use of tandem biotin and V5 tags in ChIP assays." BMC Mol Biol **10**: 6.

- Koprowski, H. (2005). "Vaccines and sera through plant biotechnology." *Vaccine* **23**(15): 1757-1763.
- Kozak, M. (1989). "The scanning model for translation: an update." *J Cell Biol* **108**(2): 229-241.
- Kroger, N. and N. Poulsen (2008). "Diatoms-from cell wall biogenesis to nanotechnology." *Annu Rev Genet* **42**: 83-107.
- Kurts, C., B. W. Robinson, et al. "Cross-priming in health and disease." *Nat Rev Immunol* **10**(6): 403-414.
- Laemmli, U. K. (1970). "Cleavage of structural proteins during the assembly of the head of bacteriophage T4." *Nature* **227**(5259): 680-685.
- Laize, V., P. Ripoché, et al. (1997). "Purification and functional reconstitution of the human CHIP28 water channel expressed in *Saccharomyces cerevisiae*." *Protein Expr Purif* **11**(3): 284-288.
- Landry, N., B. J. Ward, et al. (2010). "Preclinical and clinical development of plant-made virus-like particle vaccine against avian H5N1 influenza." *PLoS One* **5**(12): e15559.
- Lee, S. W., C. Mao, et al. (2002). "Ordering of quantum dots using genetically engineered viruses." *Science* **296**(5569): 892-895.
- Lee, Y. J., H. Yi, et al. (2009). "Fabricating genetically engineered high-power lithium-ion batteries using multiple virus genes." *Science* **324**(5930): 1051-1055.
- Levy, H., A. Or, et al. (1991). "Molecular aspects of Gaucher disease." *Dev Neurosci* **13**(4-5): 352-362.
- Lewis, J. D., G. Destito, et al. (2006). "Viral nanoparticles as tools for intravital vascular imaging." *Nat Med* **12**(3): 354-360.
- Li, K., Y. Chen, et al. (2010). "Chemical Modification of M13 Bacteriophage and Its Application in Cancer Cell Imaging." *Bioconjugate Chemistry* **21**(7): 1369-1377.
- Lico, C., F. Capuano, et al. (2006). "Peptide display on Potato virus X: molecular features of the coat protein-fused peptide affecting cell-to-cell and phloem movement of chimeric virus particles
10.1099/vir.0.82097-0." *J Gen Virol* **87**(10): 3103-3112.
- Lico, C., C. Mancini, et al. (2009). "Plant-produced potato virus X chimeric particles displaying an influenza virus-derived peptide activate specific CD8+ T cells in mice." *Vaccine* **27**(37): 5069-5076.
- Lieber, A., M. J. Vrancken Peeters, et al. (1995). "Adenovirus-mediated urokinase gene transfer induces liver regeneration and allows for efficient retrovirus transduction of hepatocytes in vivo." *Proc Natl Acad Sci U S A* **92**(13): 6210-6214.
- Lin, Y., Z. Su, et al. (2008). "Layer-by-layer assembly of viral capsid for cell adhesion." *Acta Biomater* **4**(4): 838-843.
- Loo, L., R. H. Guenther, et al. (2006). "Controlled encapsidation of gold nanoparticles by a viral protein shell." *J Am Chem Soc* **128**(14): 4502-4503.
- Loo, L., R. H. Guenther, et al. (2008). "Infusion of dye molecules into Red clover necrotic mosaic virus." *Chem Commun (Camb)*(1): 88-90.
- Luis-Arteaga, M., E. Rodriguez-Cerezo, et al. (1996). "Different tomato bushy stunt virus strains that cause disease outbreaks in solanaceous crops in Spain." *Phytopathology* **86**(5): 535-542.
- Ma, J. K., P. M. Drake, et al. (2003). "The production of recombinant pharmaceutical proteins in plants." *Nat Rev Genet* **4**(10): 794-805.

- Maliga, P. and I. Graham (2004). "Molecular farming and metabolic engineering promise a new generation of high-tech crops." *Curr Opin Plant Biol* **7**(2): 149-151.
- Mao, C., C. E. Flynn, et al. (2003). "Viral assembly of oriented quantum dot nanowires." *Proc Natl Acad Sci U S A* **100**(12): 6946-6951.
- McAleer, W. J., E. B. Buynak, et al. (1984). "Human hepatitis B vaccine from recombinant yeast." *Nature* **307**(5947): 178-180.
- McCormick, A. A., T. A. Corbo, et al. (2006). "TMV-peptide fusion vaccines induce cell-mediated immune responses and tumor protection in two murine models." *Vaccine* **24**(40-41): 6414-6423.
- Menassa, R., V. Nguyen, et al. (2001). "A self-contained system for the field production of plant recombinant interleukin-10." *Molecular Breeding* **8**(2): 177-185.
- Merzlyak, A., S. Indrakanti, et al. (2009). "Genetically engineered nanofiber-like viruses for tissue regenerating materials." *Nano Lett* **9**(2): 846-852.
- Michalet, X., F. F. Pinaud, et al. (2005). "Quantum dots for live cells, in vivo imaging, and diagnostics." *Science* **307**(5709): 538-544.
- Miller, W. A. and G. Koev (2000). "Synthesis of subgenomic RNAs by positive-strand RNA viruses." *Virology* **273**(1): 1-8.
- Mizuno, M., J. Yoshida, et al. (1998). "Adeno-associated virus vector containing the herpes simplex virus thymidine kinase gene causes complete regression of intracerebrally implanted human gliomas in mice, in conjunction with ganciclovir administration." *Jpn J Cancer Res* **89**(1): 76-80.
- Murata, Y., P. M. Lightfoote, et al. (2009). "Antigenic presentation of heterologous epitopes engineered into the outer surface-exposed helix 4 loop region of human papillomavirus L1 capsomeres." *Virol J* **6**: 81.
- Nagy, P. D., J. Pogany, et al. (1999). "RNA elements required for RNA recombination function as replication enhancers in vitro and in vivo in a plus-strand RNA virus." *EMBO J* **18**(20): 5653-5665.
- Nam, K. T., D. W. Kim, et al. (2006). "Virus-enabled synthesis and assembly of nanowires for lithium ion battery electrodes." *Science* **312**(5775): 885-888.
- Nam, K. T., R. Wartena, et al. (2008). "Stamped microbattery electrodes based on self-assembled M13 viruses." *Proc Natl Acad Sci U S A* **105**(45): 17227-17231.
- Namba, K. and G. Stubbs (1986). "Structure of tobacco mosaic virus at 3.6 Å resolution: implications for assembly." *Science* **231**(4744): 1401-1406.
- Newton-Northup, J. R., S. D. Figueroa, et al. (2009). "Bifunctional phage-based pretargeted imaging of human prostate carcinoma." *Nucl Med Biol* **36**(7): 789-800.
- Nguyen, D. M., F. R. Spitz, et al. (1996). "Gene therapy for lung cancer: enhancement of tumor suppression by a combination of sequential systemic cisplatin and adenovirus-mediated p53 gene transfer." *J Thorac Cardiovasc Surg* **112**(5): 1372-1376; discussion 1376-1377.
- Niu, Z., M. A. Bruckman, et al. (2007). "Assembly of tobacco mosaic virus into fibrous and macroscopic bundled arrays mediated by surface aniline polymerization." *Langmuir* **23**(12): 6719-6724.
- Odell, J. T., F. Nagy, et al. (1985). "Identification of DNA sequences required for activity of the cauliflower mosaic virus 35S promoter." *Nature* **313**(6005): 810-812.
- Olson, A. J., G. Bricogne, et al. (1983). "Structure of tomato bushy stunt virus IV. The virus particle at 2.9 Å resolution." *J Mol Biol* **171**(1): 61-93.

- Oster, S. K., B. Wu, et al. (1998). "Uncoupled expression of p33 and p92 permits amplification of tomato bushy stunt virus RNAs." *J Virol* **72**(7): 5845-5851.
- Panaviene, Z., J. M. Baker, et al. (2003). "The overlapping RNA-binding domains of p33 and p92 replicase proteins are essential for tombusvirus replication." *Virology* **308**(1): 191-205.
- Peabody, D. S. (2003). "A Viral Platform for Chemical Modification and Multivalent Display." *J Nanobiotechnology* **1**(1): 5.
- Plotkin, S. A. (2005). "Vaccines: past, present and future." *Nat Med* **11**(4 Suppl): S5-11.
- Pogany, J., M. R. Fabian, et al. (2003). "A replication silencer element in a plus-strand RNA virus." *EMBO J* **22**(20): 5602-5611.
- Pogue, G. P., J. A. Lindbo, et al. (2002). "Making an ally from an enemy: plant virology and the new agriculture." *Annu Rev Phytopathol* **40**: 45-74.
- Prasuhn, D. E., Jr., R. M. Yeh, et al. (2007). "Viral MRI contrast agents: coordination of Gd by native virions and attachment of Gd complexes by azide-alkyne cycloaddition." *Chem Commun (Camb)*(12): 1269-1271.
- Qiu, W., J. W. Park, et al. (2002). "Tombusvirus P19-mediated suppression of virus-induced gene silencing is controlled by genetic and dosage features that influence pathogenicity." *Mol Plant Microbe Interact* **15**(3): 269-280.
- Qu, F. and T. J. Morris (2002). "Efficient infection of *Nicotiana benthamiana* by Tomato bushy stunt virus is facilitated by the coat protein and maintained by p19 through suppression of gene silencing." *Mol Plant Microbe Interact* **15**(3): 193-202.
- Raja, K. S., Q. Wang, et al. (2003). "Hybrid virus-polymer materials. 1. Synthesis and properties of PEG-decorated cowpea mosaic virus." *Biomacromolecules* **4**(3): 472-476.
- Rajendran, K. S. and P. D. Nagy (2003). "Characterization of the RNA-binding domains in the replicase proteins of tomato bushy stunt virus." *J Virol* **77**(17): 9244-9258.
- Raska, I., K. Koberna, et al. (2004). "The nucleolus and transcription of ribosomal genes." *Biol Cell* **96**(8): 579-594.
- Ray, D. and K. A. White (1999). "Enhancer-like properties of an RNA element that modulates Tombusvirus RNA accumulation." *Virology* **256**(1): 162-171.
- Ren, Y., S. M. Wong, et al. (2006). "In vitro-reassembled plant virus-like particles for loading of polyacids." *J Gen Virol* **87**(Pt 9): 2749-2754.
- Ren, Y., S. M. Wong, et al. (2007). "Folic acid-conjugated protein cages of a plant virus: a novel delivery platform for doxorubicin." *Bioconjug Chem* **18**(3): 836-843.
- Roggero, P., M. Ciuffo, et al. (2001). "The expression of a single-chain Fv antibody fragment in different plant hosts and tissues by using Potato virus X as a vector." *Protein Expr Purif* **22**(1): 70-74.
- Russo, M., J. Burgyan, et al. (1994). "Molecular biology of tombusviridae." *Adv Virus Res* **44**: 381-428.
- Santi, L., L. Batchelor, et al. (2008). "An efficient plant viral expression system generating orally immunogenic Norwalk virus-like particles." *Vaccine* **26**(15): 1846-1854.
- Santi, L., Z. Huang, et al. (2006). "Virus-like particles production in green plants." *Methods* **40**(1): 66-76.
- Sapsford, K. E., C. M. Soto, et al. (2006). "A cowpea mosaic virus nanoscaffold for multiplexed antibody conjugation: application as an immunoassay tracer." *Biosens Bioelectron* **21**(8): 1668-1673.

- Schillberg, S., R. M. Twyman, et al. (2005). "Opportunities for recombinant antigen and antibody expression in transgenic plants--technology assessment." Vaccine **23**(15): 1764-1769.
- Schlick, T. L., Z. Ding, et al. (2005). "Dual-surface modification of the tobacco mosaic virus." J Am Chem Soc **127**(11): 3718-3723.
- Scholthof, H. B. (1999). "Rapid delivery of foreign genes into plants by direct rub-inoculation with intact plasmid DNA of a tomato bushy stunt virus gene vector." J Virol **73**(9): 7823-7829.
- Scholthof, H. B., T. J. Morris, et al. (1993). "The capsid protein gene of Tomato bushy stunt virus is dispensable for systemic movement and can be replaced for localized expression of foreign genes." Mol. Plant-Microbe Interact. **6**: 309-322.
- Scholthof, H. B., K. B. Scholthof, et al. (1995). "Identification of tomato bushy stunt virus host-specific symptom determinants by expression of individual genes from a potato virus X vector." Plant Cell **7**(8): 1157-1172.
- Scholthof, H. B., K. B. Scholthof, et al. (1996). "Plant virus gene vectors for transient expression of foreign proteins in plants." Annu Rev Phytopathol **34**: 299-323.
- Scholthof, H. B., K. B. Scholthof, et al. (1995). "Tomato bushy stunt virus spread is regulated by two nested genes that function in cell-to-cell movement and host-dependent systemic invasion." Virology **213**(2): 425-438.
- Scholthof, K. B., H. B. Scholthof, et al. (1995). "The tomato bushy stunt virus replicase proteins are coordinately expressed and membrane associated." Virology **208**(1): 365-369.
- Shenton, W., T. Douglas, et al. (1999). "Inorganic-Organic Nanotube Composites from Template Mineralization of Tobacco Mosaic Virus." Advanced Materials **11**(3): 253-256.
- Sheridan, C. (2012). "Proof of concept for next-generation nanoparticle drugs in humans." Nat Biotech **30**(6): 471-473.
- Sherman, M. B., R. H. Guenther, et al. (2006). "Removal of divalent cations induces structural transitions in red clover necrotic mosaic virus, revealing a potential mechanism for RNA release." J Virol **80**(21): 10395-10406.
- Sijmons, P. C., B. M. Dekker, et al. (1990). "Production of correctly processed human serum albumin in transgenic plants." Biotechnology (N Y) **8**(3): 217-221.
- Sikkema, F. D., M. Comellas-Aragones, et al. (2007). "Monodisperse polymer-virus hybrid nanoparticles." Org Biomol Chem **5**(1): 54-57.
- Singh, P., D. Prasuhn, et al. (2007). "Bio-distribution, toxicity and pathology of cowpea mosaic virus nanoparticles in vivo." J Control Release **120**(1-2): 41-50.
- Sit, T. L., A. A. Vaewhongs, et al. (1998). "RNA-mediated trans-activation of transcription from a viral RNA." Science **281**(5378): 829-832.
- Smith, K. M. (1935). "A NEW VIRUS DISEASE OF THE TOMATO." Annals of Applied Biology **22**(4): 731-741.
- Smith, M. L., J. A. Lindbo, et al. (2006). "Modified tobacco mosaic virus particles as scaffolds for display of protein antigens for vaccine applications." Virology **348**(2): 475-488.
- Srivastava, A. S., T. Kaido, et al. (2004). "Immunological factors that affect the in vivo fate of T7 phage in the mouse." J Virol Methods **115**(1): 99-104.
- Steinmetz, N. F., E. Bock, et al. (2008). "Assembly of multilayer arrays of viral nanoparticles via biospecific recognition: a quartz crystal microbalance with dissipation monitoring study." Biomacromolecules **9**(2): 456-462.

- Steinmetz, N. F. and M. Manchester (2009). "PEGylated viral nanoparticles for biomedicine: the impact of PEG chain length on VNP cell interactions in vitro and ex vivo." Biomacromolecules **10**(4): 784-792.
- Stoger, E., J. K. Ma, et al. (2005). "Sowing the seeds of success: pharmaceutical proteins from plants." Curr Opin Biotechnol **16**(2): 167-173.
- Storni, T. and M. F. Bachmann (2004). "Loading of MHC class I and II presentation pathways by exogenous antigens: a quantitative in vivo comparison." J Immunol **172**(10): 6129-6135.
- Strable, E., J. E. Johnson, et al. (2004). "Natural Nanochemical Building Blocks: Icosahedral Virus Particles Organized by Attached Oligonucleotides." Nano Lett **4**(8): 1385-1389.
- Suci, P. A., M. T. Klem, et al. (2006). "Assembly of multilayer films incorporating a viral protein cage architecture." Langmuir **22**(21): 8891-8896.
- Sun, J., C. DuFort, et al. (2007). "Core-controlled polymorphism in virus-like particles." Proc Natl Acad Sci U S A **104**(4): 1354-1359.
- Szittyá, G., P. Salamon, et al. (2000). "The complete nucleotide sequence and synthesis of infectious RNA of genomic and defective interfering RNAs of TBSV-P." Virus Res **69**(2): 131-136.
- Tama, F. and C. L. Brooks, 3rd (2002). "The mechanism and pathway of pH induced swelling in cowpea chlorotic mottle virus." J Mol Biol **318**(3): 733-747.
- Thanavala, Y., M. Mahoney, et al. (2005). "Immunogenicity in humans of an edible vaccine for hepatitis B." Proc Natl Acad Sci U S A **102**(9): 3378-3382.
- Thresh, J. M. (1982). "HANDBOOK OF PLANT VIRUS INFECTIONS: COMPARATIVE DIAGNOSIS (Book)." Plant, Cell & Environment **5**(3): 188-189.
- Twyman, R. M., S. Schillberg, et al. (2005). "Transgenic plants in the biopharmaceutical market." Expert Opin Emerg Drugs **10**(1): 185-218.
- Twyman, R. M., E. Stoger, et al. (2003). "Molecular farming in plants: host systems and expression technology." Trends Biotechnol **21**(12): 570-578.
- van Beijnum, J. R., R. P. Dings, et al. (2006). "Gene expression of tumor angiogenesis dissected: specific targeting of colon cancer angiogenic vasculature." Blood **108**(7): 2339-2348.
- Vezina, L.-P., M.-A. Daoust, et al. (2011-05-01). "Plants as an innovative and accelerated vaccine-manufacturing solution: a plant-based expression system could provide greater speed and capacity than other recombinant technologies at a comparatively low cost." Biopharm International **24**(5): s27(24).
- Villa, L. L., R. L. Costa, et al. (2005). "Prophylactic quadrivalent human papillomavirus (types 6, 11, 16, and 18) L1 virus-like particle vaccine in young women: a randomised double-blind placebo-controlled multicentre phase II efficacy trial." Lancet Oncol **6**(5): 271-278.
- Voinnet, O., Y. M. Pinto, et al. (1999). "Suppression of gene silencing: a general strategy used by diverse DNA and RNA viruses of plants." Proc Natl Acad Sci U S A **96**(24): 14147-14152.
- Wang, Q., E. Kaltgrad, et al. (2002). "Natural supramolecular building blocks. Wild-type cowpea mosaic virus." Chem Biol **9**(7): 805-811.
- Wang, X., Z. Niu, et al. (2008). "Nanomechanical characterization of polyaniline coated tobacco mosaic virus nanotubes." Journal of Biomedical Materials Research Part A **87A**(1): 8-14.
- White, K. A. (2002). "The premature termination model: a possible third mechanism for subgenomic mRNA transcription in (+)-strand RNA viruses." Virology **304**(2): 147-154.

- White, K. A. and T. J. Morris (1994). "Nonhomologous RNA recombination in tombusviruses: generation and evolution of defective interfering RNAs by stepwise deletions." *J Virol* **68**(1): 14-24.
- Wriggers, W., S. Chakravarty, et al. (2005). "Control of protein functional dynamics by peptide linkers." *Biopolymers* **80**(6): 736-746.
- Wu, B. and K. A. White (1999). "A primary determinant of cap-independent translation is located in the 3'-proximal region of the tomato bushy stunt virus genome." *J Virol* **73**(11): 8982-8988.
- Wu, M., T. Sherwin, et al. (2005). "Delivery of antisense oligonucleotides to leukemia cells by RNA bacteriophage capsids." *Nanomedicine* **1**(1): 67-76.
- Yamada, T., Y. Iwasaki, et al. (2003). "Nanoparticles for the delivery of genes and drugs to human hepatocytes." *Nat Biotechnol* **21**(8): 885-890.
- Yamashita, I., K. Iwahori, et al. "Ferritin in the field of nanodevices." *Biochim Biophys Acta*.
- Young, M., D. Willits, et al. (2008). "Plant viruses as biotemplates for materials and their use in nanotechnology." *Annu Rev Phytopathol* **46**: 361-384.
- Zhang, G., V. Slowinski, et al. (1999). "Subgenomic mRNA regulation by a distal RNA element in a (+)-strand RNA virus." *RNA* **5**(4): 550-561.